1954

Assembly, adjustment, and partial calibration of an infrared monochromator-spectrometer system

Skoog, Joseph Laurence

Monterey, California: U.S. Naval Postgraduate School

ASSEMBLY, ADJUSTMENT, AND PARTIAL CALIBRATION OF AN INFRARED MONOCHROMATOR-SPECTROMETER SYSTEM

JOSEPH LAWRENCE SKOOG, JR.

DIRECTIONS FOR BINDING

BIND IN
(CIRCLE ONE)

BUCKRAM
COLOR NO. 8854

FABRIKOID
COLOR_____

LEATHER
COLOR_____

OTHER INSTRUCTIONS
Letter in gold.
Letter on the front cover:

ASSEMBLY, ADJUSTMENT, AND PARTIAL CALIBRATION
OF
AN INFRARED MONOCHROMATOR-SPECTROMETER SYSTEM

JOSEPH LAURENCE SKOOG, Jr.

LETTERING ON BACK shelf
TO BE EXACTLY AS
PRINTED HERE.

SKOOG

1954

Thesis
S56

ASSEMBLY, ADJUSTMENT, AND PARTIAL CALIBRATION

OF

AN INFRARED MONOCHROMATOR-SPECTROMETER SYSTEM

by

Joseph Laurence Skoog, Jr.
Lieutenant, United States Navy

Submitted in partial fulfillment
of the requirements
for the degree of
MASTER OF SCIENCE
IN
PHYSICS

United States Naval Postgraduate School
Monterey, California
1 9 5 4

This work is accepted as fulfilling

the thesis requirements for the degree of

MASTER OF SCIENCE

IN

PHYSICS

from the

United States Naval Postgraduate School

PREFACE

The United States Naval Postgraduate School recently received a Farrand Optical Company double monochromator and spectrometer system on an indefinite loan basis from the United States Naval Ordnance Test Station, China Lake, California. The components of this particular equipment are for use in the infrared region between 1.5 and 25 microns wavelength.

Calibration data and other detailed information for proper utilization of this system were lacking and the various units had not been operated at the Naval Postgraduate School before this thesis project was undertaken at that institution during the latter half of the academic year 1954. It is hoped that efforts toward placing the system into operation and the information presented in the following pages will be of fundamental utility to others who later may use or attempt to develop further the capabilities of this equipment.

The writer desires to express his appreciation to Professor Sydney H. Kalmbach for the suggestion of the topic and for his guidance and encouragement; to Professor W. P. Cunningham for his suggestions for the improvement of this report; to Professor A. Sheingold for advice on electronic matters, and to Mr. M. K. Andrews and Chief Opticalman R. C. Moeller, U. S. Navy, for their skillful and highly cooperative assistance.

TABLE OF CONTENTS

LIST OF ILLUSTRATIONS

TABLE OF SYMBOLS AND ABBREVIATIONS

A	Absorbance factor
A_s	Pseudo-absorbance factor
b	Coefficient of linear wavelength dependence of the phase shift coefficient f
c	Wavelength position of an absorbance curve maximum value
°C	Degrees Centigrade
cps	Cycles per second
f	Coefficient of phase shift across multiple discontinuities of media
f_o	f for a designated wavelength λ_o
h	Planck's constant
k	A constant of unspecified value used in connection with y_1 values
k_1	Slope of an assumed straight line portion of a y_1 curve
k_2	Latus rectum width of an assumed parabolic absorbance curve
m	Order of interference or maximum absorbance factor
n	Index of refraction
mfd	Microfarad
R	Resolving power
rms	Root mean square
rpm	Revolutions per minute
t	Separation of two parallel reflecting surfaces used for the generation of interference fringes of equal chromatic order
y_1	Recorder stylus displacement ordinate for unabsorbed source energy
y_2	Recorder stylus displacement ordinate with contaminating absorbant only present

y_3	Recorder stylus displacement ordinate with contaminating and sample absorbants present
$\Delta\lambda$	Wavelength resolution limit
$\Delta\nu$	Wavenumber resolution limit
λ	Wavelength in microns
λ_o	Designated wavelength at which the phase shift coefficient f_o is known
μ	Microns
ν	Wavenumber in reciprocal centimeters
Ω	Ohms resistance

CHAPTER I

INTRODUCTION

1. Summary

A recording infrared monochromator-spectrometer system, intended for use in the wavelength range between 1.5 and 25 microns, has been set up and operated for the first time since acquisition. A variety of repairs, adjustments, and modifications contributed to minor improvements, but operating performance has not been made to approach anticipated characteristics.

Descriptions of the function of all system components and discussions of the theoretical and experimentally determined factors affecting the final recording of spectral responses are presented. Four distinct methods of obtaining wavelength calibration points are discussed: the method of band absorption by gases and thin films was the only method which yielded satisfactory experimental results under the conditions of limited performance characteristics. Calibration data based on this method are provided for the restricted wavelength range within which usable recorder outputs were obtained from conventional energy sources.

2. The Nature of Infrared Phenomena

Unlike the ultraviolet and visible regions of energy absorption and emission, associated with changes in the electronic configuration of atoms, most infrared phenomena are the result of changes in the vibrational and rotational energy states of molecules. At temperatures other than absolute zero, all atoms are continuously oscillating or rotating

about equilibrium positions within the molecular framework. These movements cause infrared emission or absorption phenomena, provided that changes of electric dipole moment are involved. Vibrational effects provide higher energy changes and therefore are responsible for emission and absorption spectra in the shorter wavelength portions of the infrared region, while pure rotational effects lead to phenomena in the so-called far infrared region. These effects are often superimposed, and the complexity of the spectra depend upon whether the vibrational effects are harmonic or mechanically or electrically anharmonic and upon the spacing of superimposed rotational effects. The latter characteristic is determined by the rotational moments of inertia of the molecule about its axes of rotation.

The infrared is commonly agreed to be bounded at the short wavelength limit by the red limit of human eye perception, about 0.7 micron. The long wavelength limit is an undetermined wavelength, not less than 300 microns, which overlaps the region of electronically produced microwave phenomena.

The limited optical transmittance of common materials imposes special problems in the study of infrared phenomena. Glass prisms and lenses are completely unusable beyond wavelengths of about 3 microns and various alkali halides are suitable for transmission of infrared only to wavelengths of approximately 28 microns. Gratings are required as dispersing devices at longer wavelengths.

Fortunately, the reflectivity coefficient of most mirror surfaces increases as wavelength increases, and gold or silver deposits on glass

are excellent for redirection of infrared rays. Furthermore, aberrations and astigmatism effects are usually small within any infrared system.

Since infrared radiations from most emitters are of very low power per unit area, most studies of infrared phenomena are made by observing characteristic absorption actions of specific molecules in the presence of a source of wide-band continuous infrared radiation.

3. Infrared Spectroscopy

An infrared spectroscopic system capable of sufficient resolution can yield data which are sufficiently precise to justify deductions as to the mechanical properties of molecules and the modes of vibratory oscillations, rotations, and overtone combinations between the systems of atoms. Scientific publications of such observations and deductions are very numerous.

Characteristic spectral effects are associated with many radicals, with their designated atoms and bond forms, regardless of the total composition of molecules to which they may be attached or the presence of other molecules (see Figure 1). This fact, plus the advent of integrated systems capable of scanning infrared absorption characteristics of mixed liquids or vapors or thin films and yielding a continuous recording of the absorption spectrum in several minutes, has brought about an enormous commercial interest in these methods. Such systems are capable of providing sufficiently accurate quantitative analyses to compete with more conventional methods, and production control problems are particularly well-suited to employment of these systems.

4. The U. S. Naval Postgraduate School Infrared Monochromator-Spectro-

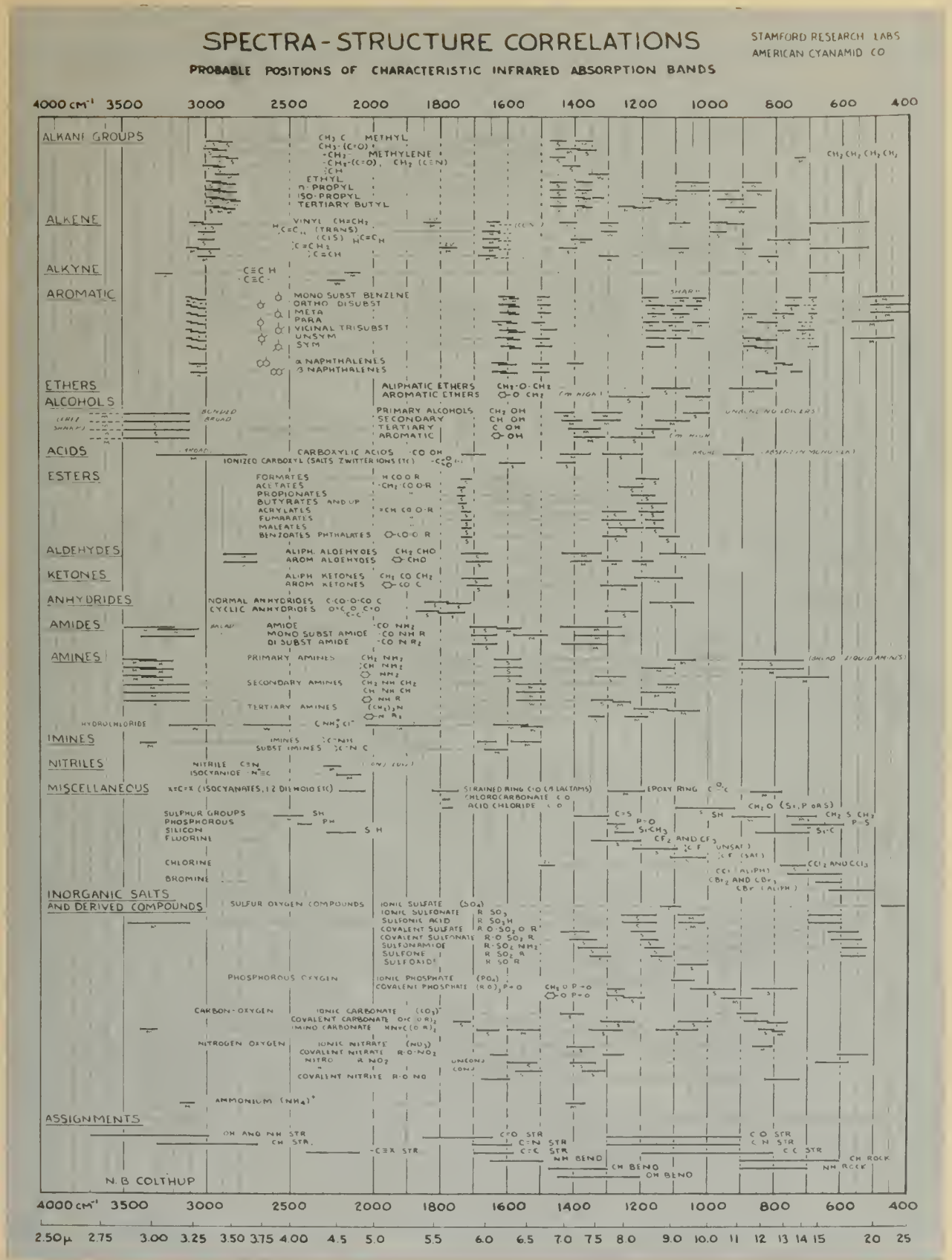

FIGURE 1

CHART OF INFRARED ABSORPTION BANDS
FOR PRINCIPAL ATOMIC FUNCTIONAL GROUPS

meter System

The Farrand Optical Company infrared monochromator at this institution, activated in the process of this thesis project, consists essentially of two large potassium bromide prisms arranged so that each prism disperses incident radiation twice; gold-plated mirrors to control the path of the transmitted energy; variable slits for control of resolution and total emergent energy, and a motor-driven drive system which determines the wavelength of radiation emerging from the exit slit and provides vernier dial indication of that wavelength.

Monochromatic infrared radiation from the monochromator may be focused upon a bolometer to generate an electrical signal. This signal may then be amplified and passed through a discriminator circuit to reduce spurious effects upon a recording device. The amplifier and discriminator units received with the monochromator are products of the W.S. McDonald Co., Inc., Cambridge, Mass. Alternate detection systems include the Golay pneumatic detector and simple thermocouple devices. Connection of these units renders the monochromator proper a part of a monochromator-spectrometer system.

Wide-band continuous emitters used with this system include the Globar and Nernst glowers. No absorption cells are provided with this system, but non-interacting gases may be admitted directly into the monochromator casing for purposes of analysis or calibration.

Accessories and modifications to the original equipment have been made to allow operation of the monochromator and detector within a constant temperature enclosure. A means of indicating wavelength vernier

dial position directly on the recorder trace also has been provided.

5. Calibration of the Monochromator-Spectrometer

In addition to accomplishing necessary repairs and adjustments to establish satisfactory operation, it was originally intended that precision calibration of this system would be accomplished by utilization of some or all of the following methods:

a. Selective transmission by a Christiansen filter.

b. Line emission spectra of mercury, sodium, helium, and hydrogen in the near-infrared region.

c. Band absorption spectra of suitable gases and thin films.

d. Interference fringes of equal chromatic order.

CHAPTER II

DESCRIPTION OF SYSTEM COMPONENTS

1. The Monochromator

The monochromator is a prismatic dispersion apparatus shown schematically by Figure 2. Radiant energy received through the silver chloride entrance window A and passing entrance slit B is reflected by fixed Newtonian mirror C and collimated by mirror D to form a parallel beam incident upon potassium bromide prism E. The dispersed beam is reflected from the Littrow mirror assembly F, undergoes further dispersion through the first prism, and is reflected in turn by mirrors D and C to center slit G, where a similar path and double dispersion process begins. Monochromator radiation from exit slit H may be allowed to pass through exit window J or may be reflected from plane mirror K and ellipsoidal mirror L to focus at detector M.

All mirrors are gold-plated for optimum reflectivity over the 1.5 to 25 micron range of this version of the instrument. The KBr prisms are fixed, have minimum linear dispersion of 1.35 millimeters per micron at about 4.5 microns and maximum linear dispersion of 10 millimeters per micron at 25 microns.

The wavelength of radiation at the exit slit is dependent upon the position of the Littrow mirror assembly, which is driven from a synchronous motor through a gear assembly, drive shaft N, and a cam and follower arrangement. A vernier dial system P indicates mirror assembly position in terms of microns of wavelength and is direct-reading to 0.01 micron.

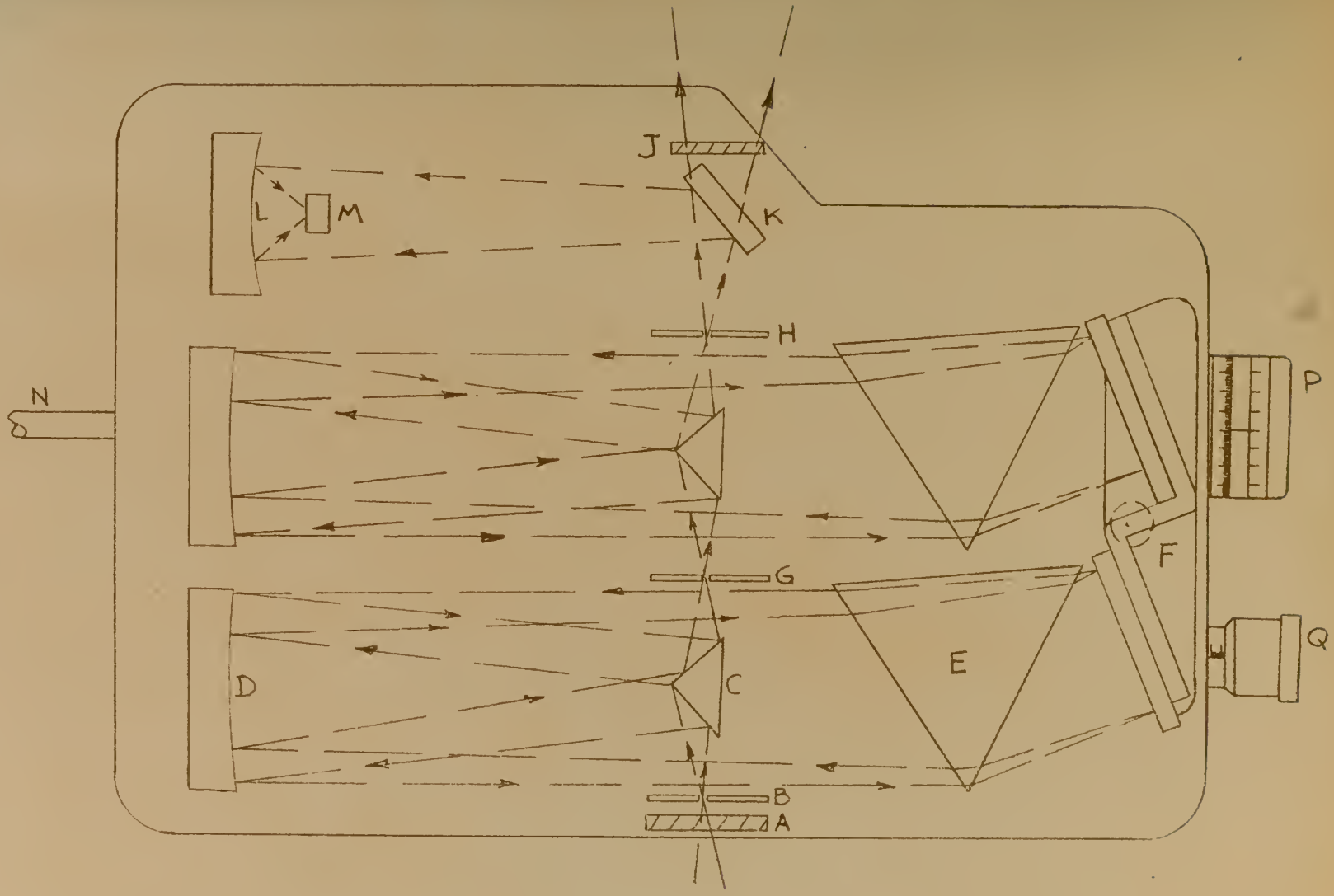

FIGURE 2

SCHEMATIC DRAWING OF MONOCHROMATOR

The drive system is single-speed for any one installed gear cluster: the furnished cluster causes the wavelengths between 1.5 and 25 microns to be scanned at a constant rate in 4.9 minutes.

The entrance, center, and exit slits of this instrument are always equal to each other, but may vary during the operating cycle. Initial setting of slits width is made and indicated by means of dial 0: Selection of cams may then be made to allow the mirror assembly drive to also control slits width such that constant linear slits width, constant band width, or constant $h\nu$ product are obtained at the exit slit. (All work during this project was done with constant slits widths.) The entrance and exit slits are curved for image curvature compensation.

The monochromator cover is gastight, hence suitable gases may be admitted directly to this portion of the optical path. Conversely, evacuation of this space to reduce carbon dioxide and water vapor absorption effects may be accomplished. Baffle plates within the cover serve to reduce stray radiation paths and attendant false energy at the detector when the cover is in place.

Overall rated energy transmission of this assembly is 11% at 15 microns. The manufacturer's data lists a theoretical resolution limit of 0.015 microns at 15 microns.

Figure 3 is a photograph of the monochromator with cover removed, showing size and arrangement details.

2. The Chopper and Reference Signal Generator

A means for system rejection of stray monochromator energy inputs and random direct current fluctuations in amplifier output is essential.

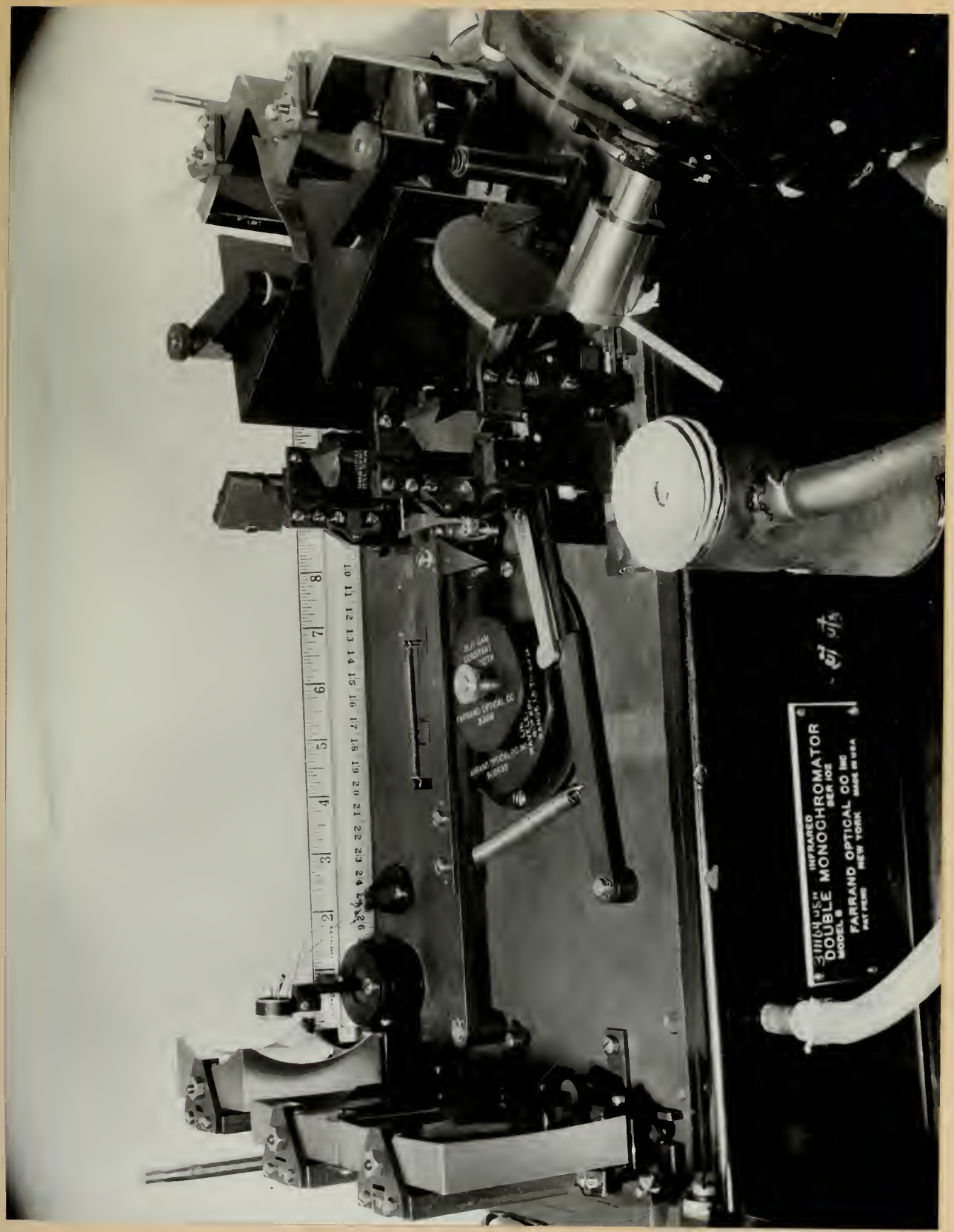

FIGURE 3

PHOTOGRAPH OF MONOCHROMATOR

The chopper and reference signal generator are fundamental units for this purpose.

The chopper consists of a radially segmented metal blade, with the first and third quadrants mirror-surfaced and the second and fourth quadrants cut away. This blade is mounted on the shaft of a 1200 rpm synchronous motor in such a position that radiant energy travelling the intended path between the source and monochromator entrance slit is alternately reflected to the entrance slit and allowed to be lost from the usable path. This chopper action, together with the smoothing effect of the detector time constant, results in the formation of a 40 cps detector response which is essentially a sine wave. The energy delivered to the entrance window is of course a fixed portion of the source energy for any particular wavelength.

The same synchronous motor which turns the chopper blade is also used to rotate a commutator assembly which is so arranged that a fixed external battery voltage is caused to form a 40 cps square wave of constant magnitude. This assembly is known as the reference signal generator.

Means are provided for shifting the commutator brush rigging of the reference signal generator so as to put the reference signal in proper phase with respect to the detector signal. The amplified detector signal is filtered to reject all except 40 cps components, and is mixed with the reference signal at the discriminator input to permit discriminator response proportional to the magnitude of the detector signal and to the degree that the detector and reference signals approach

zero and 180 degrees phase relationships.

3. The Bolometer and Amplifier

The detector provided with this system is a Baird Associates, Inc. bolometer with a silver chloride window, 2.77 ohms resistance, and rated performance characteristics as follows:

Time constant - 0.003 second

Response - 0.3 rms volts per peak watt

Noise - 5×10^{-9} rms volts

The resistance changes of the bolometer due to incident radiant energy acting upon the thin blackened metallic sensitive element are utilized in the most common manner: a Wheatstone bridge arrangement with a fixed battery voltage across one diagonal is tapped across the opposite diagonal for a signal voltage proportional to the bolometer resistance change.

Figure 4 is a schematic presentation of the amplifier circuit. The signal voltage from the bridge network is passed via a high-gain transformer to two conventional resistance-coupled amplifying stages, after which a narrow 30-50 cps bandpass filter acts to suppress all but the principal 40 cps signal generated by chopper interruption of the input energy. The filtered signal is resistance-coupled to a third amplifying stage, coupled via a gain-control potentiometer to a fourth amplifying stage, and finally resistance-coupled to a phase-splitting stage which develops similar but opposite-phased 40 cps signals across matched plate and cathode follower resistances.

All stages are intended to operate Class A. The input transformer

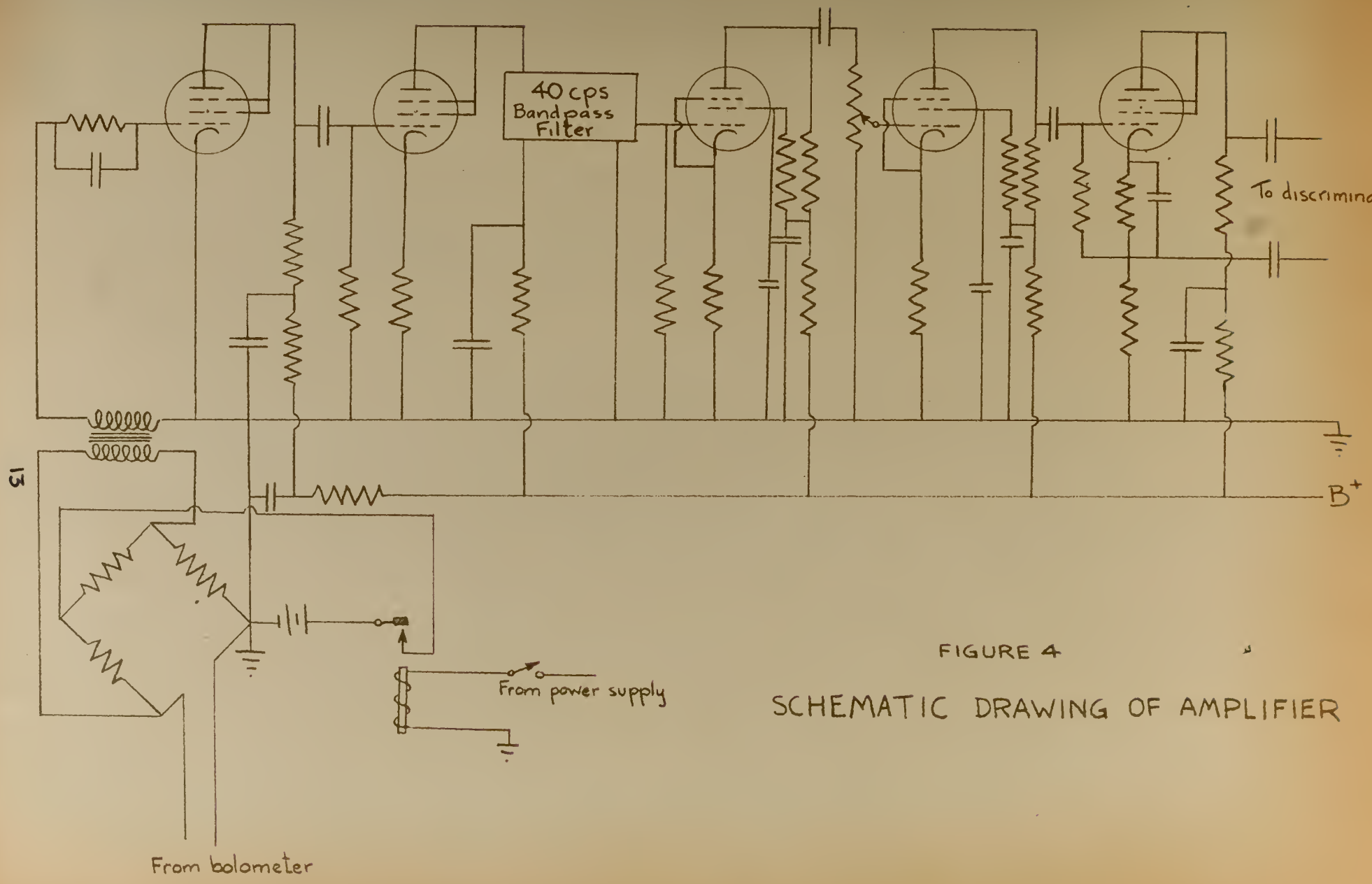

FIGURE 4

SCHEMATIC DRAWING OF AMPLIFIER

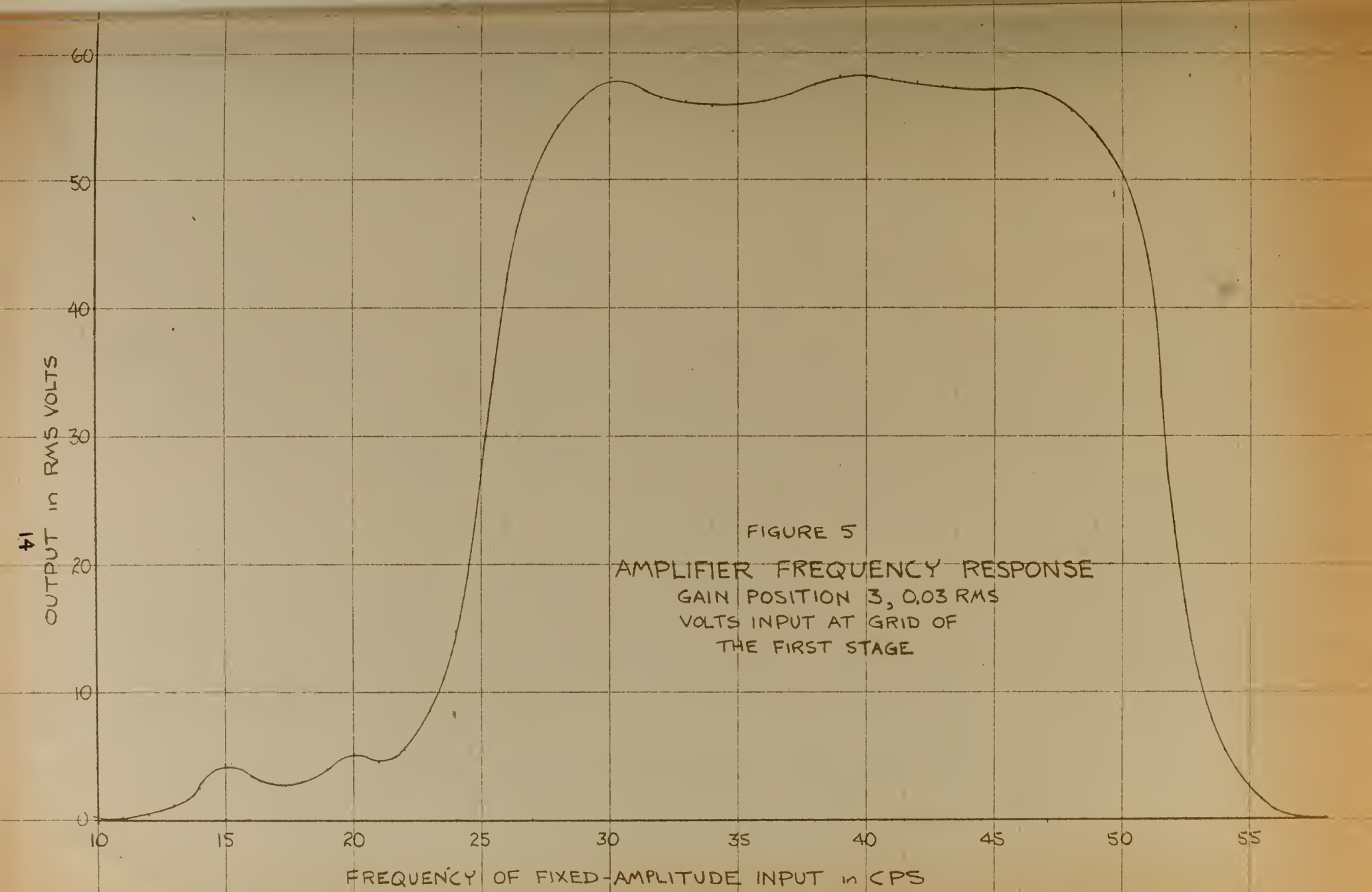

FIGURE 5

AMPLIFIER FREQUENCY RESPONSE

GAIN POSITION 3, 0.03 RMS VOLTS INPUT AT GRID OF THE FIRST STAGE

and filter are specially constructed and are heavily shielded against stray electromagnetic effects. A solenoid circuit is provided such that the bolometer battery voltage is removed when the amplifying system is off or when a manually operated switch is used to reduce bolometer heating effects between periods of actual use.

A frequency response curve for the amplifier at nominal gain was obtained by applying 0.03 rms volts between ground and the grid of the first stage, using various frequencies from a test oscillator, and measuring rms volts across the push-pull output leads. Results are depicted by Figure 5 and reveal the excellence of the rejection of signals appreciably different from 40 cps.

4. The Power Supply and Discriminator

The power supply and discriminator are built within the same chassis and are schematically represented by Figure 6. Conventional techniques are used for the generation of rectified and filtered filament voltages, regulated and filtered plate voltages, and a voltage to operate the previously-described bolometer battery solenoid.

The amplifier and reference generator signals are combined at the grid inputs to the first stage of the discriminator such that in-phase reinforcement of signals occurs on one side of the symmetric arrangement and opposing signals 180 degrees out of phase are presented at the opposite grid. The direct current component of cathode follower voltage differences is directed to a balanced amplifying stage and the output to the recorder is taken across matched triode plate leads for that stage. The tendency of the discriminator to reject effects due to direct cur-

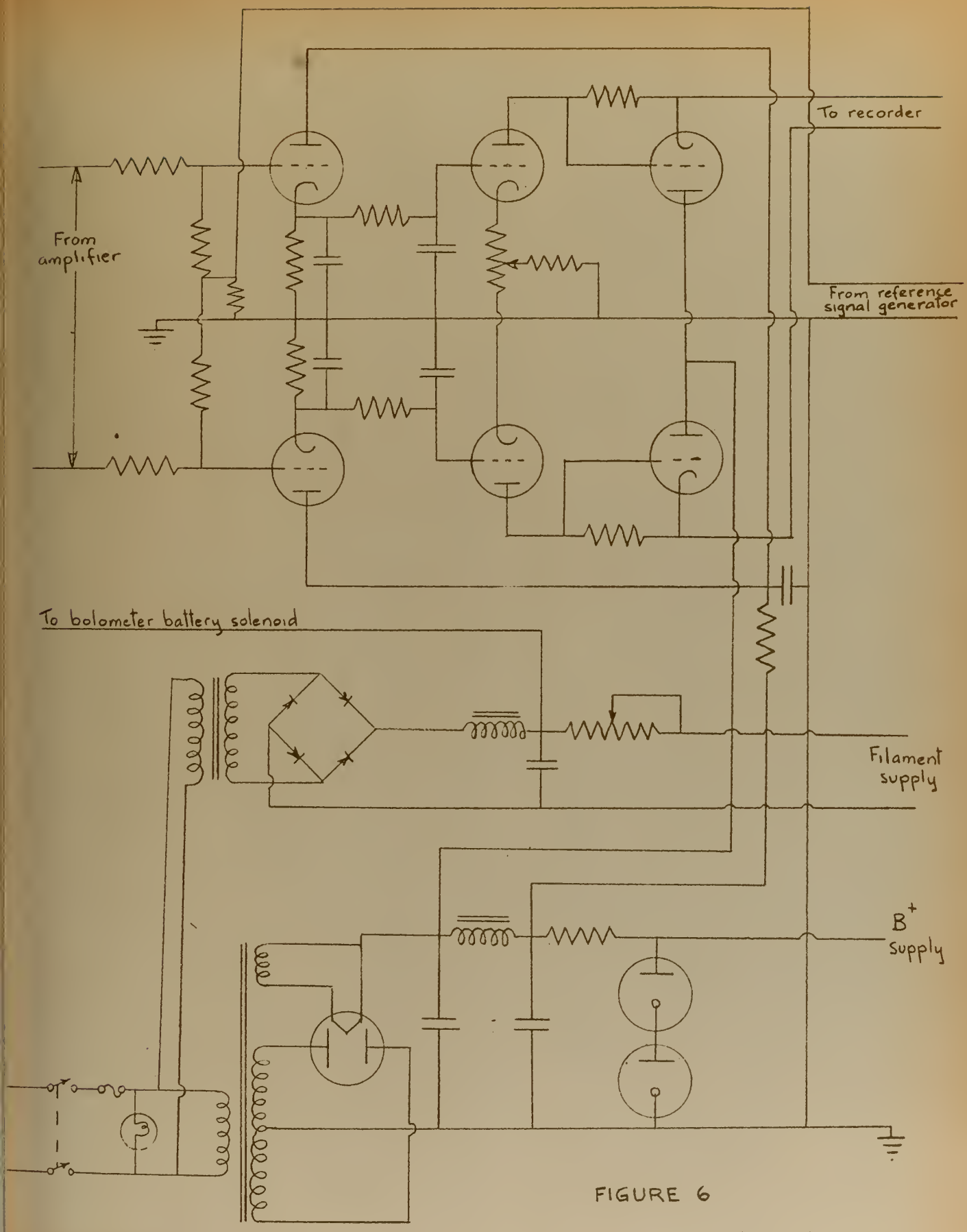

FIGURE 6

SCHEMATIC DRAWING OF
POWER SUPPLY AND DISCRIMINATOR

rent changes in the amplifier output and the need for careful phase adjustment between the amplifier and reference generator signals are apparent.

A determination of the linearity of direct current discriminator response relative to various rms voltage magnitudes of 40 cps input was made, since recorder traces would be expected to accurately reflect the magnitude of signals developed at the bolometer. Figure 7 presents the data obtained, using approximately 2 ohms output shunting resistance (see Section 5 following), and reveals fair linearity of response.

5. Auxiliary Components

a. Source Holder and Outer Fixed Mirror

A refractory-lined chamber with a cored metal jacket is provided for mounting and reducing the indirect heating effects of various sources. Hoses were connected to admit a cooling agent to the core and it was found that water or other liquids could not be used, due to leakage problems which could not be overcome except by manufacture of a replacement holder. Compressed air was therefore provided as a cooling agent and was found to be satisfactory for the sources used.

A fixed concave gold-surfaced mirror is mounted off-axis to direct rays emerging from a round hole in the source holder to the chopper blade, thence to form an image of the source at the monochromator entrance slit.

b. Temperature Control System

The originally-received system included a large Plexiglass

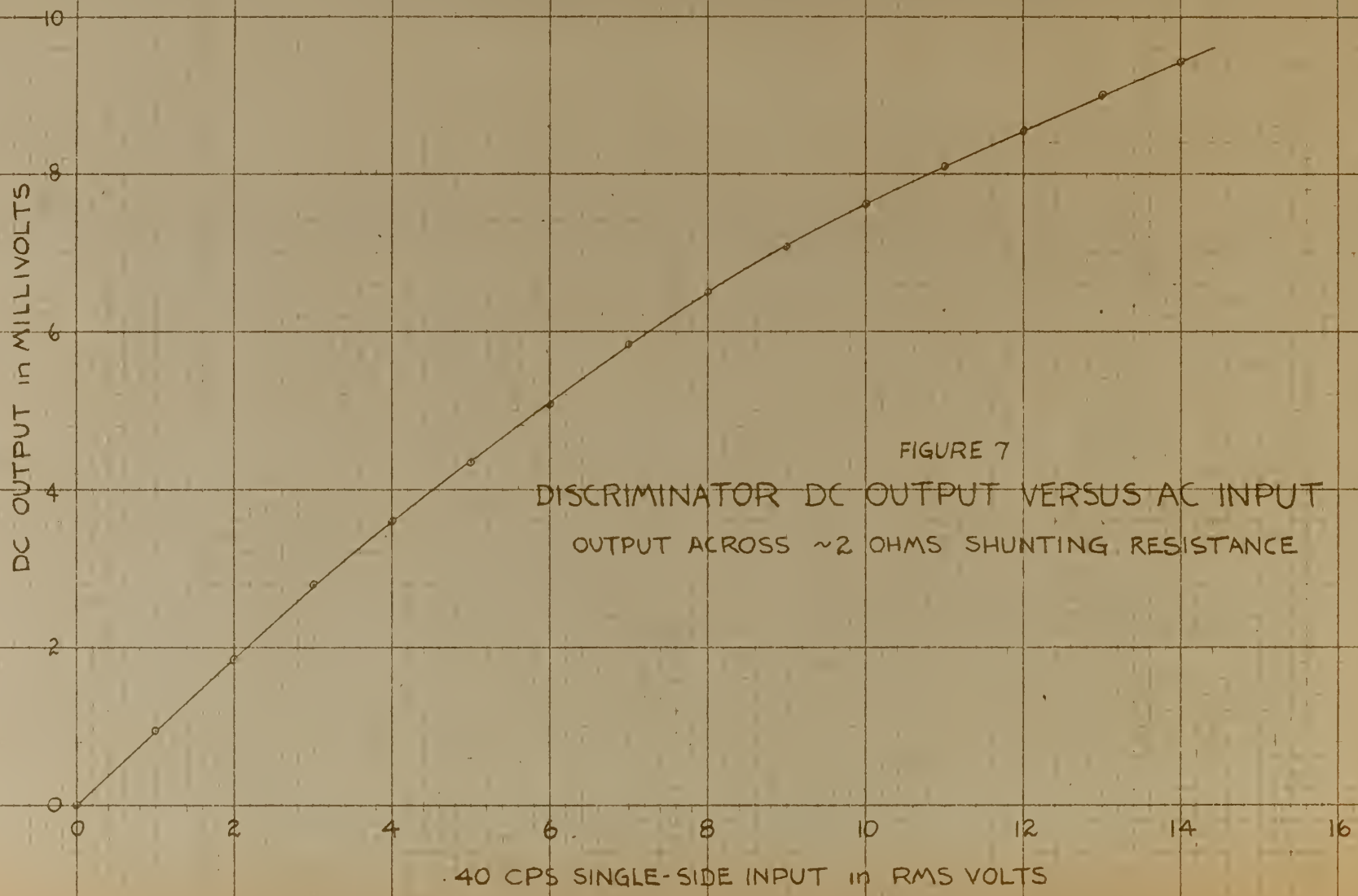

FIGURE 7

DISCRIMINATOR DC OUTPUT VERSUS AC INPUT

OUTPUT ACROSS ~2 OHMS SHUNTING RESISTANCE

enclosure surrounding the monochromator and those accessory units also mounted on its heavy steel foundation, as well as the amplifier, placed underneath the monochromator foundation. The only apparent use of this enclosure was as a dirt and moisture safeguard when the equipment was idle, since various essential controls were inoperative when the enclosure was in place. A decision to utilize this outer casing to facilitate accurate temperature control of the monochromator region was made and was subsequently found to have been thoroughly justified.

The amplifier was removed from the enclosure to allow access to the gain control and bolometer voltage off-on switch and to permit operation at lower temperatures. Controls for operation of the chopper-reference generator motor and the monochromator drive motor were relocated on a panel forming part of the constant-temperature enclosure. Access holes with sliding covers were provided for reach-rod operation of the slits width control and for insertion of a crank for manual operation of the wavelength drive system. Cable and hose runs were modified to render the outer casing more nearly airtight.

A drying light circuit and thermostat-controlled relay were present in the original arrangement: these were used for temperature control within the enclosure. A small electric blower was rigged for the purpose of minimizing temperature gradients due to slow air circulation. Trays for calcium

chloride and soda lime were installed within the enclosure for the reduction of undesirable water vapor and carbon dioxide absorption effects along that part of the energy path outside of the monochromator casing.

It was anticipated that a Globar source operated at rated voltage within the air-cooled source holder would be used for most absorption observations. Since the equilibrium operating temperature using this source would be the highest of all expected sources, a determination was made of the heat transfer characteristics of the constant-temperature enclosure with this source in use. Figure 8 presents the data obtained and shows that equilibrium is reached 21.0°C above ambient temperature in approximately six hours. Irregularities in the data are attributed solely to differences in the rate of change of ambient and enclosure temperatures. A thermostat setting of 45.0°C was then selected on the basis that ambient temperature of the small room could be maintained below 24.0°C and thermostat control would thereby be preserved. (An enclosure temperature of 45°C was subsequently found to preserve thermostat control with Nernst glower operation, although the ballasting resistors used for those sources elevated ambient temperatures to about 30°C.). A 200-watt light was rigged in the vicinity of the source holder to act as a Globar simulator and help maintain temperature when the Globar was not in use.

An index mark was established on the thermostat control and

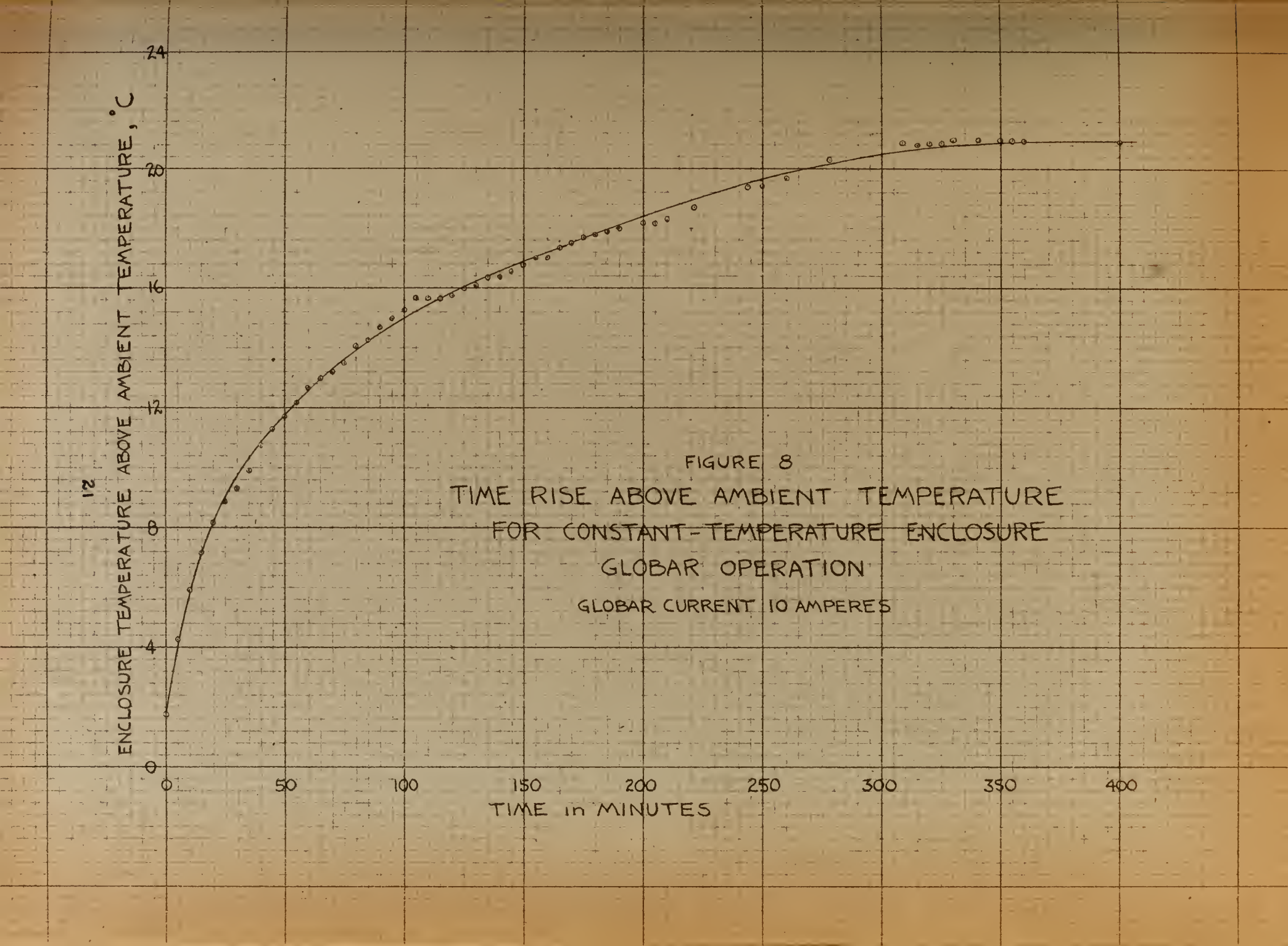

FIGURE 8

TIME RISE ABOVE AMBIENT TEMPERATURE
FOR CONSTANT-TEMPERATURE ENCLOSURE
GLOBAR OPERATION

GLOBAR CURRENT 10 AMPERES

experimentation revealed that + 17.5 marker intervals provided 45.0°C operation.

c. Recorder

The recorder selected for use with this system is the Leeds and Northrup Co. Speedomax Type G. Long periods of use revealed that the excellent time constant, sensitivity, and over-run characteristics of this recorder did not act as the limiting factor on system performance at any time. The wide flexibility of choice in signal strengths to yield full scale deflection and the ability of the recorder to withstand transient signals beyond full scale deflection values were found to make this recorder well suited for this system.

A gear combination to provide a recorder paper feed rate of 16 inches per minute was established: this is the maximum rate obtainable with the drive motor which is a part of this unit.

d. Hand Drive System

The motor-driven monochromator drive system has only one speed and is not reversible. It was found to be possible to remove one gear of the drive train and to attach a hand drive crank while the constant-temperature enclosure remained in place. Accordingly, a hand crank was fabricated and an access hole was provided. The following advantages were thereby gained:

(1) Observations of recorder stylus position or of waveforms and meter readings at any point in the system can be observed for a selected vernier wavelength. A series of

such observations can be used to obtain expanded presentations of spectral responses.

(2) The possibility of high drive speed limiting the effective resolution of spectral response details can be avoided.

(3) Examination of a limited wavelength region, search for a particular form of recorder response, or repeated runs for determination of optimum choice of equipment control settings can be accomplished much more quickly.

It is recognized that static observations might be expected to be different from those obtained at normal drive speed, and this effect was rather carefully investigated. Vernier wavelengths at which well-defined recorder responses occurred by the two methods were never observed to differ by more than 0.01 micron. (Lost motion equal to about 0.025 micron is apparent when the drive system is reversed, and care was taken to always approach vernier wavelength settings from the short wavelength direction.)

It is not possible to restore motor drive without lifting the constant-temperature enclosure. Foresight is therefore required in scheduling the use of hand drive observations relative to desired normal drive observations.

e. Vernier Wavelength Synchronizing Signal and Plate Load Shunting Resistor Circuit

A make-and-break cam-operated microswitch is attached to the monochromator wavelength drive shaft and it was desired to utilize this device to provide signals at the recorder which could be

associated with known positions of the wavelength vernier dial. The recorder is capable of providing only one trace, hence it was necessary to allow any such signals to be superimposed on the normal discriminator output, but only at such times that discontinuities in the recorder trace would be acceptable.

A discussion of the suitability of a variable shunting resistor across the discriminator output to the 6500 ohm recorder is given in Chapter IV.

Figure 9 depicts schematically the circuit which was evolved in response to these needs. The RC time constant for condensor charge and discharge is seen to be essentially independent of

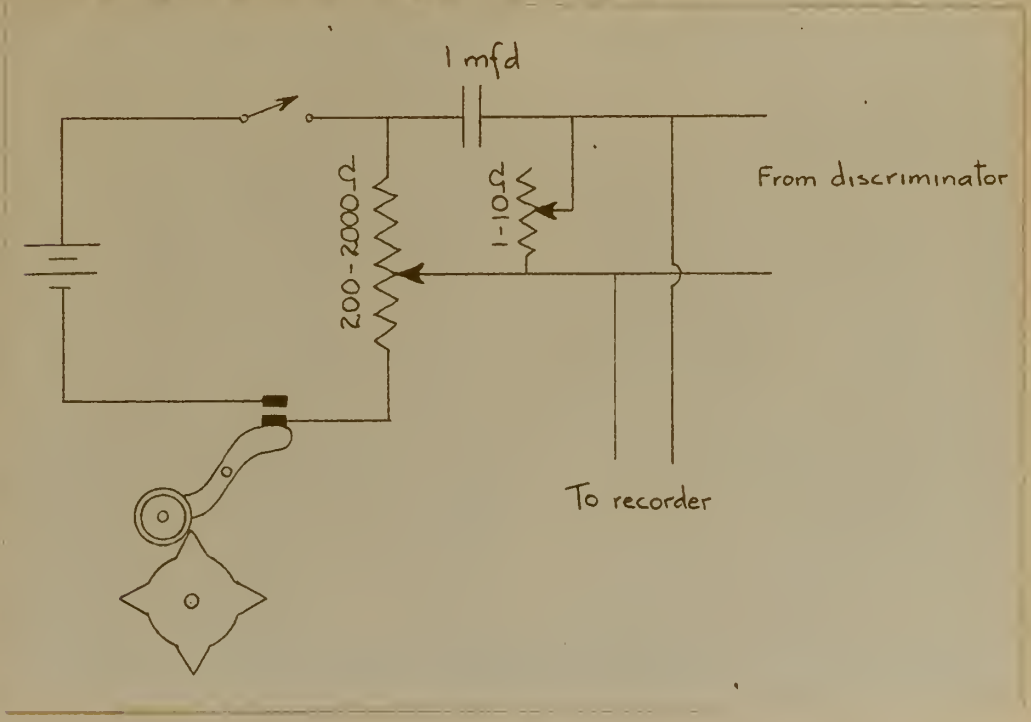

Figure 9
Schematic Drawing of Vernier Wavelength Synchronizing Signal and Plate Load Shunting Resistor Circuit

the plate load shunting resistance; conversely, the value set on that resistor is very nearly the net impedance seen as external

load by the discriminator.

The hand drive system was used to carefully determine the wavelength vernier positions corresponding to each differentiated pip created by the closing or opening of the cam-driven microswitch. Figure 10 is a table of these readings. It was found that cam action timing was essentially independent of drive speed for rates up to that of normal drive. Changes of these values due to mechanical wear or microswitch adjustment must be anticipated, however.

The recorder paper feed was found to be sufficiently uniform that linear interpolations between synchronizing signals one or two microns apart were accurate within the limits of interpolation accuracy.

f. Gas Sampling and Evacuation System

The space within the monochromator cover has two external connections. Suitable adaptors were fitted and hoses were led to these connections. Figure 11 is a schematic presentation of the gas sampling and evacuation system which was established. With this arrangement it is possible to:

(1) Evacuate the monochromator casing for observations with fixed minimum carbon dioxide and water vapor effects present along the external optical path only.

(2) Slowly bleed in a dried sample of selected gas to a measured pressure.

(3) Flush the gas sample with dry nitrogen to the external atmosphere.

Table of Vernier Wavelength Readings Corresponding to
Various Wavelength Synchronizing Signals
(All readings in microns)

1.611	5.409	9.422	13.221	17.236	21.035
1.660	5.672	9.471	13.485	17.285	21.299
1.922	5.722	9.735	13.535	17.549	21.349
1.972	5.986	9.784	13.797	17.599	21.609
2.235	6.035	10.048	13.848	17.859	21.659
2.285	6.298	10.098	14.108	17.909	21.922
2.548	6.348	10.359	14.159	18.172	21.972
2.598	6.609	10.409	14.422	18.222	22.235
2.858	6.660	10.672	14.471	18.485	22.285
2.909	6.922	10.721	14.735	18.535	22.549
3.172	6.972	10.985	14.784	18.798	22.599
3.222	7.236	11.035	15.048	18.848	22.858
3.485	7.285	11.299	15.098	19.109	22.909
3.535	7.549	11.349	15.358	19.159	23.171
3.798	7.599	11.610	15.409	19.421	23.221
3.848	7.858	11.660	15.672	19.471	23.485
4.108	7.909	11.922	15.722	19.734	23.535
4.159	8.172	11.972	15.986	19.784	23.797
4.422	8.222	12.236	16.035	20.048	23.848
4.471	8.485	12.286	16.299	20.098	24.108
4.735	8.534	12.549	16.349	20.359	24.159
4.784	8.797	12.599	16.609	20.409	24.422
5.048	8.848	12.859	16.660	20.672	24.471
5.098	9.108	12.909	16.922	20.722	24.735
5.358	9.158	13.172	16.972	20.986	24.784

Figure 10

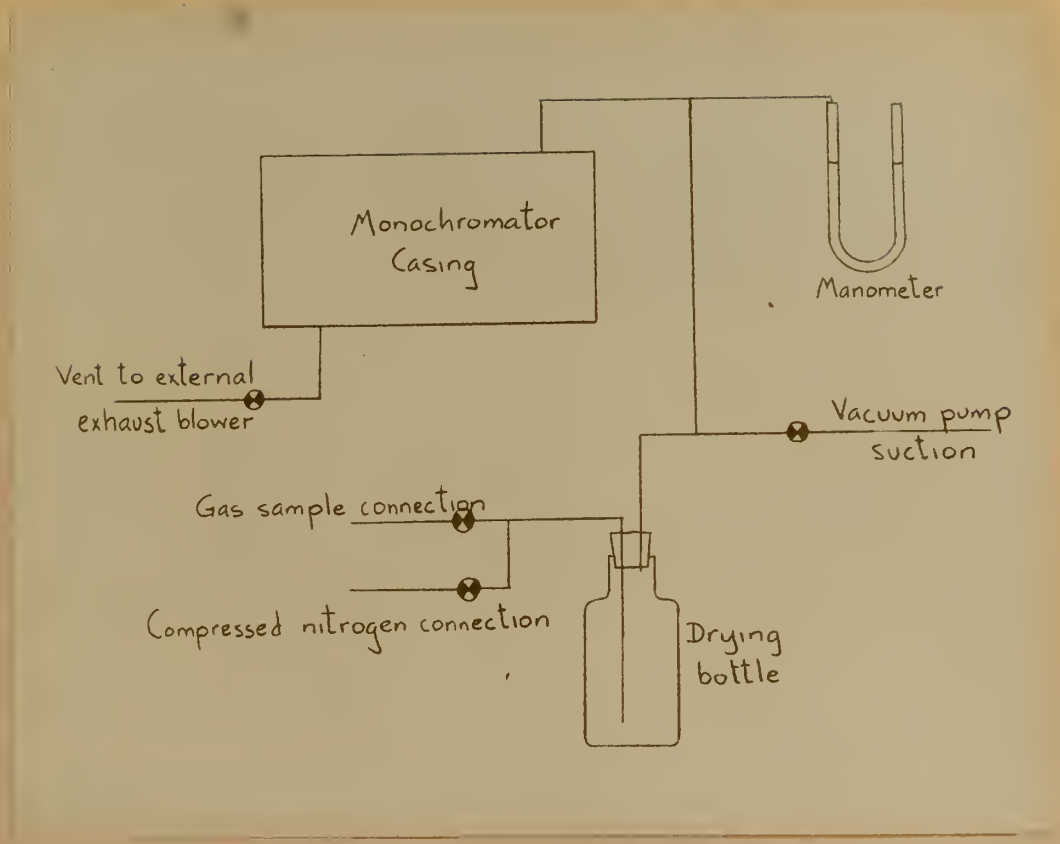

Figure 11
Schematic Drawing of Gas Sampling and Evacuation System

Figure 12, a photograph of the assembled system, shows many of the system components and may render the preceding descriptions more clear. The gas sampling and evacuation system and the power supply - discriminator chassis are below the field of view.

6. An Alternate Detector and Amplifier System: The Golay Unit

The Golay infrared detector is a wartime development invented by Dr. Marcel J. E. Golay of the Army Signal Corps Engineering Laboratories. Impressive practical problems were overcome in developing the detector, but the principle is simple. Infrared radiation passing through the

FIGURE 12

PHOTOGRAPH OF ASSEMBLED SYSTEM

rock salt entrance window falls upon an absorbing membrane mounted in the center of a small gas-filled chamber. Expansion of the gas due to heating of the membrane creates a pressure which is transmitted via a narrow duct to another gas-filled chamber, the top of which is covered by a small flexible mirror membrane. (The opposite side of this membrane is in a larger ballasting gas space: an analogy with the human ear is quite apparent.)

Light from an incandescent filament is passed through a lens system and a ruled grid and is then reflected from the mirror membrane to a photocell, again by way of the ruled grid. The amount of visible light reaching the photocell is determined by the degree of overlap between the grid and its own image from the flexible mirror. (The overlap is due to image blurring as the mirror changes radius of curvature, rather than by translation of the image pattern.)

A 10 cps chopper is used to interrupt incident energy in this system. The modulation of the light falling upon the photocell is utilized to create an electrical signal at the photocell and this signal is amplified and passed to a discriminating circuit not unlike that of the McDonald apparatus in principle. The "reference signal generator" in this system is a separate incandescent filament and photocell combination: the same chopper blade which interrupts the detected energy also interrupts the visible light between this filament and photocell. Analagous waveforms are thus generated, and proper phasing is accomplished by adjusting the position of the "reference generator" filament.

Rated performance characteristics of the detector are remarkably

high in view of the anticipated qualities of the original pneumatic action. Sensitivity and the time constant of response are strongly dependent upon the gas and gas pressure used in the pneumatic portion of the detector: a typical unit has a rated time constant of 3 milliseconds and an equivalent noise input of 0.014 ergs per second. Final output noise from the associated amplifier is rated less than 6×10^{-11} watts.

Figure 13 is a photograph of the Golay unit. The chopper-"reference generator" assembly is shown mounted directly in front of the detector: it is more efficient in practice to put this unit close to the source or at the monochromator entrance window.

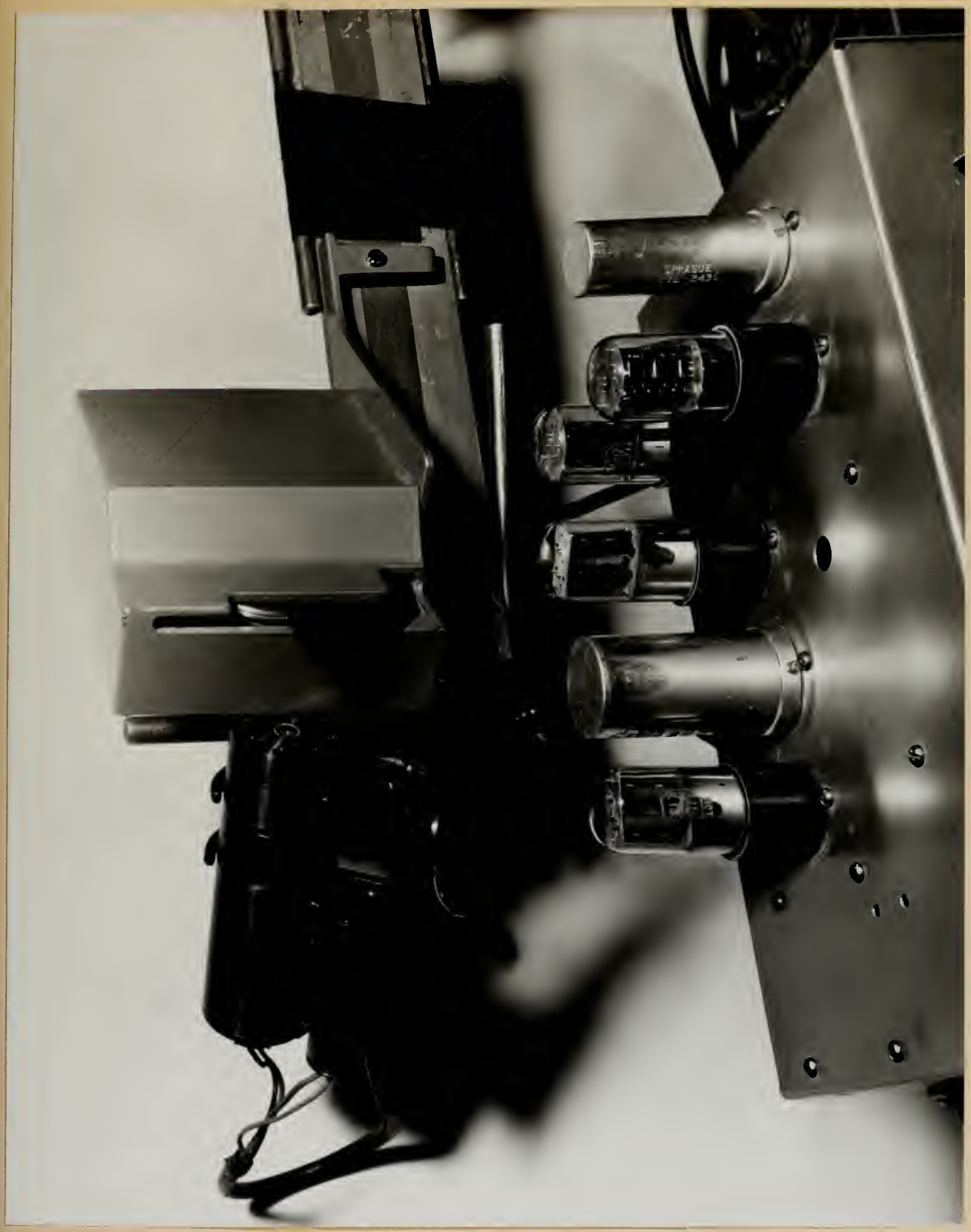

FIGURE 13

PHOTOGRAPH OF GOLAY UNIT ASSEMBLY

CHAPTER III

THEORY AND PRELIMINARY REMARKS

1. Theoretical Resolution Limits for the Monochromator

Data for the index of refraction of potassium bromide at 25°C and in the wavelength range of interest was obtained from Gundelach (11) and is presented by Figure 14. Data for the rate of change of index of refraction with temperature, $\frac{dn}{dt}$, is also available for the general region, but not as a specific function of wavelength. It will therefore be assumed that at operating temperatures of 45°C the curve of Figure 14 will undergo translation without appreciable alteration of shape. In any event, the primary purpose of determination of theoretical resolution limits is to gain an appreciation for the approximate values involved at various wavelengths.

The Rayleigh criterion of resolution leads to the formula for resolving power R of a simple prism:

$$R = B \frac{dn}{d\lambda},$$

where B is twice the mean prism thickness traversed by the dispersed beam and $\frac{dn}{d\lambda}$ is the rate of change of index of refraction with wavelength, the slope of a curve such as Figure 14 at a particular wavelength. (B is the same for a single simple prism or a series of simple prisms if the mean distances travelled through the dispersing media are the same.) Now R is defined as $\frac{\lambda}{\Delta\lambda}$, the wavelength under consideration divided by the wavelength resolution limit at that wavelength. Hence it is apparent

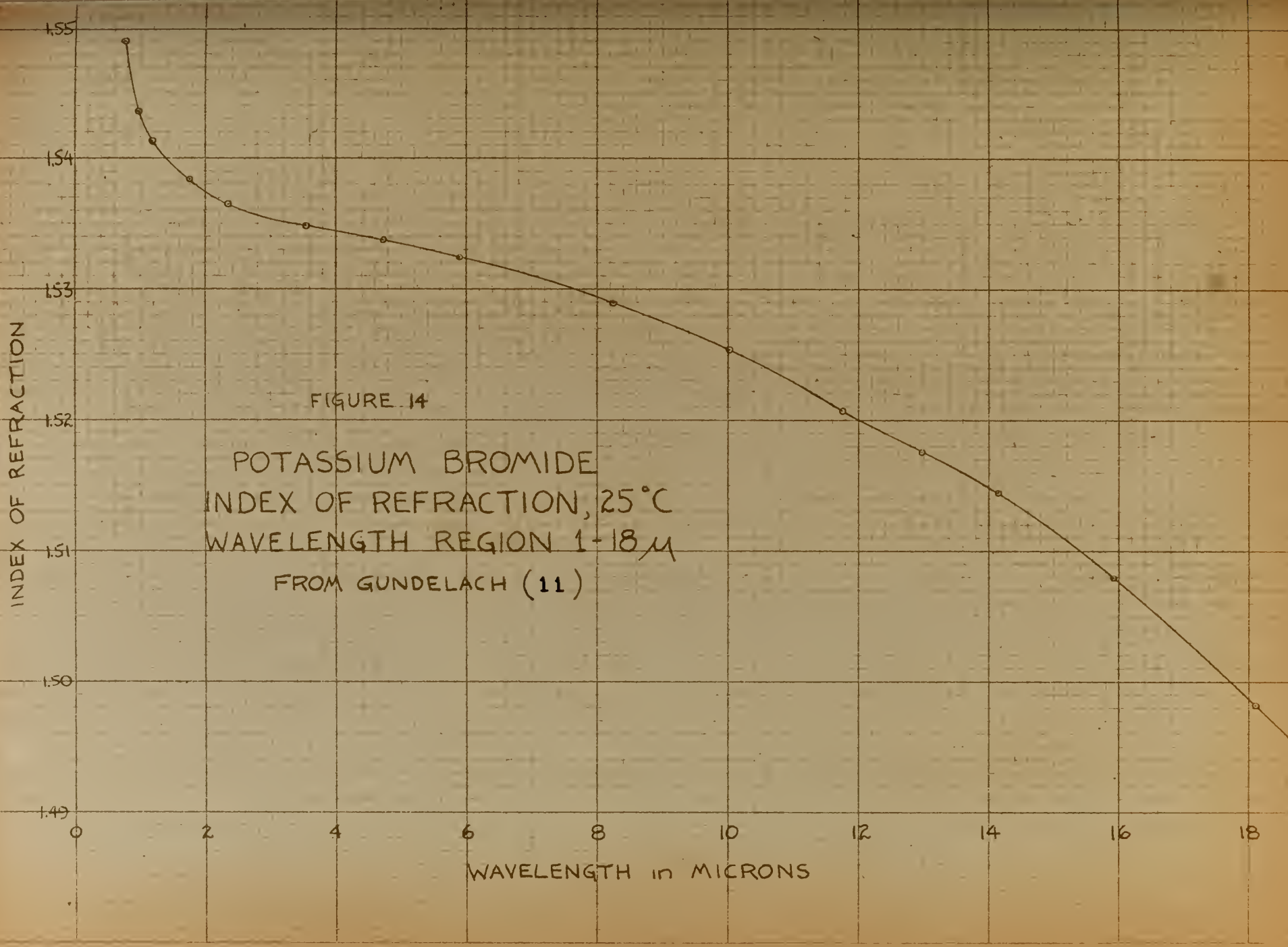

FIGURE 14

POTASSIUM BROMIDE
INDEX OF REFRACTION, 25°C
WAVELENGTH REGION 1-18 μ
FROM GUNDELACH (11)

that $\Delta\lambda = \frac{\lambda}{R} = \frac{\lambda}{B\frac{dn}{d\lambda}}$.

The wavenumber resolution limit $\Delta\nu$ in reciprocal centimeters may be calculated from the fact that $\nu = \frac{10^4}{\lambda}$ or $|\Delta\nu| = \frac{10^4}{\lambda^2}\Delta\lambda$, where the wavelength λ is expressed in microns.

$$\text{Thus } |\Delta\nu| = \frac{10^4}{B\lambda\frac{dn}{d\lambda}}.$$

An assumption that a mean value of 80% of the prism face widths are actually utilized in the four dispersions through the 8.4 centimeter equilateral prisms of this monochromator appears to be reasonable and leads to coincidence with the manufacturer's stated theoretical resolution limit of 0.015 microns at 10 microns. Calculated values of $\Delta\lambda$ and $\Delta\nu$, based on this assumption, the preceding formulae, and slopes obtained from Figure 14 are shown below:

λ, microns	$\frac{dn}{d\lambda}$, microns^{-1}	R	$\Delta\lambda$, microns	$\Delta\nu$, centimeters^{-1}
1.5	0.0049	1320	0.0011	5.1
2	0.0033	885	0.0023	5.6$^+$
3	0.0012	325	0.0092	10.3
4	0.0009	240	0.017$^-$	10.4
5	0.0010	270	0.018$^+$	7.4
6	0.0012	325	0.018$^+$	5.1
7	0.0015	405	0.017$^+$	3.5

λ, microns	$\frac{dn}{d\lambda}$, microns^{-1}	R	$\Delta\lambda$, microns	$\Delta\nu$, centimeters^{-1}
8	0.0018	485	0.017^{-}	2.6
9	0.0021	565	0.016	2.0^{-}
10	0.0024	645	0.015^{+}	1.6^{-}
11	0.0026	700	0.016^{-}	1.3
12	0.0025	670	0.018	1.2^{+}
13	0.0024	645	0.020	1.2
14	0.0029	780	0.018	0.9
15	0.0035	940	0.016	0.7
16	0.0041	1100	0.015^{-}	0.6^{-}
17	0.0045	1210	0.014	0.5
18	0.0047	1260	0.014	0.4

These values are presented graphically by Figure 15.

2. Factors Affecting the Ultimate Recorder Presentation of Spectra

a. Resolution

The effective resolution of the system, ordinarily determined by the width of the monochromator exit slit, has a very considerable effect upon the recorder presentation of spectra. As the bandwidth of wavelengths simultaneously passed by the exit slit increases, existing irregularities of the true spectrum are smoothed, of course. Of more importance is the fact that the apparent position of distinctive spectral characteristics will shift according to the resolution. The best way of demonstrating the existence of this effect is perhaps by means of a simple sketch,

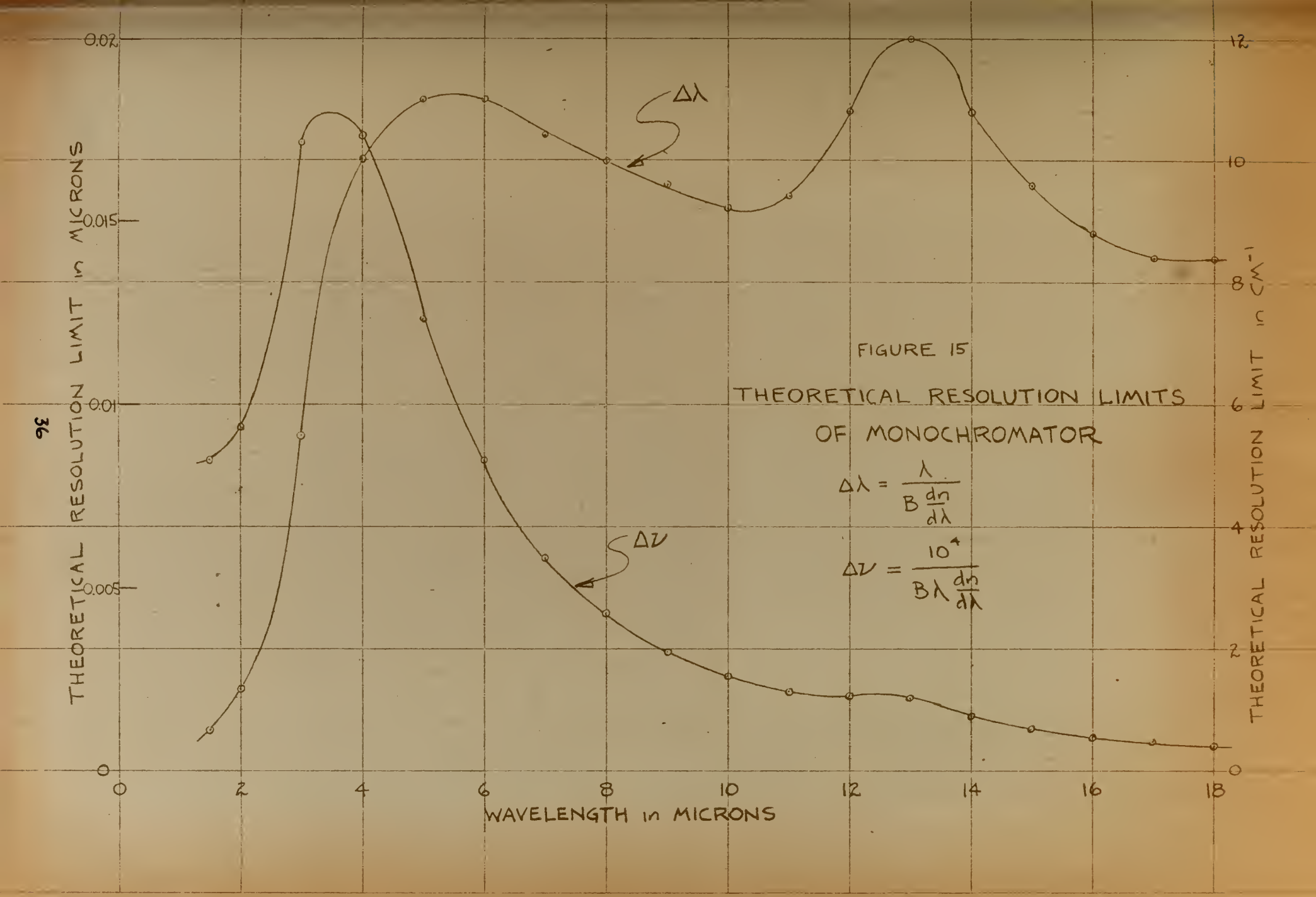

FIGURE 15

THEORETICAL RESOLUTION LIMITS OF MONOCHROMATOR

$$\Delta\lambda = \frac{\lambda}{B\frac{dn}{d\lambda}}$$

$$\Delta\nu = \frac{10^4}{B\lambda\frac{dn}{d\lambda}}$$

Figure 16, and a non-rigorous analysis.

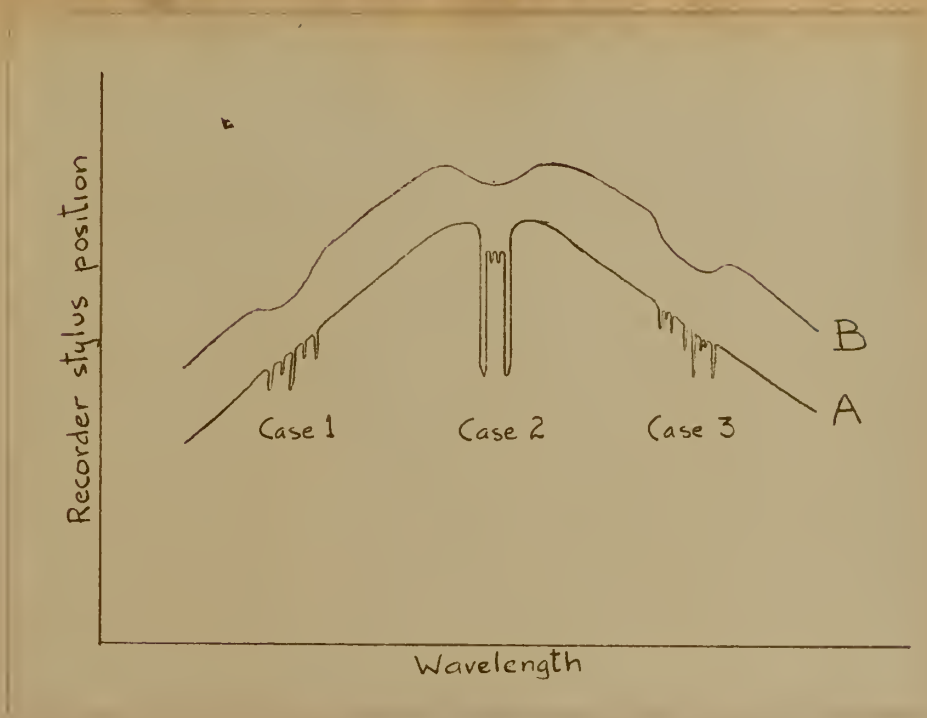

Figure 16

The Effect of Resolution on the Apparent Position of Spectral Characteristics

Imagine that curve A represents a true existing absorption spectrum. Since the detector will respond according to the mean energy being received across the bandwidth which it "sees", a low-resolution presentation of the same spectrum would appear similar to curve B. Three distinct cases are apparent:

Case 1: A symmetrical band spectrum in a region of unsymmetric source energy, leading to a shift of the apparent band center toward the lower source energy wavelengths. This effect may be compensated by calculating the transmittance or absorbance, whereby the absorption effect is expressed as a fraction of incident energy.

Case 2: A symmetric band spectrum in a region of symmetric or constant source energy. No shift of the apparent band center occurs for this case.

Case 3: An unsymmetric band spectrum. Generally, a shift occurs which is dependent on the center of gravity of absorption dips present within the existing bandwidth. A precise compensation for this effect is not practicable for the very complex unsymmetric absorption bands usually found.

Many infrared spectrometers provide a device which regulates the source energy monochromator input so that it is constant over a selected range of wavelengths. Other spectrometers exist which continuously determine the energy transmitted along each of two paths, one of which includes the absorption sample chamber, while the other path includes an evacuated chamber identical to the sample chamber. Electronic or other means are then used to compute the ratio of the energies along the two paths and the output is directly related to transmittance or absorbance.

Since this spectrometer system includes neither of the just-described refinements, calibration data will be based on symmetric absorption bands whenever feasible. Conversion of spectra dips to curves related to absorbance will normally be accomplished where Case 1 or Case 3 apply.

This discussion is obviously equally applicable to cases where the characteristic spectral region is a maximum due to filter action or emission spectra.

b. Unsymmetric Source Energy Distribution in the Wavelength Vicinity of Symmetric Spectral Characteristics

The conversion of spectral maxima and minima to transmittance or absorbance factors does not completely compensate for the effects of Case 1 preceding. This fact is demonstrated by Figure 17 and an analytical approach for absorption minima as follows:

Let y_1 represent the ordinates of unabsorbed source energy recorder response, assumed to form a straight line, $y_1 = k_1\lambda$.

Let y_3 represent the ordinates of recorder response with absorbant present.

Let A represent absorbance as a function of wavelength, typified by a parabolic curve with true wavelength center c, maximum absorbance factor m, and latus rectum width k_2.

Then $y_3 = y_1(1 - A)$.

And the assumed absorption curve characteristics are expressed by: $(\lambda - c)^2 = k_2(m - A)$.

Thus $A = m - \frac{(\lambda - c)^2}{k_2}$ with $m \leq 1$ and $A \geq 0$ as additional limitations.

and $y_3 = k_1\lambda\left[1 - m + \frac{(\lambda - c)^2}{k_2}\right]$.

or $y_3 = k_1\left[\lambda - m\lambda + \frac{\lambda^3}{k_2} - \frac{2c\lambda^2}{k_2} + \frac{c^2\lambda}{k_2}\right]$.

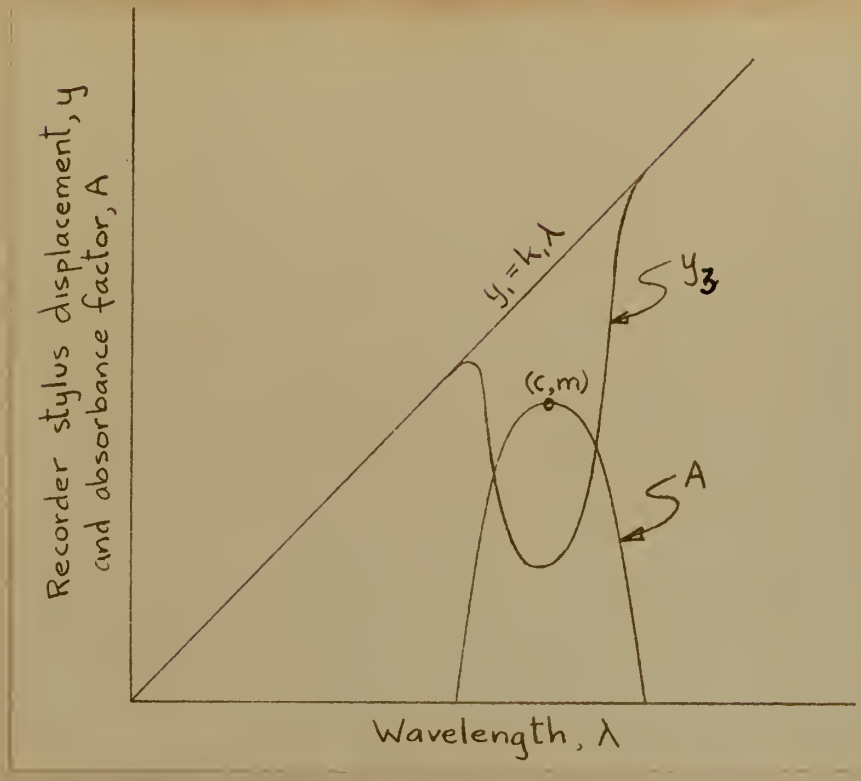

Figure 17
The Effect of Unsymmetric Source Energy Distribution in the Wavelength Vicinity of Symmetric Spectral Characteristics

Minimum y_3 occurs when $\frac{dy_3}{d\lambda} = 1 - m + \frac{3\lambda^2}{k_2} - \frac{4c\lambda}{k_2} + \frac{c^2}{k_2} = 0$.

or $\lambda^2 - \frac{4c\lambda}{3} + \frac{c^2}{3} + \frac{k_2}{3} - \frac{mk_2}{3} = 0$.

or $\lambda = \frac{\frac{4c}{3} \pm \sqrt{\frac{16c^2}{9} - 4\left(\frac{c^2}{3} + \frac{k_2}{3} - \frac{mk_2}{3}\right)}}{2}$

$= \frac{2c}{3} \pm \sqrt{\frac{c^2}{9} + \frac{k_2}{3}(m-1)} < c$ for $m < 1$ or $k_2 \neq 0$.

For cases where $m = 1$ or $k_2 = 0$:

$$\lambda = \frac{2c}{3} \pm \sqrt{c^2/9} = c, \cancel{c/3}$$

(A second derivative test shows c/3 to be a maximum and the requirement $m \leq 1$ leads to an unlikely further condition for its existence, $k_2 \geq 4c^2/9$.)

It is thus apparent that the minimum value of y_3 will generally occur at the true position of maximum absorption only if 100% absorption occurs ($m = 1$) or the absorption band has zero width ($k_2 = 0$). Neither of these conditions are realizable in practice, but due attention is to be paid toward approaching these conditions where possible.

It is also apparent that the actual y_1 curve for a source spectrum without strong irregularities may be approximated by a straight line provided the region of absorption dip be narrow. It is to be noted that the amount of shift of the minimum is independent of k_1, the slope of the unabsorbed source energy curve, provided λ values be expressed in terms of abscissa distance from the point of ky_1 ordinate is zero.

A similar discussion may be readily applied to filter maxima, leading to the desirability of maximum transmittance and a minimum bandwidth of passed wavelengths in the characteristic region.

c. Contaminating Absorbants

With this system, the effects of carbon dioxide and water vapor absorption are continuously present. In the presence of

these or other contaminating absorbants, the previously-discussed problem becomes modified as follows:

Let y_1 represent the ordinates of unabsorbed source energy recorder response as before.

Let y_2 represent the ordinates of recorder response with contaminating absorbant(s) only present.

Let y_3 represent the ordinates of recorder response with contaminating absorbant(s) and sample absorbant present.

In practice, the y_2 curves are to be observed with a minimum amount of contaminating absorbants in the constant - temperature enclosure and an evacuated monochromator casing, while the superimposed y_3 curves are to be obtained with the same contaminating absorbant concentrations in the outer enclosure and a pure absorbant sample within the casing or an absorbant film placed in the external path. No complicating factor due to partial replacement of one absorbant by another is introduced by this procedure.

Now at any wavelength the net transmittance factor for the entire path is the product of the transmittance factor for energy passage through contaminating absorbants outside the monochromator casing and the transmittance factor for energy passage through the sample absorbant within the monochromator casing. (A constant transmittance factor associated with passage through the evacuated monochromator may be omitted from consideration.) It is therefore readily deducible that the absorbance factor for the sample, A, equals $1 - \frac{y_3}{y_2}$ or $\frac{y_2 - y_3}{y_2}$.

For any cases in which the effect of contaminating absorbants is negligible in the immediate wavelength region of interest, it is proposed to make only the y_3 recording. Then $A = \frac{y_1 - y_3}{y_1}$. A true and complete y_1 curve is not readily obtained, due to the continuously present contaminating effects. However, since the determination of absorbance peak locations but not magnitudes are to be carried out in this project, a pseudo-absorbance factor, A_s, will be determined for these cases such that $A_s = \frac{ky_1 - y_3}{ky_1}$, where k is a constant of unspecified magnitude for the determination of each absorbance curve. In this manner, a single representative spectral response curve for a source may be taken at low resolution, estimated compensations for contaminating influences faired in, and a table of ky_1 values made in arbitrary units. In subsequent determinations of A_s using the same source, these tabulated values of ky_1 may be plotted to an arbitrary scale in the vicinity of interest and used.

d. Monochromator Drive Speed

It is obvious that there exists a maximum rate at which any spectrum may be scanned without the response time of the detector, characteristics of the amplifier and discriminator, or the response time of the recorder either limiting the effective resolution or causing irregular displacements of spectral characteristics. It is considered most practical to determine experimentally whether or not the fixed monochromator motor drive speed is causing these effects with any particular spectrum.

3. The Christiansen Filter

The Christiansen filter consists of a powder of crystalline or glassy substance suspended in a transparent medium. At those wavelengths at which equality of indices of refraction for the powder and medium exists, the suspension is optically homogeneous and transmits maximum energy. The transparent medium may be a liquid contained in a transparent cell or may be air, with the powder mounted on a thin transparent film in direct contact with air. Various combinations of powder and suspension medium yield characteristic transmission frequencies in the ultraviolet, visible, or infrared regions. There may be several transmission frequencies for a particular filter, depending upon the number of intersections of the curves of refractive index.

Since the variation of index of refraction with temperature is generally different for the two components of the filter, the transmission frequencies are temperature-dependent. It is to be noted that the transmission frequencies are not dependent upon the percentage composition of the mixture, although the maximum transmittance may be expected to vary with composition.

When using the filter as a calibration device, it is desirable that a sharp, well-defined transmission peak be used. This property is dependent upon a large angle of intersection between the curves of refractive index and upon the size of the powder particles. Optimum particle size is slightly more than the wavelength of the transmission peak. The presence of many smaller particles will lead to the filter being semi-opaque due to diffusion effects over a wide range of frequencies below the peak frequency, while numerous particles appreciably

larger than required will simply exert a larger true absorption effect at all frequencies.

Since the rejection of wavelengths either side of the transmission peak is due to refractive scattering, maximum efficiency will be obtained if incident energy is normal to the filter surface and only that energy emerging nearly normal to the filter surface is allowed to reach the detector.

4. Line Emission Spectra

The defined short wavelength limit of the infrared spectrum includes line emission and absorption effects due principally to electron changes of orbital quantum number. Infrared emissions of this type correspond to changes in low energy states of atoms, ordinarily occupied by a significant number of electrons only under conditions of strong excitation. Electric arcs in media of certain ionized atoms yield moderately intense emission spectra in this region: arc tubes available and yielding suitable emissions of wavelength greater than 1.5 microns include helium (2.0581 and 4.0450 microns), hydrogen (1.8751, 2.6300, 4.0500, and 7.4000 microns), mercury (a number of mild emissions below 3.7 microns and strong emissions at 3.9425 and 4.0159 microns), and sodium (1.8459 and 4.0449 microns).

These emissions are advantageous for calibration purposes because of the simplicity of their spectra and the accuracy with which they are known. On the other hand, the total energy represented by any one emission line is small and glass or quartz envelopes for the arcs are characterized by a marked decrease in transmittance as the infrared

larger than required will simply exert a larger true absorption effect at all frequencies.

Since the rejection of wavelengths either side of the transmission peak is due to refractive scattering, maximum efficiency will be obtained if incident energy is normal to the filter surface and only that energy emerging nearly normal to the filter surface is allowed to reach the detector.

4. Line Emission Spectra

The defined short wavelength limit of the infrared spectrum includes line emission and absorption effects due principally to electron changes of orbital quantum number. Infrared emissions of this type correspond to changes in low energy states of atoms, ordinarily occupied by a significant number of electrons only under conditions of strong excitation. Electric arcs in media of certain ionized atoms yield moderately intense emission spectra in this region: arc tubes available and yielding suitable emissions of wavelength greater than 1.5 microns include helium (2.0581 and 4.0450 microns), hydrogen (1.8751, 2.6300, 4.0500, and 7.4000 microns), mercury (a number of mild emissions below 3.7 microns and strong emissions at 3.9425 and 4.0159 microns), and sodium (1.8459 and 4.0449 microns).

These emissions are advantageous for calibration purposes because of the simplicity of their spectra and the accuracy with which they are known. On the other hand, the total energy represented by any one emission line is small and glass or quartz envelopes for the arcs are characterized by a marked decrease in transmittance as the infrared

region is entered.

5. Absorption Spectra

The phenomena of molecular band spectra have been discussed. Absorption media which can be readily utilized for calibration of this system include gases and thin films, subject to the following conditions:

a. The absorption media must be non-toxic, relatively pure, and locally available.

b. Gas samples must not interact appreciably with the steel, gold, rubber, silver chloride, or potassium bromide of the monochromator and must be readily separable from water vapor.

c. Absorption bands used for calibration should preferably be symmetric.

d. Absorption bands used for calibration must be accurately described by available publications, preferably with the aid of a graphical or recorder presentation of the entire region of interest.

e. Absorption bands should be selected at appropriate intervals throughout the range of calibration.

On the basis of fulfilling an optimum combination of the preceding conditions, carbon dioxide, ammonia, and methane gases and a thin film of nitrocellulose (collodion) were selected for use.

6. Interference Fringes of Equal Chromatic Order

The use of two infrared-transparent flat surfaces, spaced a small fixed distance apart in air to generate multiple reflection interference effects, provides a calibration device with a unique advantage: if only several wavelength calibration points be otherwise obtained with accuracy,

a series of evenly-spaced and equally accurate points may be obtained across the entire wavelength range of the monochromator with a minimum of manipulative procedures.

The elementary approach to transmitted energy interference fringes of equal chromatic order generated by a multiple reflection device leads to interference maxima of order m such that $m\lambda$ equals twice the separation distance of the parallel reflecting surfaces, t, (for normal incidence and reflection). In practice, this approach leads to inaccuracies of the order of one percent, due to the assumption that phase changes at media discontinuities are zero or 180 degrees. For purposes such as intended here, it is expedient to use an equation $m\lambda = 2t + f\lambda$ and to determine f experimentally. If the reflecting surfaces be freshly silvered, a paper by Koehler (13) indicates that f may be expressed satisfactorily as a linear function $f = f_o + b(\lambda - \lambda_o)$, where f_o is the phase shift coefficient at a wavelength λ_o ; that f_o and f will lie between 0.9 and 1.0, and that the coefficient of wavelength dependence, b, will be quite small for the infrared region.

The determination of the separation distance t and the phase shift coefficient f may therefore be experimentally determined by the use of monochromatic light at a number of wavelengths in the visible region and at several wavelengths in the infrared. Provided Koehler's experimental observations for the linear wavelength dependence of f in the visible region is found to extend as expected to the infrared region, a multiplicity of calibration points may then be obtained.

A simple calculation reveals that a separation of the parallel plates by 0.016 centimeter will provide 200 maxima in the wavelength

range between 1.5 and 25 microns: this is perhaps more than an optimum number of maxima, but fewer maxima requires a lesser plate separation and correspondingly greater difficulties in fabrication of a spacing device.

CHAPTER IV

EXPERIMENTAL PROCEDURE AND RESULTS

1. General

The best performance obtained from the system up to the time of this report was highly disappointing. A large predominance of the time available for the conduct of the project was devoted to attempts to improve the magnitude of reproducible signals at the recorder and a number of minor successes were realized. However, the maximum energy inputs available and optimum choices of the various controls have never yielded recorder traces of usable magnitude with 2.00 millimeter slits width beyond about 17 microns or with slits width less than 0.3 millimeter at any wavelength, except with unacceptable accompanying spurious effects. Furthermore, the resolution obtainable with these slits widths prohibits detailed observations of spectra and precise calibration.

An obvious defect in the monochromator is the etched surface of one of the prisms: the amount of energy lost to the detector due to this defect is not readily determined and resurfacing the prism face was not feasible within the available time.

Descriptive material written by the manufacturer of the monochromator does not give direct evidence that markedly superior performance characteristics are to be expected: the minimum slits width used in connection with any recorder response curve is 0.50 millimeter and the best long wavelength response curve shown in that material is free of excessive spurious responses to about 19 microns only. There are

references to intended use "in the field" with output band widths of 0.5 to 0.3 micron. On the other hand, the potassium bromide prisms which are a part of this version of the monochromator become superior to sodium chloride prisms only for use with wavelengths longer than about 12 microns and are considerably less satisfactory in the 3 to 7 micron region. It is thus apparent that the instrument was designed for superior performance in the longer wavelength region.

Present-day recording infrared prism spectrometer systems exist which may be favorably compared with high quality gratings with regard to the detailed resolution of the fine structure of molecular absorption bands: resolutions of from one to two reciprocal centimeters at 10 microns, roughly equal to the theoretical resolution limits, have been demonstrated. (See McAlister, Matheson, and Sweeney (14) and Oetjen, Kao, and Randall (18).) Although such systems may be more expensive and elaborate than the one under discussion, it is the conclusion of the writer that results thus far obtained represent unacceptable utilization of the components and the precision workmanship present in this system.

Figure 18 is a partial reproduction of the manufacturer's linear dispersion curve for the monochromator. (The ratio of proportionality between these values of linear dispersion and corresponding values of dispersion, $\frac{dn}{d\lambda}$, calculated from the Gundelach data is fairly uniform.) Bandwidths in microns may be calculated for various exit slit widths directly from the manufacturer's linear dispersion data: Figure 19 shows such derived exit slit bandwidths for various slits widths and

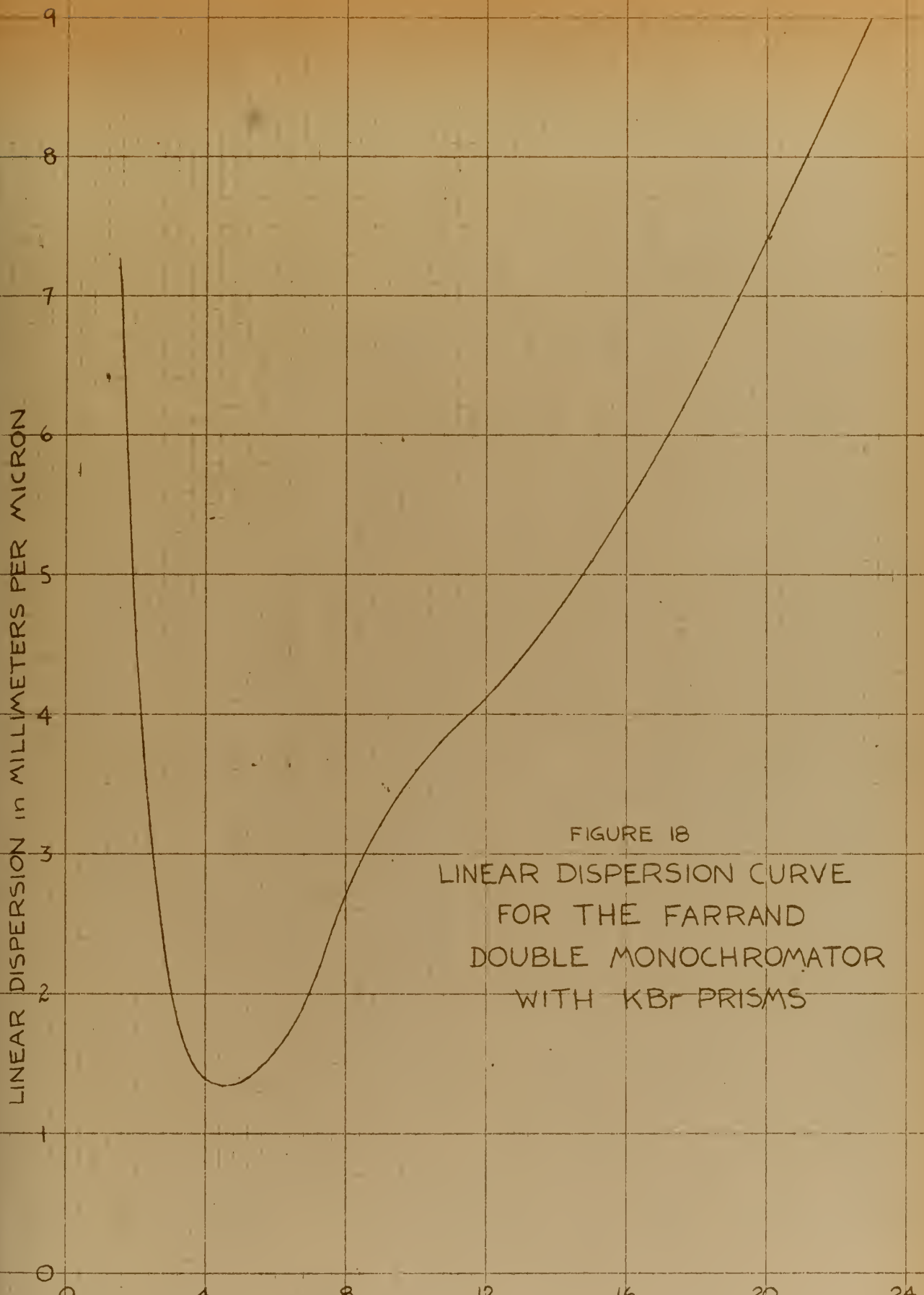

FIGURE 18

LINEAR DISPERSION CURVE FOR THE FARRAND DOUBLE MONOCHROMATOR WITH KBr PRISMS

delineates the zone of slits widths with which reproducible and usable recorder traces are obtainable. Also shown for comparison is the previously-calculated curve of theoretical resolution limits. It is obvious that the theoretical resolution limits are meaningless when bandwidths of never less than 0.065 micron are simultaneously presented to a detecting device which is effectively equally sensitive to all wavelengths within that band.

It is feasible to check optical alignment of the monochromator only by trial and error methods for each individual adjustment or by passing a visible monochromatic emission through the unit and performing coordinated adjustments to optimize overall transmission. The latter procedure unfortunately involves partial disassembly of the prism and Littrow mirror mountings, since the assembled monochromator is mechanically prevented from assuming a mirror position which will accomodate any part of the visible spectrum: this procedure was eventually followed and it was found to be difficult to restore, let alone improve, the optical alignment of the instrument. A large portion of the original vernier wavelength correction was removed in this process, however.

The manufacturer of the monochromator does not refer in any way to the particular amplifying units which are a part of this system, and it is the conclusion of the writer that these units are not best-suited for this purpose. At minimum amplifier gain, available outputs to a recorder system presenting the recommended impedance to the discriminator are far in excess of those required by the recorder but are completely unsatisfactory in terms of smoothness of response. The output shunt-

FIGURE 19

EXIT SLIT BANDWIDTHS FOR VARIOUS SLITS WIDTHS AND A COMPARISON CURVE OF THEORETICAL RESOLUTION LIMITS. SHADING INDICATES REGION OF USABLE SLITS WIDTHS

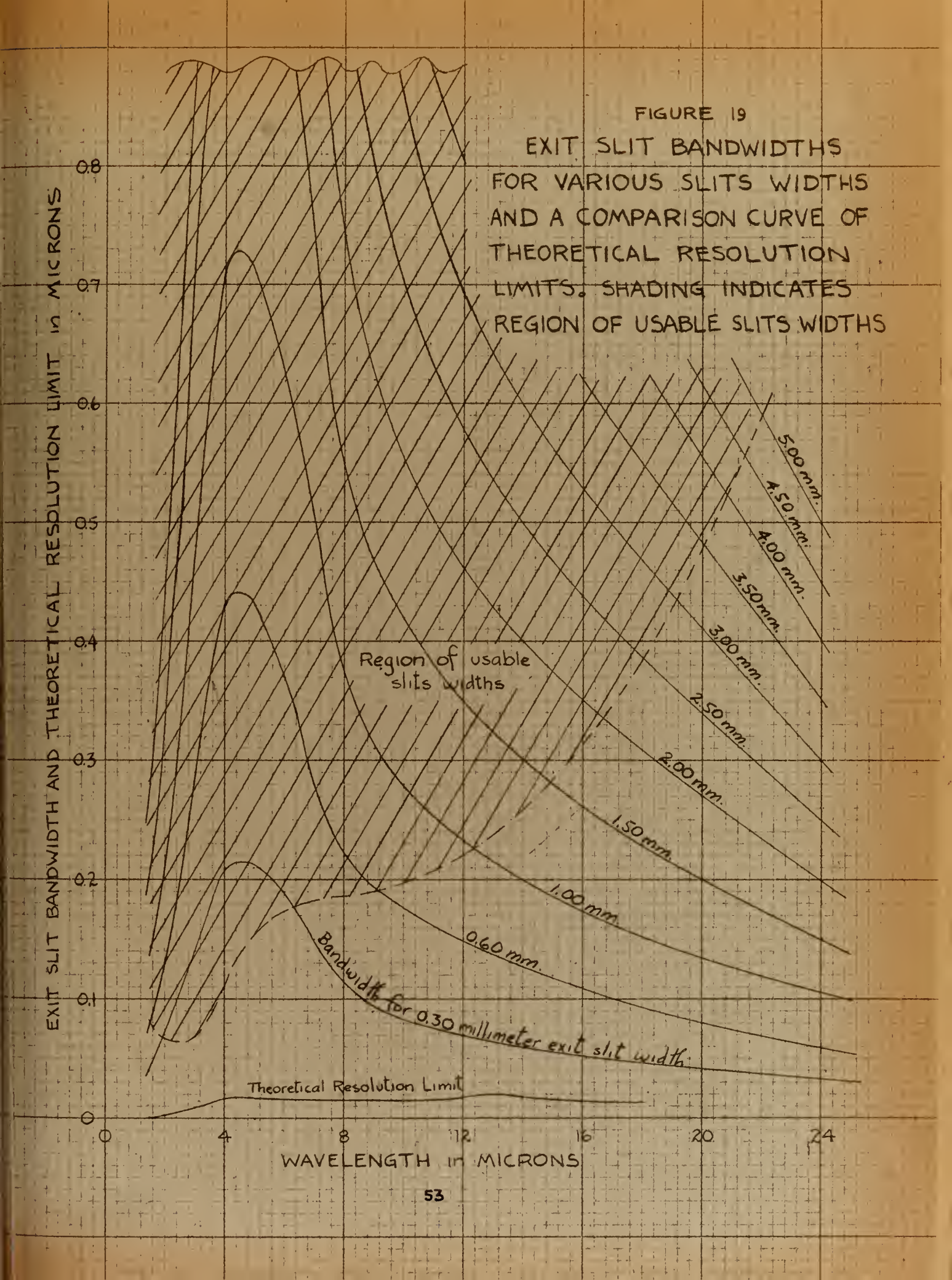

ing variable resistor arrangement described in Chapter II was found to be an expedient method of reducing the recorder signal and simultaneously improving signal-to-noise ratio. An electronic system capable of generating a smaller output but with less self-noise and susceptibility to chassis vibration effects would obviously be superior.

Principally for the benefit of subsequent users of this system, effective modifications and adjustments accomplished during this project are listed below:

a. Replaced unshielded cables with shielded cables where applicable.

b. Installed the amplifier in a spring suspension.

c. Placed rubber vibration pads under the main equipment foundation.

d. Adjusted the brush rigging of the reference generator to approach zero and 180 degrees phasing with the detector signal.

e. Increased the reference generator battery voltage from 22.5 to 45 volts.

f. Realigned the positions of the external concave mirror, source holder, chopper mirror, and bolometer holder to maximize bolometer response. Shimmed the chopper mirror to partially compensate for its departure from flatness.

g. Provided a common conductor between all chassis and a true ground.

h. Installed a Sola constant voltage transformer to stabilize the alternating current feed to the power supply.

The following modifications or adjustments were found to provide no noticeable improvement in system performance:

a. Provided an electromagnetic shield cage around the amplifier.

b. Re-evacuated the bolometer and bled in dry nitrogen to about one millimeter pressure.

c. Temporarily reduced the resistance of R24 and R25 plate and cathode matched resistors of the amplifier phase-splitting stage in an attempt to improve the reference signal waveform.

d. Adjusted R13 of the power supply to provide 12.6 volts rated filament voltage for the 12SJ7 amplifier tubes.

Step-by-step waveform analyses and noise measurements throughout the amplifying system revealed no correctable conditions which were recognized to represent a malfunction. Distortion of the reference generator square wave was observed when the amplifier output leads were paralleled with the reference generator input to the discriminator, even though the amplifier was turned off. This effect rendered perfect phasing of the reference and detector signals impossible, but efforts to correct this condition were unsuccessful. The oscilloscope presentations also revealed the irregularity of chopper mirror reflection and this condition was partially compensated as mentioned above.

With regard to improvement of detector-reference signal phasing, it is to be remarked that the radial edges of the chopper mirror presently begin to cut across the ray bundle which will form the entrance slit image of the source in a direction along the major axis of the elliptical bundle. The detector signal waveform, smoothed by the 3

millisecond bolometer time constant, is thus very nearly a sine wave. Relocation of the chopper and reference generator mounting such that the chopper mirror edges would cut in a direction along the minor axis would steepen the sides of the detector signal waveform and render proper discriminator input phasing more nearly attainable. An observed shift of phase relationships with change of slits width due to this same effect would also be reduced by this alteration. Since this change would represent an improvement of much less magnitude than that being sought, available time was not devoted to this refinement during this project.

It was observed that the presence of the bolometer in the amplifier circuit had no significant effect when the bolometer was receiving no direct energy input and that increasing the battery voltage across the bolometer network from 1.5 to 3.0 volts increased the final output without appreciable immediate change in signal-to-noise ratio. It was also observed, however, that bolometer-induced noise was a general function of its total energy dissipation and that use of the 3.0 volt battery arrangement must be restricted to shorter periods of time if bolometer noise is to remain below a level of significance.

Grounding the case of the Leeds and Northrup Speedomax recorder is recommended by the manufacturer. It was found, however, that this is undesirable in this case, for the direct current recorder inputs are provided with a capacitor path to the case and moderately fast voltage swings properly generated by the various spectra are too readily lost to ground. Trial installation of a variable resistance between the

recorder case and ground was found to provide a usable method of controlling the recorder signal-to-noise ratio, but this device was less successful than the discriminator output variable shunting resistor and was removed.

The limitation of resolution or irregular displacement of recorder traces due to excessive monochromator motor drive speed was not observed at any time.

As might be expected, maximum usable recorder signals were obtained with the discriminator output balanced for zero signal with median displacement of the recorder stylus, and the discriminator balance control should not be used as a zero-adjust feature for the recorder. A direct current millivoltmeter was installed across the output shunting resistor to facilitate this adjustment. A switch was also installed to open the voltmeter lead at all other times, to protect the meter against transients and to allow direct-reading dial calibration of the output shunting resistor.

Tentative substitution of an Esterline-Angus moving coil type recorder was made and it was found that controllable signals were still obtained only when the output shunting resistor was used. Since superior damping characteristics were ineffective in the case of the severe random effects introduced with the desired signal from this system, a return was made to the Speedomax, with its better over-run characteristics, scale flexibility, and resistance to transient shocks.

Figure 20 shows the high sensitivity and strong susceptibility of the system to transient effects. Traces (a) through (g) were made with

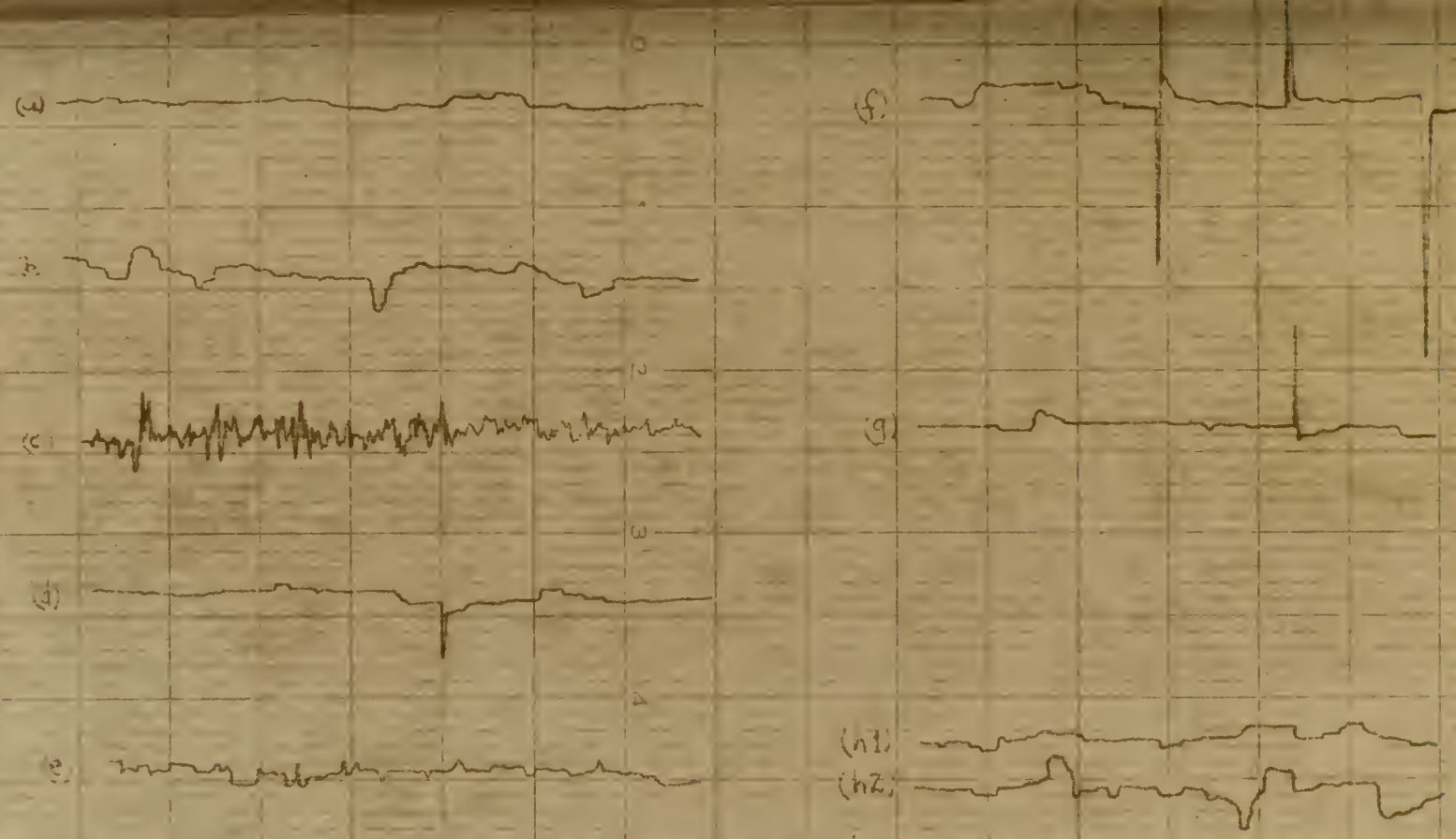

FIGURE 20

SAMPLE	TRANSIENT EFFECTS UPON THE SYSTEM
(a)	50 - 3 - 3 - 2.3 - 1.5 - 45 - S - 1.2 - X - X - X (bolometer off)
(b)	Power supply shifted to bypass constant voltage transformer
(c)	Removed common ground connections
(d)	Turned on small photographic timer on same AC feeder
(e)	Increased amplifier gain control to position 4.
(f)	Dropped paper clips on amplifier chassis
(g)	Slammed outer door of building
(h1)	Turned on bolometer with Nernst glower source
(h2)	Walked past operating Nernst glower

moderate gain and plate shunting resistance and with the bolometer turned off: trace (h) was taken with the bolometer on and shows the effect of the mild air motion due to merely walking within several feet of an uncovered Nernst glower. On several occasions, the passage of low-flying aircraft was sufficient to cause effects upon a recorder trace!

A code system intended to present necessary information as to various system variables is utilized on all spectral response traces and is demonstrated and explained herewith:

50-3-6-2.3-3.0-45-S-1.2-46.0-7.0-1.50

Slits width: 0.50 millimeters.

Amplifier gain control in position 3.

Recorder range: 6 millivolts full scale deflection.

Discriminator output shunting resistor set at 2.3 ohms.

Bolometer battery voltage: 3.0 volts.

Reference generator battery voltage: 45 volts.

Power supply is via Sola constant voltage transformer.
(NS indicates power supply to be direct from AC utility circuit.)

Reference generator brush rigging index at position 1.2.

Temperature of constant-temperature enclosure: 46.0°C.

Recorder stylus position on index scale with zero energy input: 7.0.

Monochromator wavelength vernier setting at start of recorder trace: 1.50 microns.

2. Comparison of Detector-Amplifier Systems

In view of the poor overall performance of the system, trial substitution of the Golay detector and amplifying system for the bolometer and McDonald amplifying units was made. Results were even less impressive

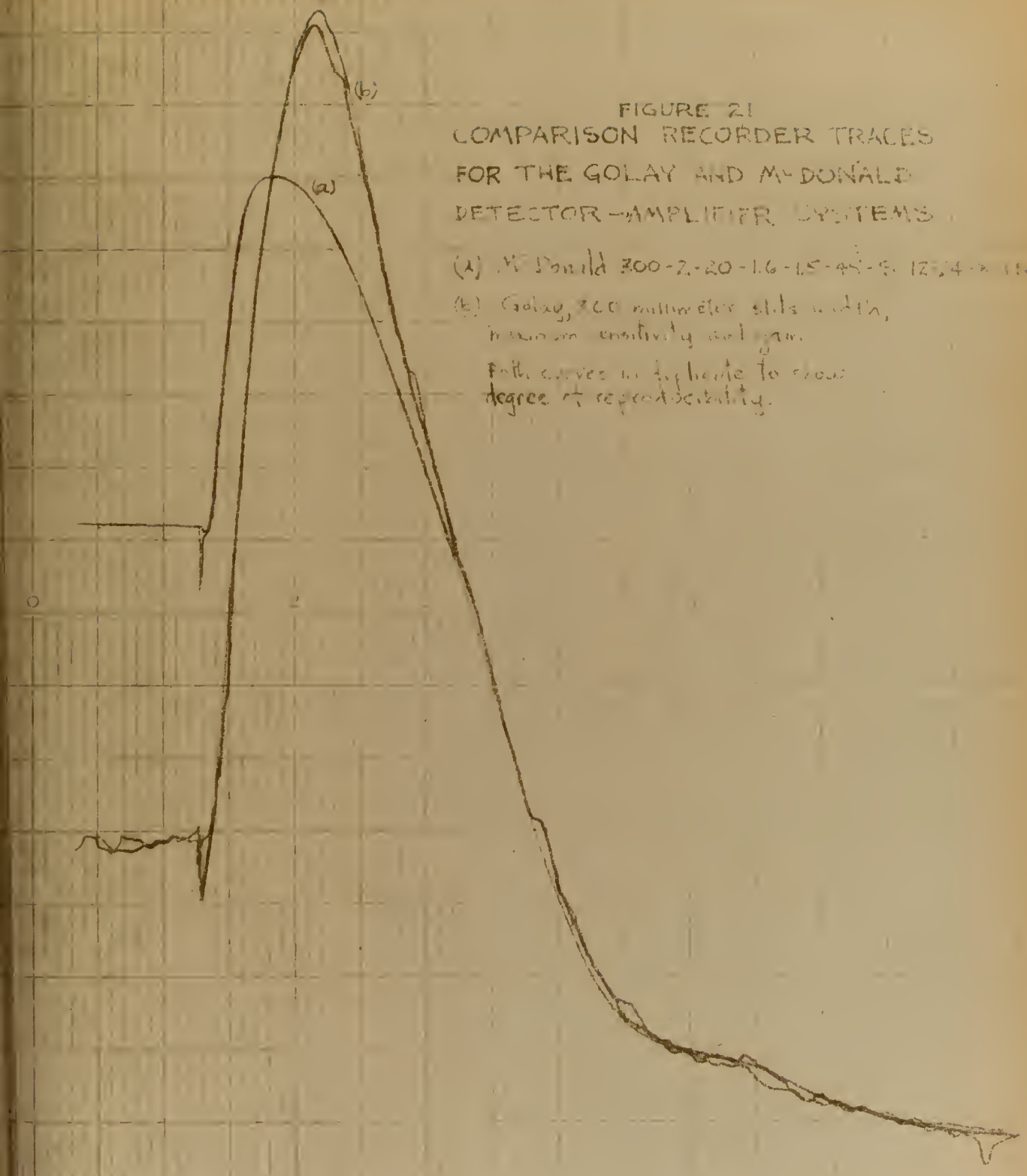

FIGURE 21
COMPARISON RECORDER TRACES
FOR THE GOLAY AND McDONALD
DETECTOR-AMPLIFIER SYSTEMS

(a) McDonald 300-2.-20-1.6-1.5-45-5-12,4-x-110

(b) Golay, 300 millimeter slit width,
maximum sensitivity and gain.

Both curves on log scale to show
degree of reproducibility.

then with the original system: the Golay units exhibited a much larger detector time constant and a considerably less reproducible trace, as shown by Figure 21.

The Golay detector and amplifier had not been utilized since purchase several years ago. Tubes were checked and found satisfactory, the circuit was traced without finding any discrepancies, reasonable waveforms were observed at the external test connections, and the detector was adjusted for optimum response according to the manufacturer's instructions. Excessive background signal due to stray light from the chopper filament reaching the detector was somewhat reduced by applying dull black paint to the chopper blade and part of the lamp envelope. Improvement in the output signal was observed, but it is likely that inherent performance characteristics were not developed in the time devoted to trial of this system.

An attempt to obtain usable results by connection of the most sensitive galvanometer on hand across the signal diagonal of the bolometer Wheatstone bridge was also unsuccessful. The magnitude of obtainable displacements of the galvanometer index was entirely insufficient for utilization of this method.

3. Comparison of Sources

Three types of infrared continuous-spectra emitters were used during the course of this project: a nichrome wire coil, the Nernst glower, and the Globar.

The nichrome wire coil was a conventional heating element, reshaped to a higher linear turns density, and operated at 8 amperes current. It

was easy to handle and had stable load characteristics, but emitted considerably less energy than the other two types of emitter.

The Nernst glower is a high resistance ceramic rod composed principally of rare earth oxides such as zirconia, yttria, and thoria, and is maintained at an appropriate radiation temperature by an electric current. Units used during this project were approximately one millimeter in diameter and two centimeters long and had thin platinum leads attached with a ceramic cement. These units were old and it is considered likely that aging had a deleterious effect, but the writer considers these sources to be less desirable than either of the other two types, for the following reasons:

a. The Nernst glower is difficult to handle and mount without breaking either the rod or the cemented lead connections.

b. The spectral distribution is much less smooth and less similar to a black body emitter.

c. The glower must be preheated by a flame torch or a specially constructed heater to permit starting.

d. A large negative temperature coefficient of resistivity necessitates large series ballast resistors. These ballast resistors emit sufficient heat to raise the room temperature to an uncomfortable level.

e. An image of this thin source cannot be made to fill the entrance slit opening of the monochromator at higher settings of slits width.

f. Minor disturbances in the atmosphere surrounding these units cause completely unacceptable changes of output, as previously shown by Figure 20.

The Globar is a resistance heating carborundum element: those used as sources for calibration data during this project are one-quarter inch in diameter and about four inches long, and were operated at 10 amperes rated current. Silver-coated ends reduce localized heating effects where clip type leads are attached. These elements are very brittle and have a small negative temperature coefficient of resistivity, necessitating small ballast resistors. They change resistance with use and are reported to have a short operating life. No Globar failed in use during this project, however, and their self-starting characteristics, fair emissive stability, and the strong similarity of their spectrum to that of a black body emitter lead to their preferred use by the writer.

A comparison of recorder traces obtained from the Globar and the Nernst glower at two different slits widths is shown by Figure 22. The 175 milliamperes operating current for the Nernst glower is less than rated value, but five out of six available units were broken or failed during use at 200 to 250 milliamperes current and a higher load was not risked with the remaining unit. The inherent difference in stability (and other transient effects in the case of following recorder traces) are best shown by the portion of the trace prior to the start of the monochromator drive.

4. The Effect of Temperature Upon Monochromator Wavelength

An investigation of the effect of temperature upon the actual wavelength passed by the monochromator at a particular vernier reading fully justified the effort devoted to modifying the Plexiglass casing to provide operation within a constant-temperature enclosure.

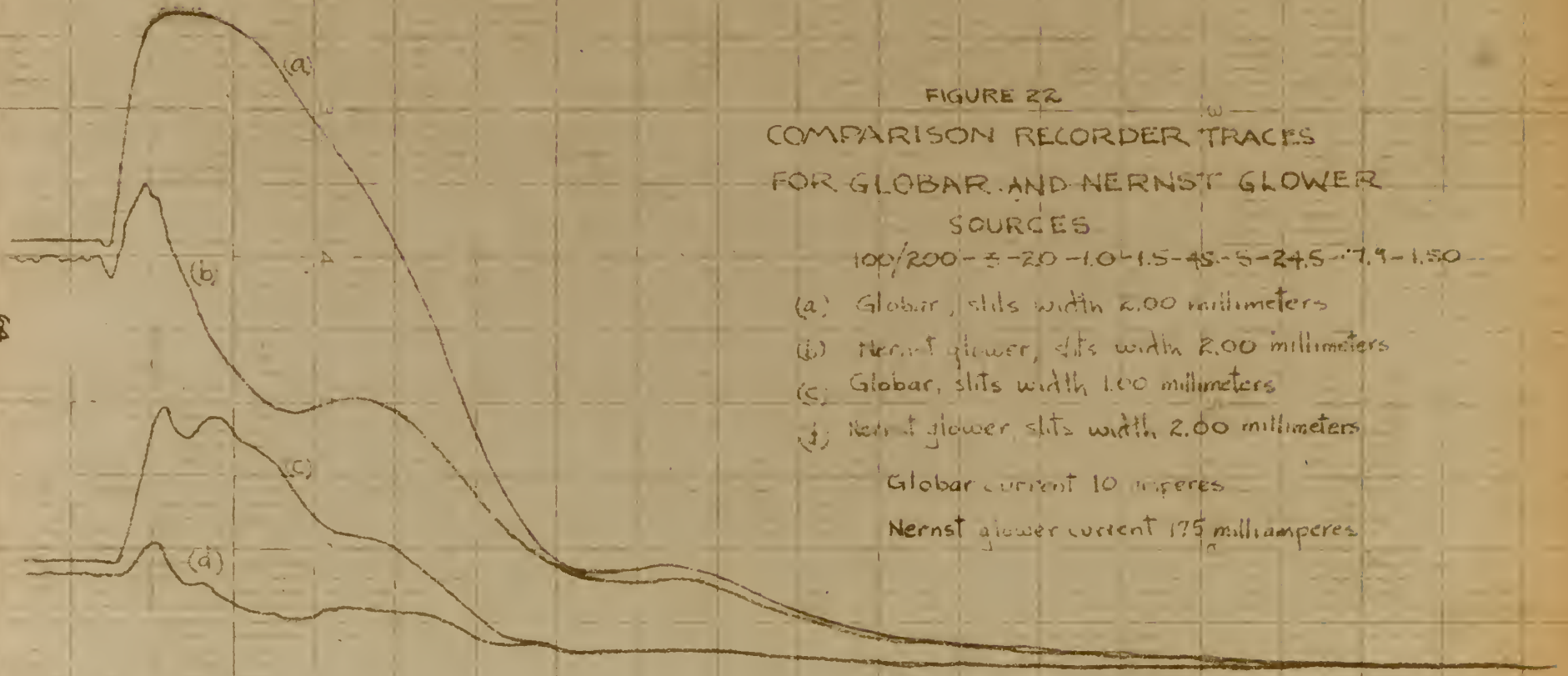

FIGURE 22

COMPARISON RECORDER TRACES FOR GLOBAR AND NERNST GLOWER SOURCES

100/200 - 3 - 2.0 - 1.0 - 1.5 - 4.5 - 5 - 24.5 - 7.9 - 1.50

(a) Globar, slits width 2.00 millimeters

(b) Nernst glower, slits width 2.00 millimeters

(c) Globar, slits width 1.00 millimeters

(d) Nernst glower slits width 2.00 millimeters

Globar current 10 amperes

Nernst glower current 175 milliamperes

Inasmuch as the shift of true spectral position of the major features of an absorption band is known to be negligible for temperature changes of a few degrees, it was decided to simply observe the temperature-induced shift of a sharp symmetrical absorption dip, using an essentially fixed mixture of absorbant gases and identical controlled variables other than temperature. Conversion of recorder readings to absorbance was thus obviated for this case.

The room was thoroughly ventilated for several hours, after which the monochromator cover was sealed and the outer enclosure was installed. The thermostat system was left off and the carbon dioxide and water vapor naturally present within the outer enclosure were allowed to remain without reduction as a source of absorption bands. Another hour was allowed for temperature equalization before a recorder trace of carbon dioxide and water vapor absorptions of a Globar emission spectrum was taken and individual recorder stylus positions versus vernier wavelength readings were taken with the hand drive. This process was repeated about 12 hours later with the constant-temperature enclosure brought to 44°C. Figure 23A shows the superimposed recorder traces, reveals the very appreciable temperature effect, and indicates that carbon dioxide and water vapor concentrations did not vary sufficiently to provide a significant contribution to the shift of the symmetric strong dip at vernier readings of 2.30 microns at 26°C and 2.53 microns at 44°C. The shift can be attributed primarily to the change of index of refraction of KBr with temperature. The increased magnitude of response at the higher temperature was noticed on other occasions, but no investigation sufficient to warrant an attempt to explain this

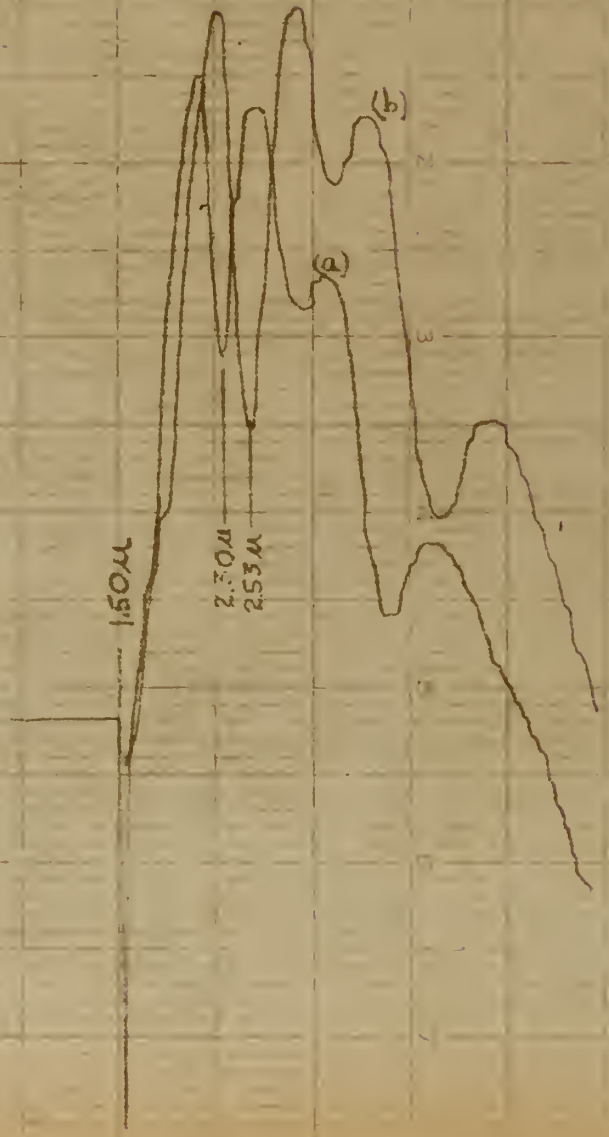

FIGURE 23A

EFFECT OF TEMPERATURE UPON MONOCHROMATOR WAVELENGTH

50-3-2-18-1.5-45-5-1.2-26/44-X-1.50

(a) Recorder trace at 26°C

(b) Recorder trace at 44°C

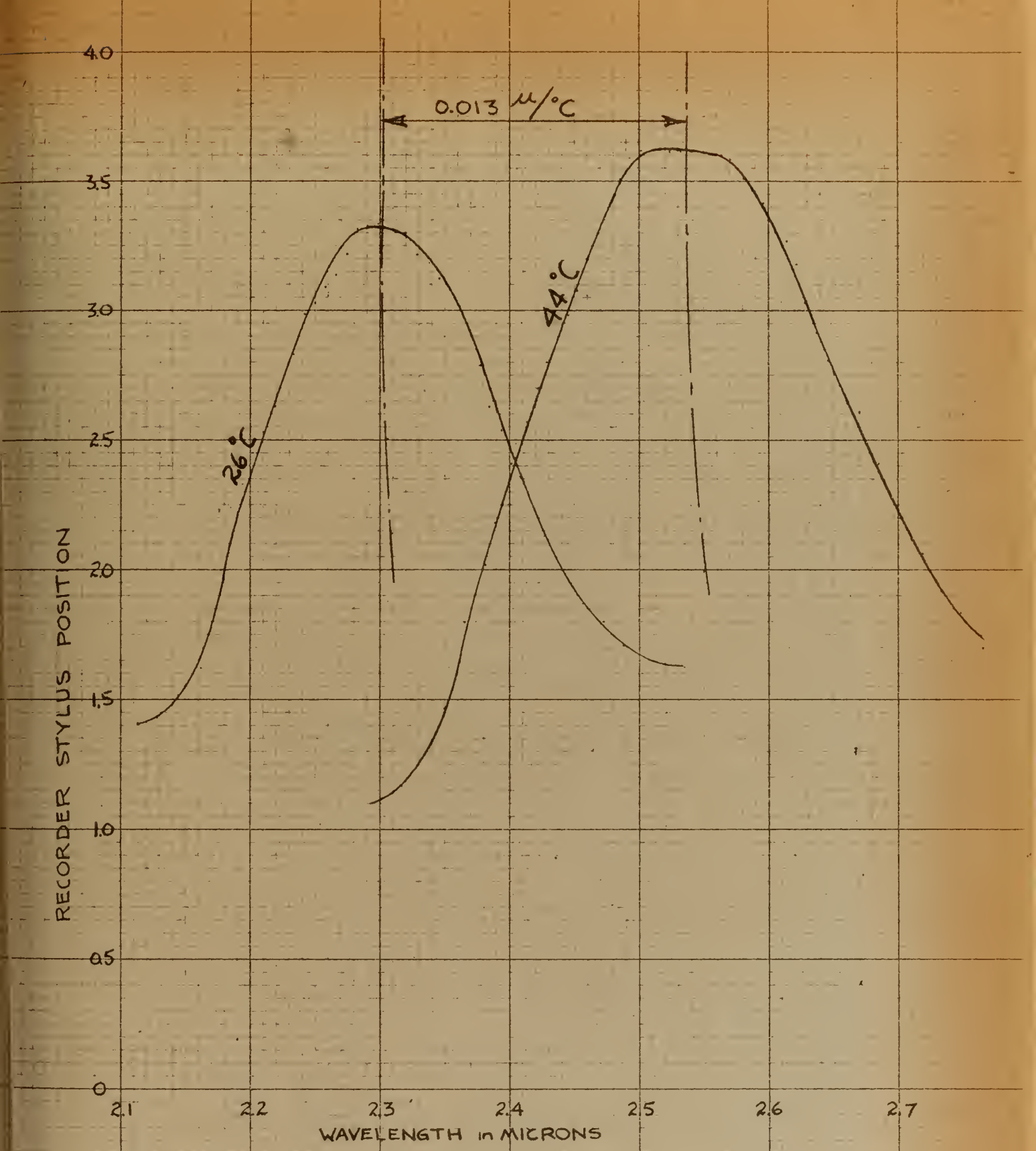

FIGURE 23B

MANUAL DRIVE OBSERVATIONS OF THE 2.69-2.76 μ CARBON DIOXIDE DOUBLET BAND AT 26°C AND 44°C, SHOWING EFFECT OF TEMPERATURE UPON THE MONOCHROMATOR WAVELENGTH

effect was made.

Figure 23B is a plot of the individual recorder stylus positions versus vernier wavelength readings taken by means of the hand drive. Symmetry axes are shown and a temperature coefficient of 0.013 microns per degree Centigrade is established for this wavelength region. (This absorption dip is that of the carbon dioxide 2.69 - 2.76 doublet bands.)

Further operation and calibration of the system was at 45°C and determination of a curve of temperature coefficients versus wavelengths was not undertaken. It was observed at this time that variations in temperature of the order of ± 1°C are permitted by the installed thermostat. This undesirable situation should be corrected by installation of a precision thermostat when available.

5. The Effect of Slits Width on Monochromator Wavelength.

The effect of resolution upon the apparent position of distinctive portions of a spectral trace has been discussed. It was desired, however, to determine whether or not a change of slits width per se would cause a shift of wavelengths passed by the monochromator.

The strong symmetrical absorption dip used for determination of temperature effect was also used for the determination of slits width effect. Individual readings of recorder stylus position versus vernier wavelength were taken with the manual drive for slits widths of 0.50 and 1.00 millimeters in immediate succession. Since temperature, absorbant gas concentration, and all other controllable variables except slits width and recorder zero adjust were constant, conversion of readings to absorbance was again obviated. Due to the near-symmetry of the absorption dip and the emission spectrum in this vicinity, it is con-

sidered that effects due to resolution difference would be negligible.

Figure 24 is a plot of the observed data at the two different slits widths. It is apparent that slits width changes per se do not affect the apparent position of a characteristic region of a spectral response trace to any significant degree.

6. Calibration Method Results

Most of the originally considered methods of calibration were not successfully utilized in the experimental procedure.

a. Emission Spectra

An appreciable amount of time was devoted to attempts to obtain responses to the line emission spectra of helium, hydrogen, mercury, and sodium arcs. Maximum total response was obtained from a General Electric Corp. AH-3 mercury vapor lamp from which the outer protective glass envelope had been removed. Resolution was so poor at slits widths yielding reproducible results, however, that the response to the doublet near 4 microns was spread across about one micron of recorder presentation. Furthermore, carbon dioxide absorption along portions of the energy path outside the monochromator case produced an interfering effect for which accurate compensation was not possible. This mode of obtaining calibration points was therefore abandoned.

b. Christiansen Filter

A Christiansen filter using air as the transparent medium was attempted in preference to one requiring construction of

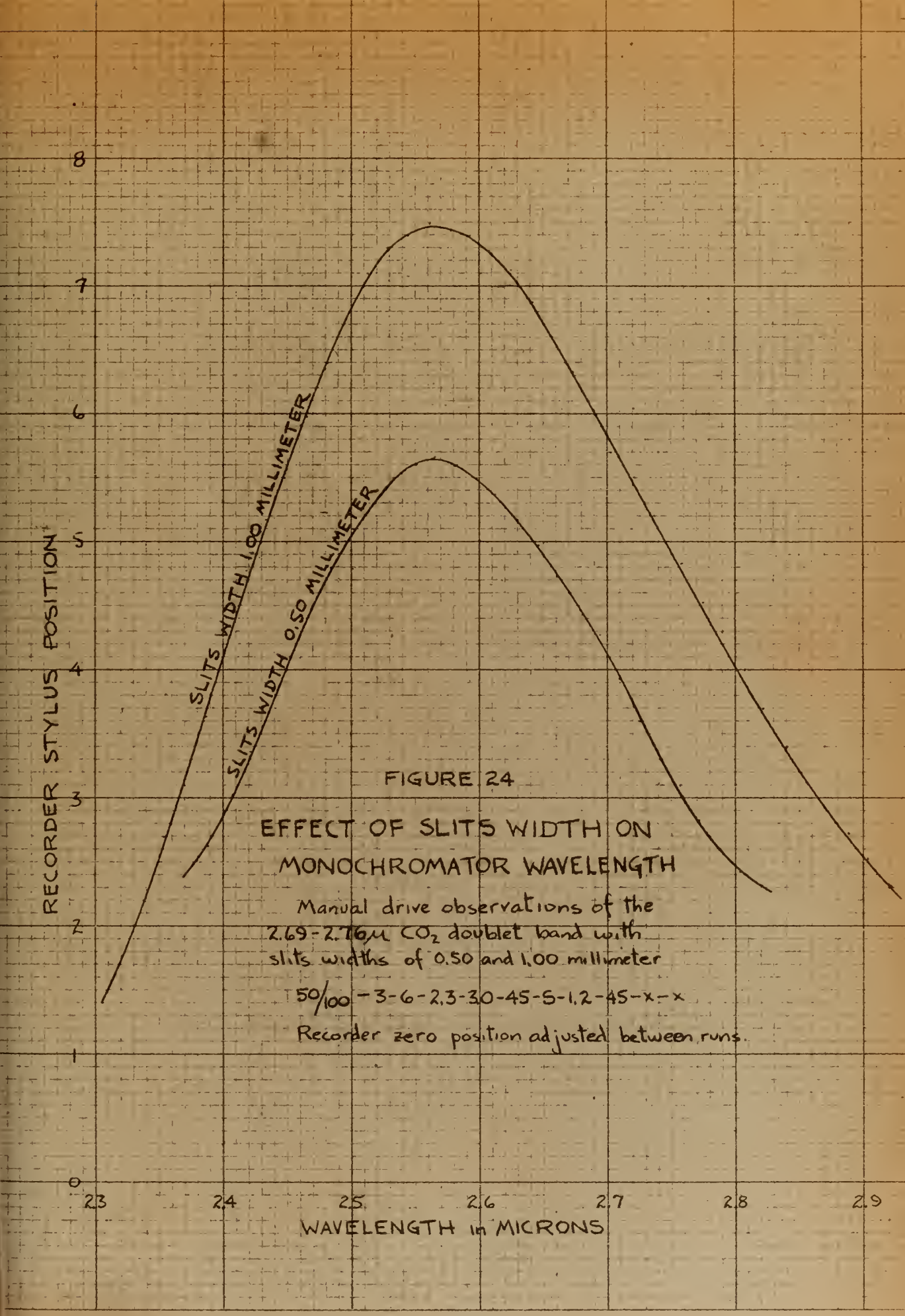

FIGURE 24

EFFECT OF SLITS WIDTH ON MONOCHROMATOR WAVELENGTH

Manual drive observations of the 2.69-2.76μ CO_2 doublet band with slits widths of 0.50 and 1.00 millimeter

50/100 - 3 - 6 - 2.3 - 3.0 - 4.5 - 5 - 1.2 - 4.5 - x - x

Recorder zero position adjusted between runs.

an infrared transparent cell for a liquid suspension type filter. Of the various powder components for which data was obtained, quartz was selected for several reasons:

(1) Quartz crystals of high purity were available.

(2) The transmission frequency of an air-quartz filter (7.35 microns) was nearest the high energy portion of source emission spectra.

(3) The transmission peak for properly sized quartz particles was particularly well-defined.

The insolubility of quartz in water led to another advantage in that powdered quartz particles of uniform size were obtained by means of a method suggested by Barnes and Bonner (4). Stoke's Law, assuming spherical particles, was used to calculate the velocity of fall in water for the various particle sizes desired. Quartz was ground to a fine powder with an agate mortar and the powder was placed in a cylinder of water of sufficient height to provide a convenient time of fall. By repeatedly shaking the suspension and discarding portions which did not settle out within narrow time limits each side of calculated values, lots containing a predominance of particles of desired size were obtained. The efficacy of this separation scheme is revealed by Figure 25, a microphotograph of residual particles obtained after carrying out this process for a calculated spherical diameter of 40 microns. A small portion of off-size particles is acceptable and is to be expected when the separation process is begun from a mixture which fills the entire settling column.

FIGURE 25

MICROPHOTOGRAPH OF QUARTZ PARTICLES SEPARATED FROM A RANDOM MIXTURE BY SELECTIVE TIME OF FALL IN WATER

Filters were prepared with various particle size lots and with varying thicknesses of powder mounted between two thin layers of nitrocellulose. It was found that an extremely thin dusted layer of the quarts powder was sufficient to appreciably suppress the transmission of wavelengths at which the source emissions were intense. It was also found to be impossible to obtain a reproducible definitive transmission peak in the 7.4 micron region, due to low source intensity in that region and the fact that the nitrocellulose mounting films failed to transmit about half of the incident energy at that wavelength. (Alternate available films of cellophane, pliofilm, Duco household cement, cellulose acetate, and Glyptal resin are all characterized by low transmittance in this region.)

c. Interference Fringes

The method of interference fringes of equal chromatic order was originally intended to be the primary calibration method. Two potassium bromide discs 1 3/16 inches in diameter and one-half inch thick were obtained and were sent away for professional polishing to optical flatness. A holder designed to receive these discs with a sliding fit and to provide variable spring compression about the periphery of the retaining bonnet was made. A pedestal and bracket assembly to mount the holder at the exit slit of the monochromator were also made and a portion of the monochromator light baffle system was duplicated with suitable modifications for use when the holder was installed.

Invar was originally selected as the material to be used for the

spacer ring, due to its markedly lower temperature coefficient of expansion, but was not locally obtainable in suitable form. Stainless steel, Class 1A, annealed, was selected as an alternate material due to its resistance to corrosion and accurately known temperature coefficient. A ring intended to be 0.006" ± 0.001", of uniform thickness ± 0.0001", 1 3/16" outside diameter and 1" inside diameter was machined from heavy sheet stock. (The machining process consisted of boring the inside diameter; milling the surrounding region to approximate thickness; mounting the useful region between cylinders of brass bar stock so that an inside shoulder fitted the inside diameter and the outer shoulders held the ring in compression about its periphery; turning the spacer ring and the mounting cylinders to proper outside diameter; and hand-lapping the spacer ring to uniform thickness.)

Figure 26 is a photograph of the interference discs installed in the holder. Spring loading of the retaining bonnet is apparent. A portion of the modified light baffle system is attached to the holder. The spacer ring is shown between the butting surfaces of the mounting cylinders.

The two potassium bromide "flats" were found to be completely unsatisfactory when returned from the polishing activity: none of the four sides were flat to within ten wavelengths of sodium light when tested on an optical flat. The manufacture of a suitable polishing lap of 17% beeswax and 83% rosin was accomplished by Professor Kalmbach and repolishing of the discs was commenced with the benefit of his direct demonstrations and supervision.

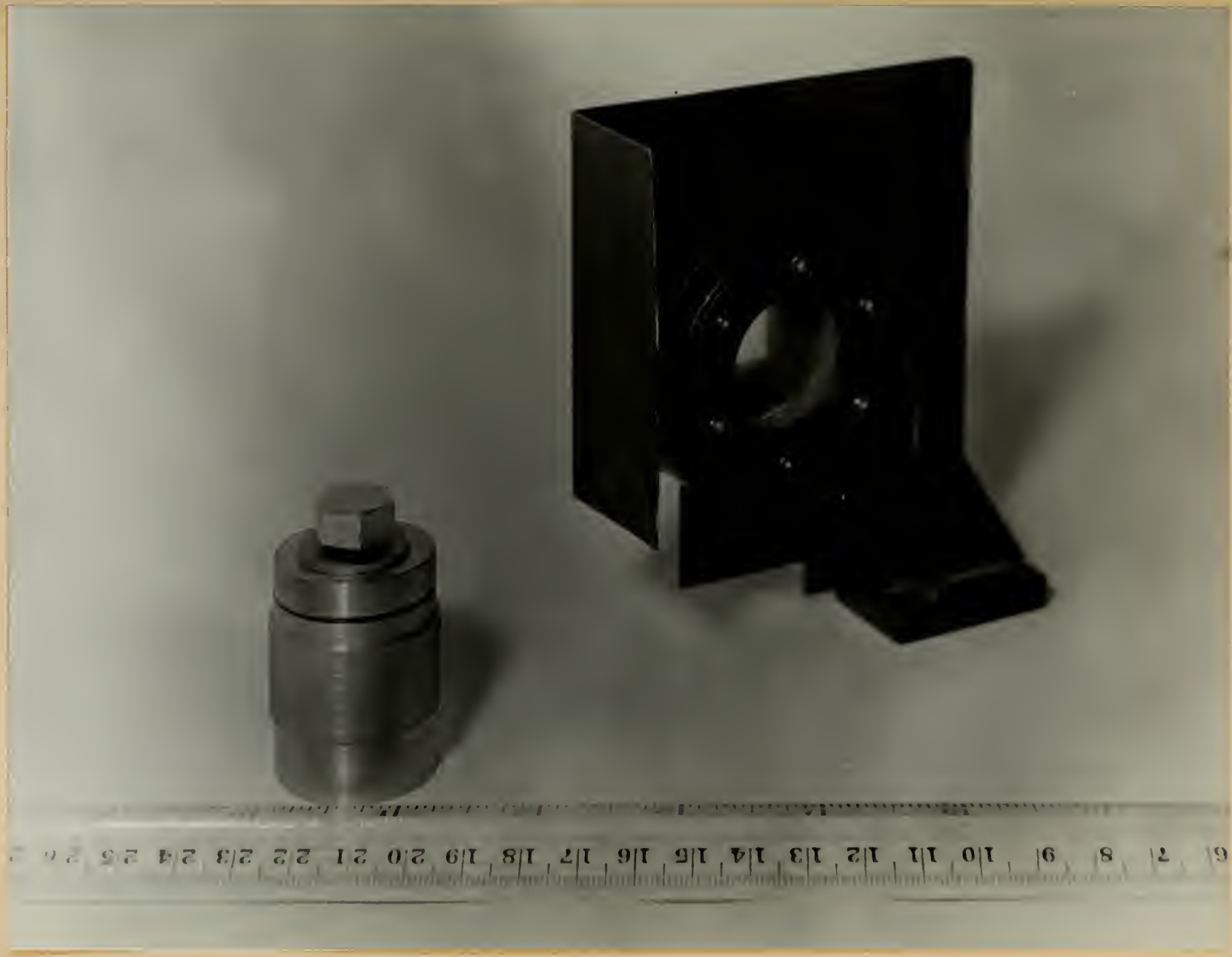

FIGURE 26

PHOTOGRAPH OF INTERFERENCE DISCS HOLDER ASSEMBLY AND SPACER RING

This portion of the project was dropped, however, due to overall time requirements and doubt that useful data beyond the range of absorption methods would be obtainable.

d. Band Absorption Spectra

The method of calibration by means of band absorption spectra of gases and thin films proved to be useful, subject to these severe limitations:

(1) Reproducible usable recorder traces were obtainable only for wavelengths of 8 microns or less. (The 9.4 and 10.4 micron absorption bands of carbon dioxide were discernible only under conditions of unusable resolution.)

(2) Negligible reduction in carbon dioxide and water vapor contaminating absorbant effects was accomplished by the use of trays of soda lime and calcium chloride within the outer casing.

(3) Obtainable resolution prevented direct comparisons with available data. In the case of unsymmetric absorption regions, the accuracy-limiting factor for calibration points sometimes became the estimation of the wavelength at which known detailed absorption spectra would yield a spectral minimum under conditions of poor resolution.

7. Calibration Data from Absorption Spectra

Recorder response curves were obtained for the selected absorbants according to previously-described procedures. Separate runs with optimum choice of control settings were made for each region of interest for each

absorbant. At least four recorder traces were obtained on each run in order to assure that a trace selected for calibration purposes was representative and free from severe transient effects in the region of interest.

All absorption calibration curves were taken with a Globar source operating at 10 amperes current. A low-resolution response curve for this source, with estimated compensation for the broad 5-8 micron water vapor band and multiple bands of carbon dioxide and water vapor between 1.5 and 2.0 microns, is shown by Figure 27. Derived values of ky_1 for this source are also shown by this figure and were subsequently used for calculation of carbon dioxide pseudo-absorbance factors.

No attempt was made to utilize water vapor as a calibration absorbant: the strong 5-8 micron absorption region is too diffuse for low-resolution use and it was considered undesirable to increase water vapor concentration, even in the outer casing, in order to develop usable responses to other bands.

Figures 28 through 36 show the selected recorder traces, together with derived absorbance curves.

Vernier Wavelength in microns	y_1	ky_1	Vernier Wavelength in microns	y_1	ky_1
1.61	3.85	70.0	6.30	1.60	29.0
1.92	5.00	90.8	6.61	1.36	24.6
2.23	5.44	98.5	6.92	1.16	21.0
2.55	5.51	100.0	7.23	1.00	18.2
2.86	5.47	99.3	7.55	0.84	15.3
3.17	5.32	96.5	7.86	0.69	12.5
3.48	5.10	92.5	8.17	0.57	10.3
3.80	4.81	87.3	8.48	0.47	8.52
4.11	4.48	81.3	8.80	0.37	6.71
4.42	4.05	73.5	9.11	0.29	5.26
4.73	3.58	64.6	9.42	0.23	4.18
5.05	3.04	55.2	9.73	0.20	3.64
5.36	2.60	48.5	10.05	0.18	3.27
5.67	2.22	40.3	10.36	0.16	2.91
5.99	1.87	34.0			

ky_1 in terms of percent maximum y_1.

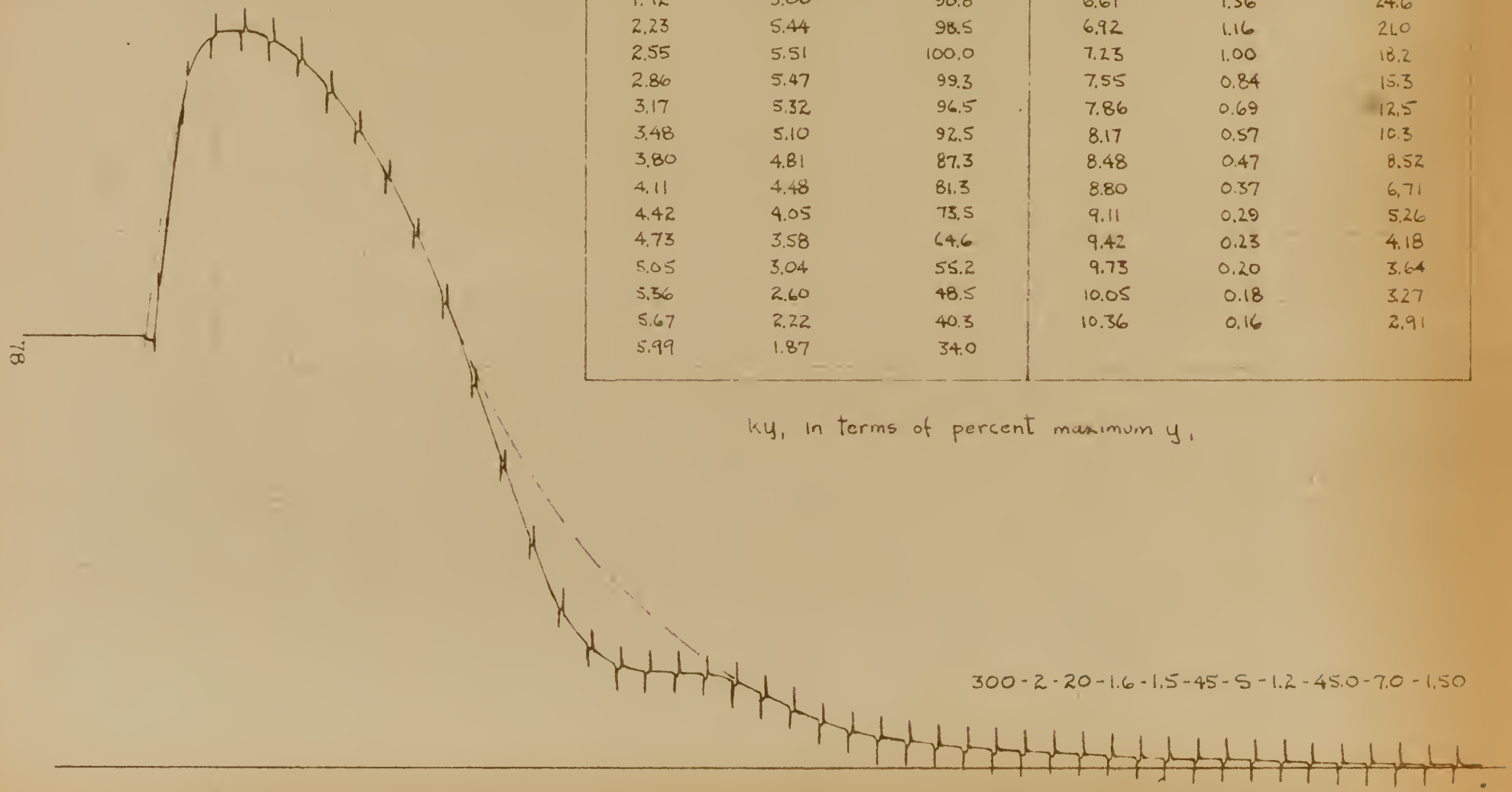

FIGURE 27

LOW RESOLUTION RESPONSE CURVE FOR 10 AMPERE GLOBAR OPERATION, WITH DERIVED VALUES OF ky_1

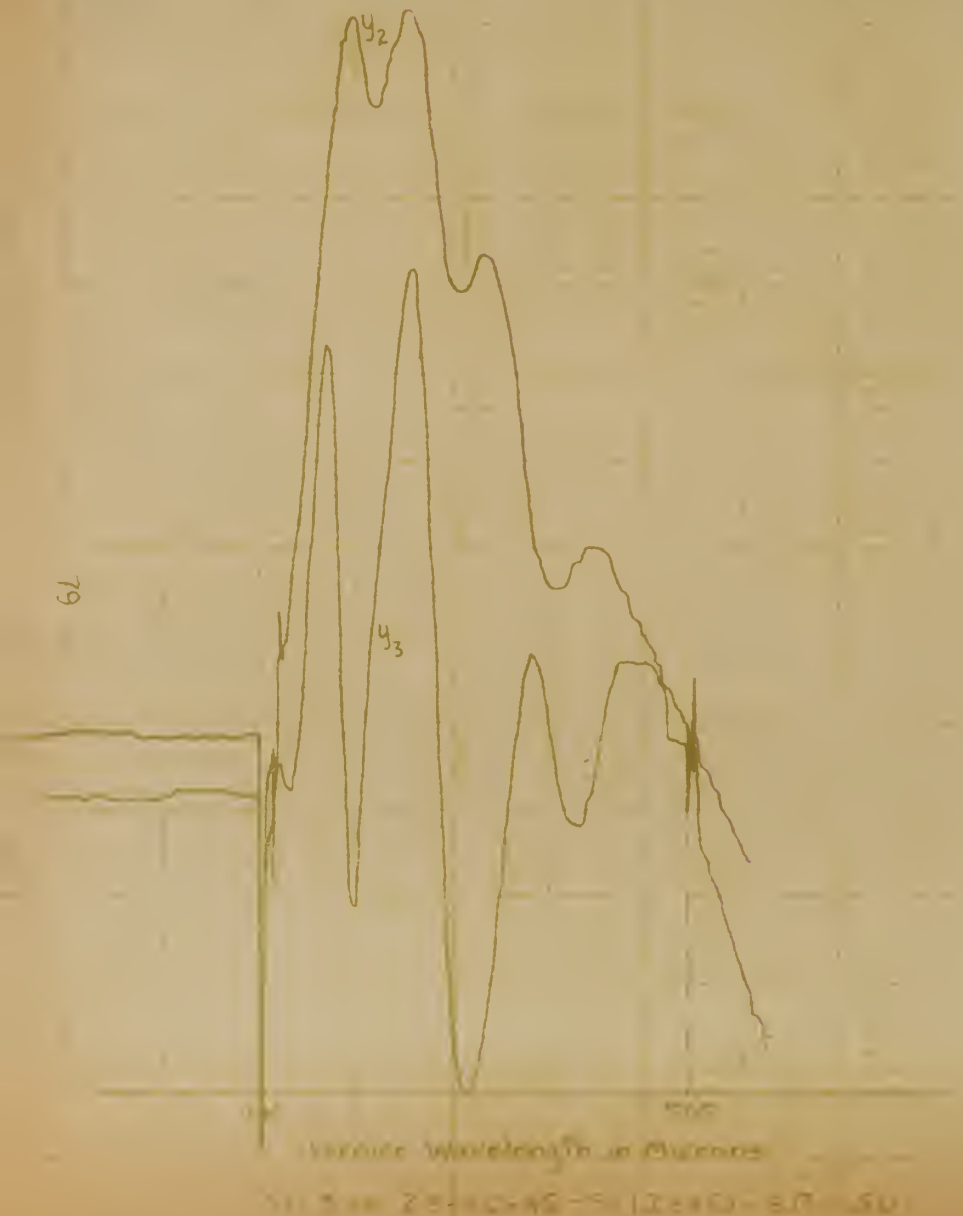

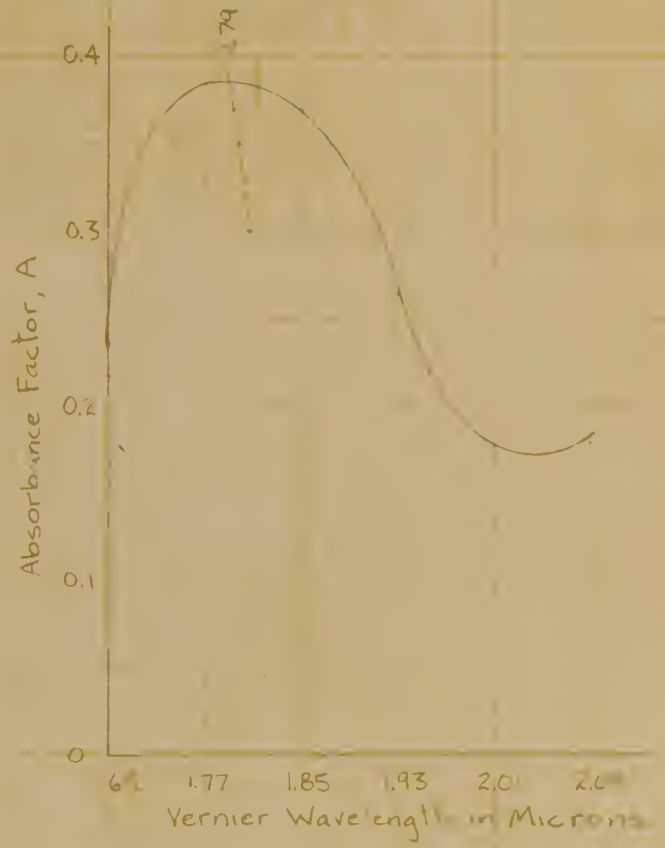

FIGURE 28

1.8 MICRON METHANE ABSORPTION BAND
RECORDER TRACE AND ABSORBANCE CURVE

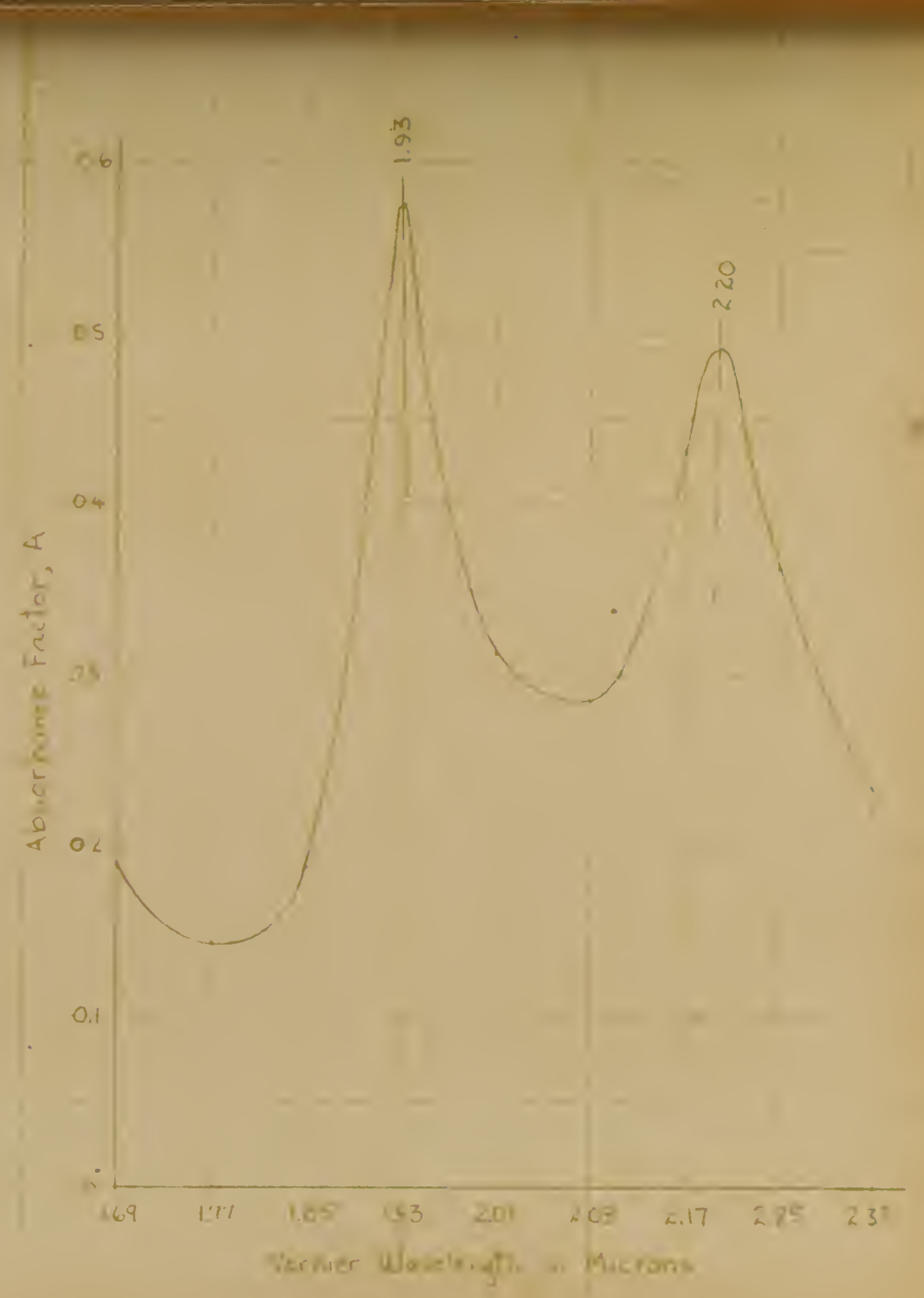

FIGURE 25

2.0 and 2.2 MICRON AMMONIA ABSORPTION BAND RECORDER TRACE AND ABSORBANCE CURVE

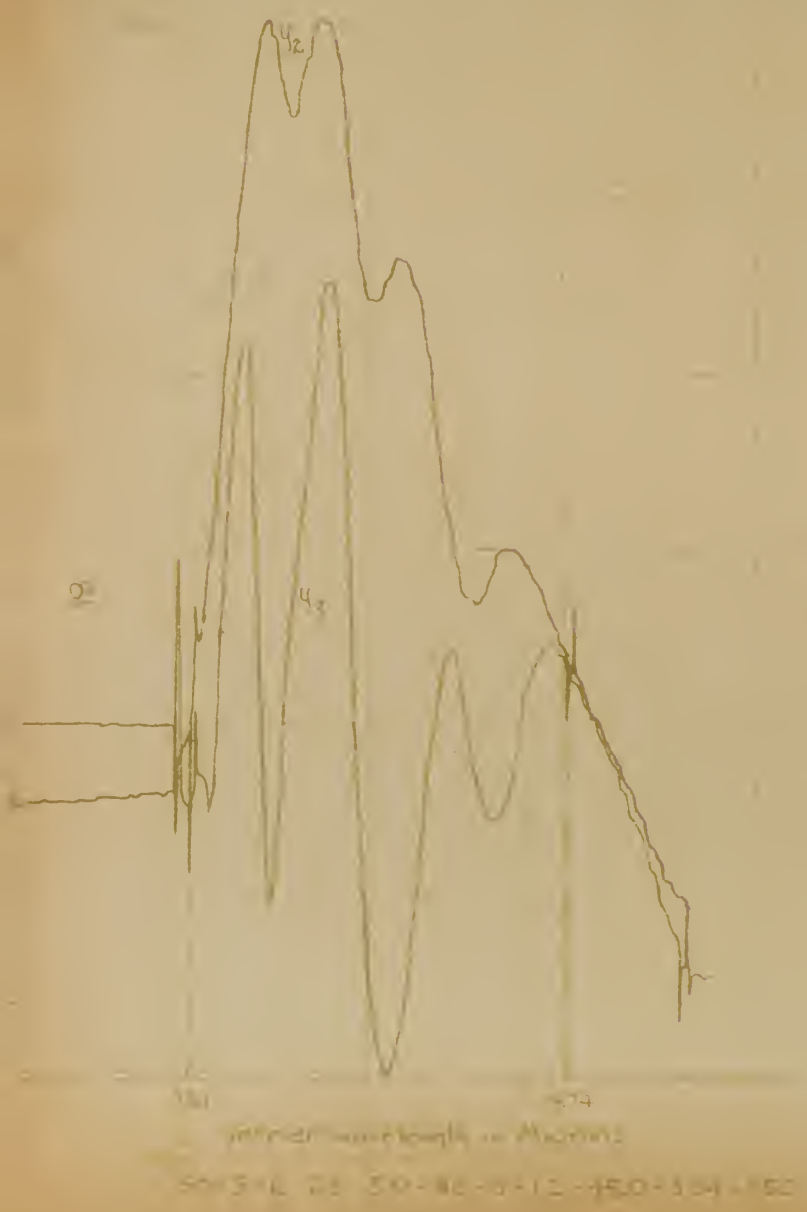

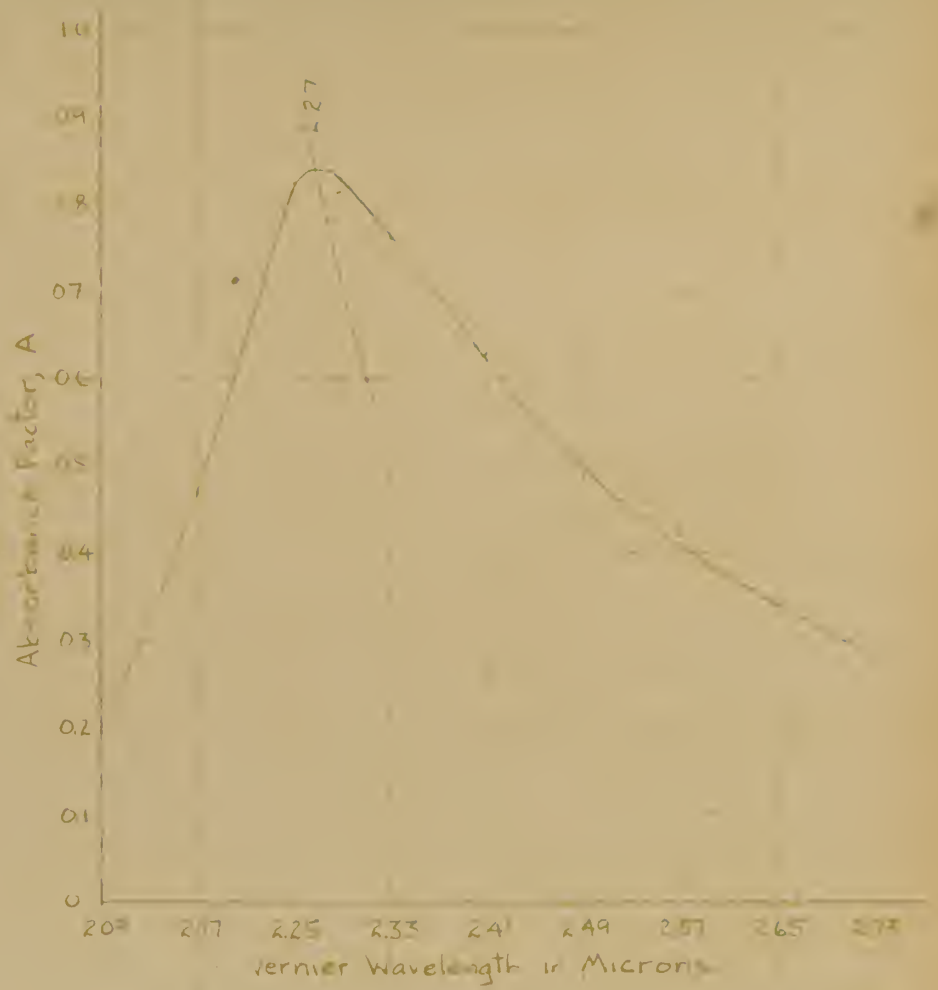

FIGURE 30

2.3 MICRON METHANE ABSORPTION BAND
RECORDER TRACE AND ABSORBANCE CURVE

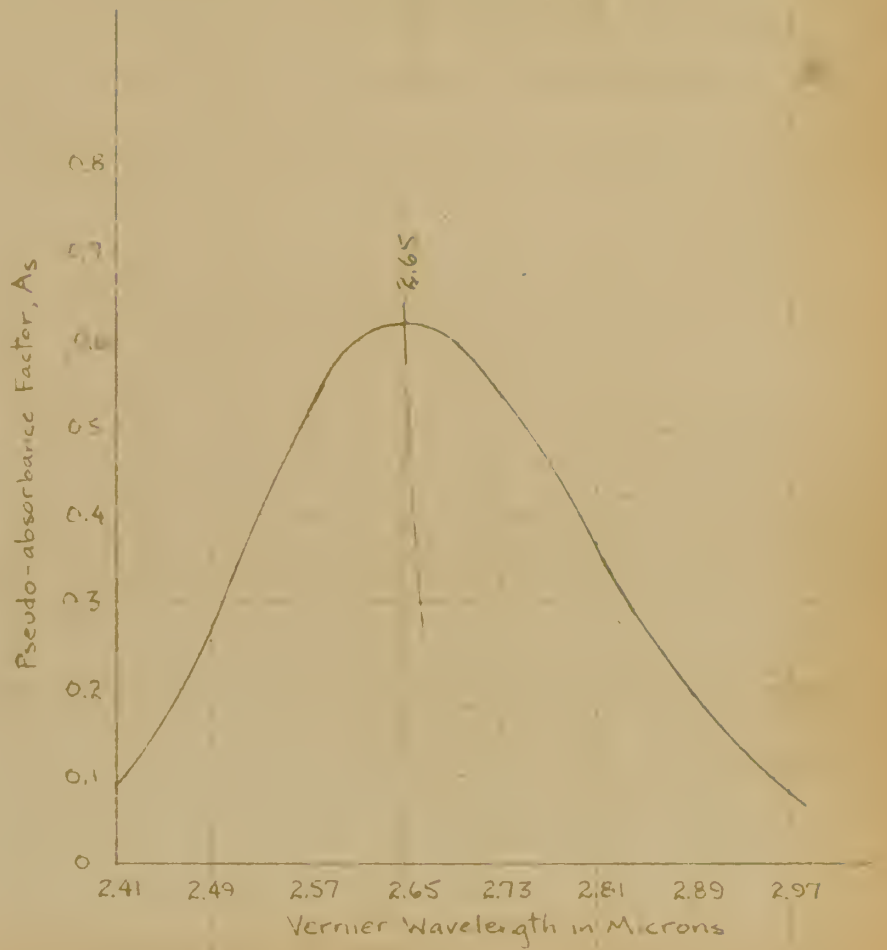

FIGURE 31

2.7 MICRON CARBON DIOXIDE ABSORPTION BAND RECORDER TRACE AND ABSORBANCE CURVE

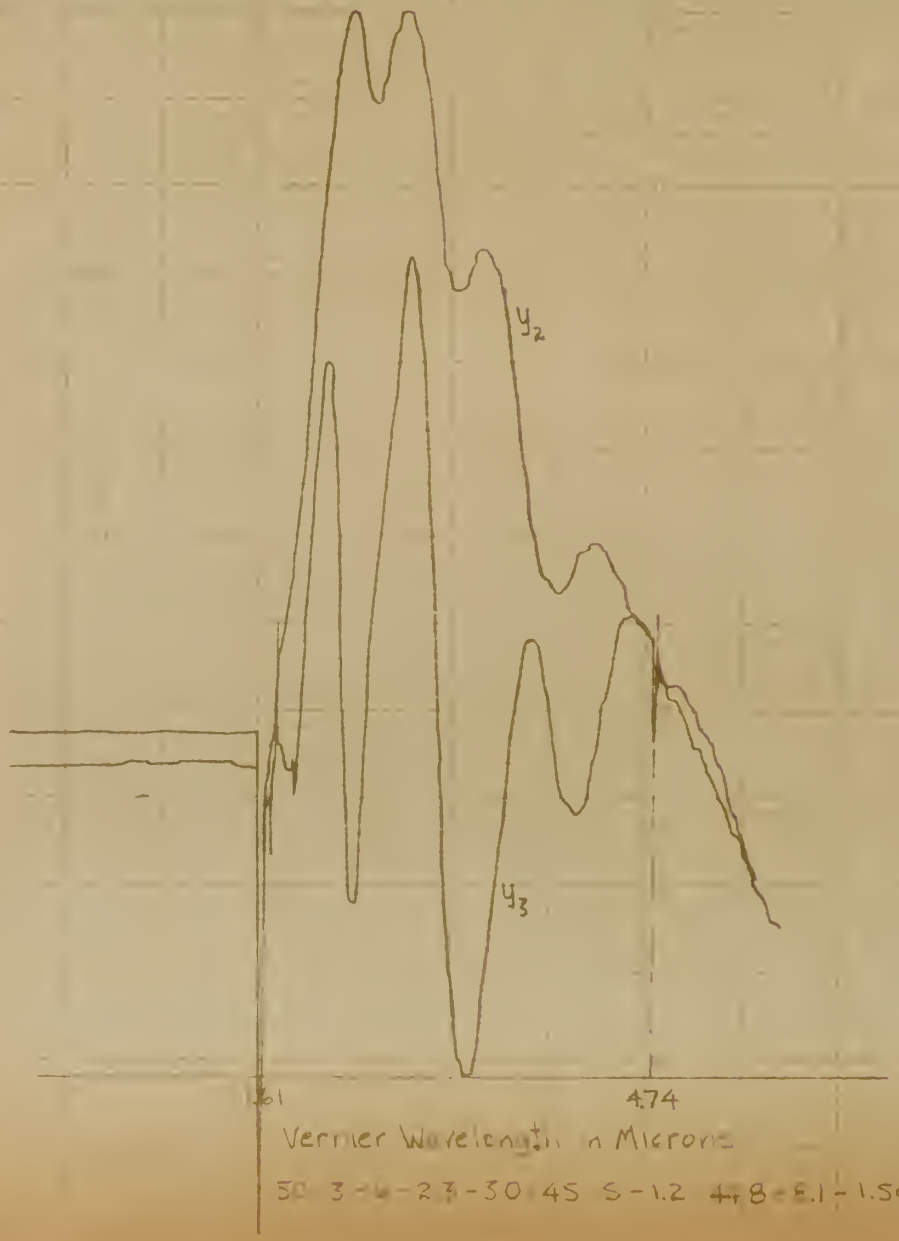

50 3-4-2.3-30.45 S-1.2 4.8-8.1-1.50

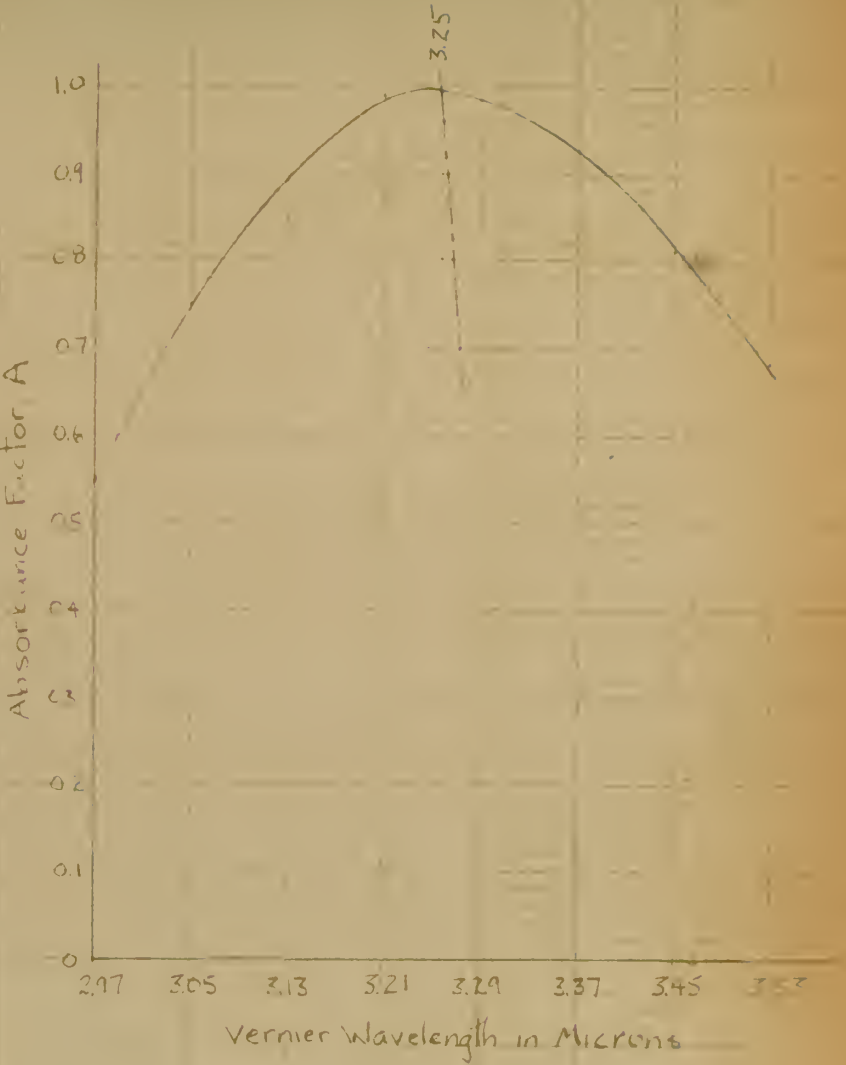

FIGURE 32

3.3 MICRON METHANE ABSORPTION BAND RECORDER TRACE AND ABSORBANCE CURVE

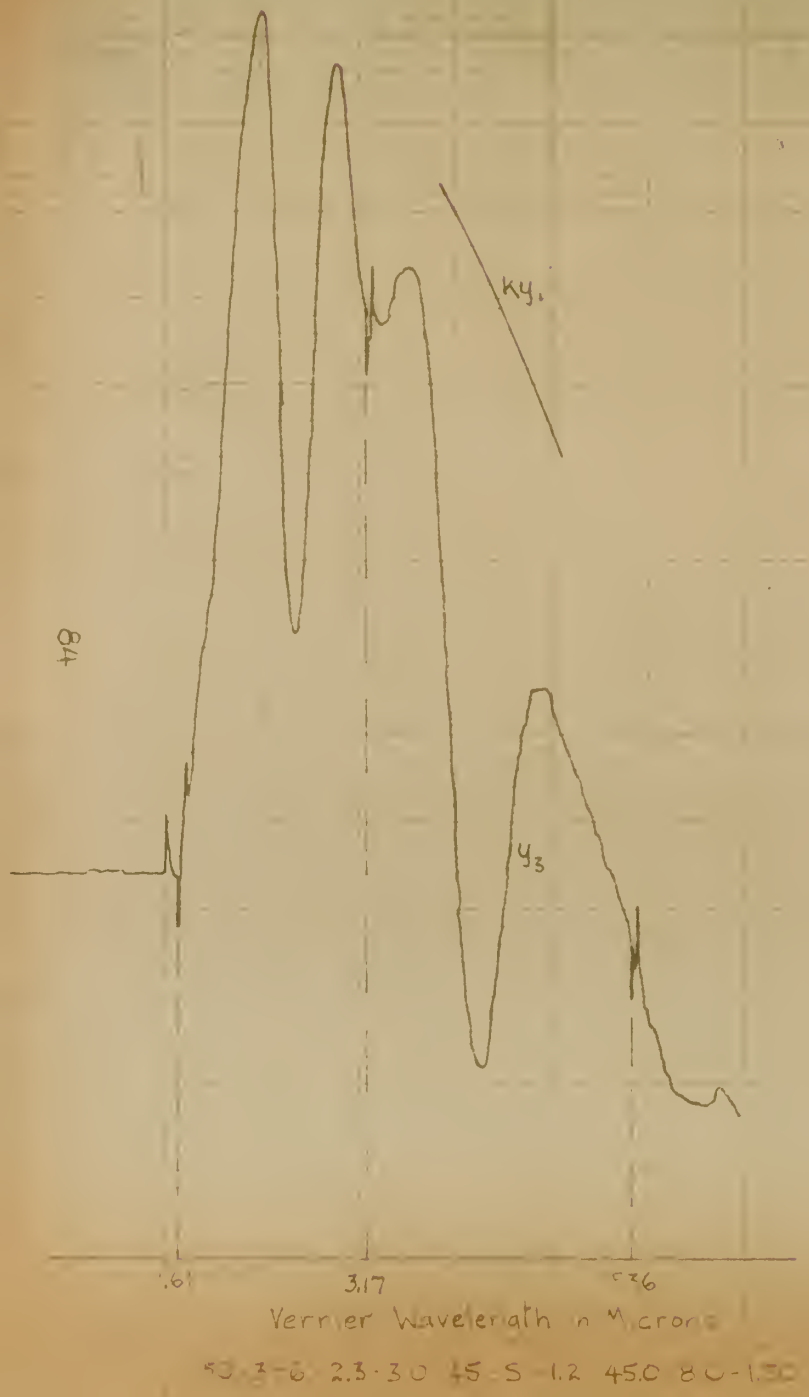

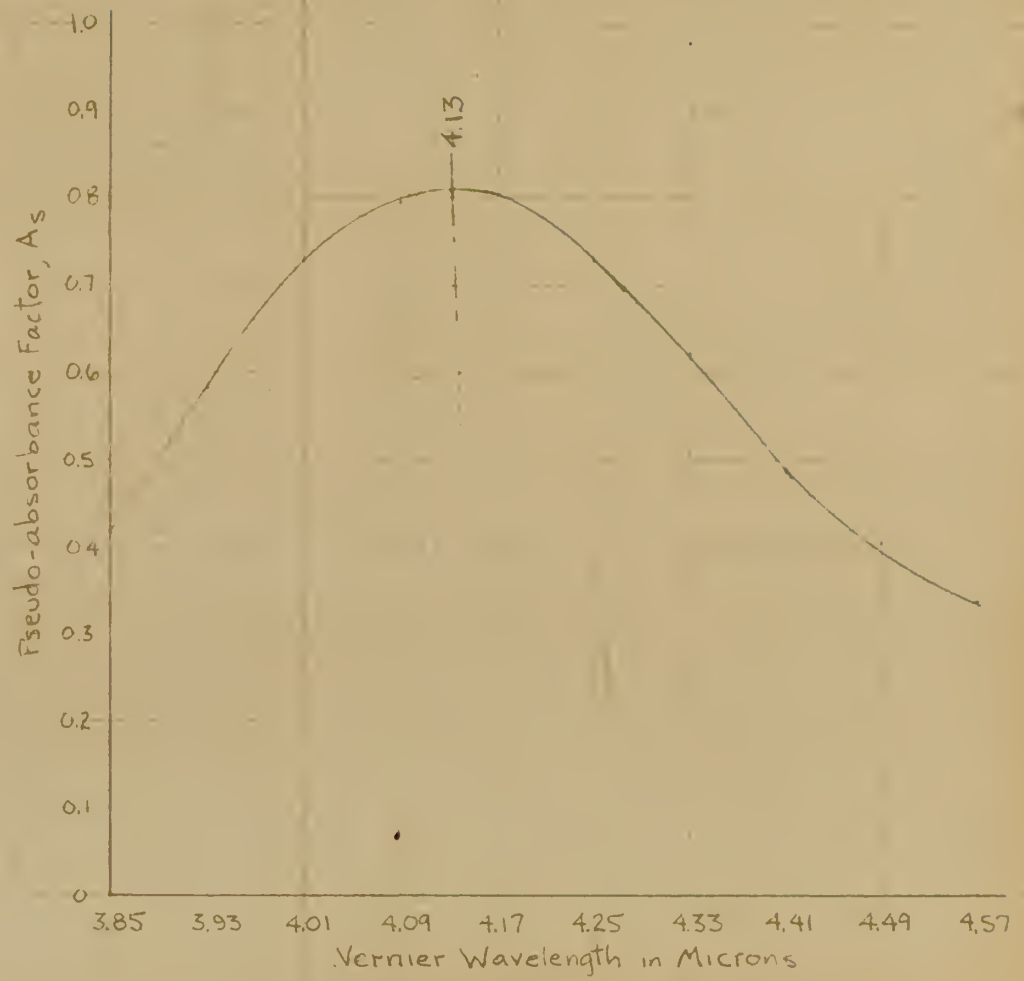

FIGURE 33

4.3 MICRON CARBON DIOXIDE ABSORPTION BAND
RECORDER TRACE AND ABSORBANCE CURVE

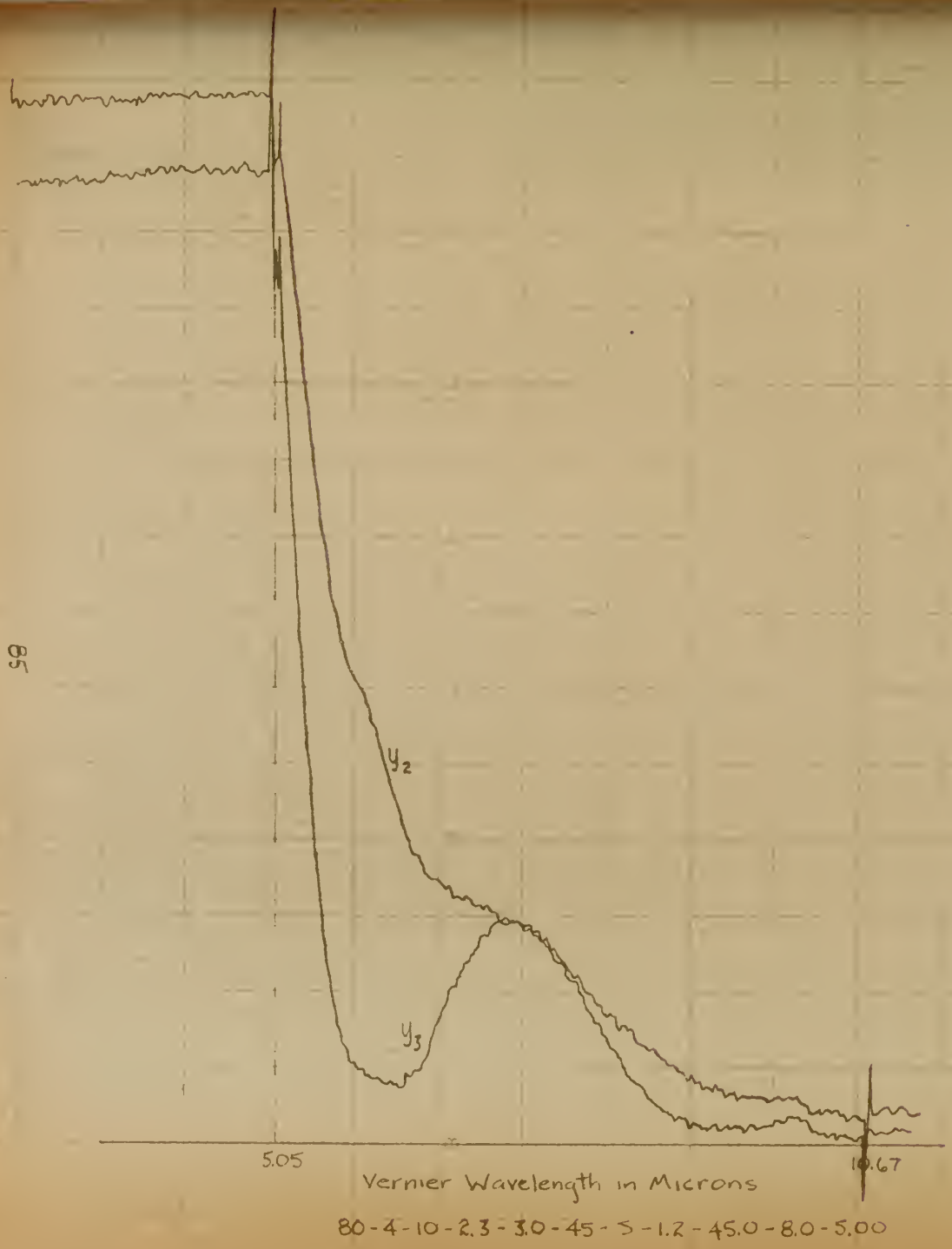

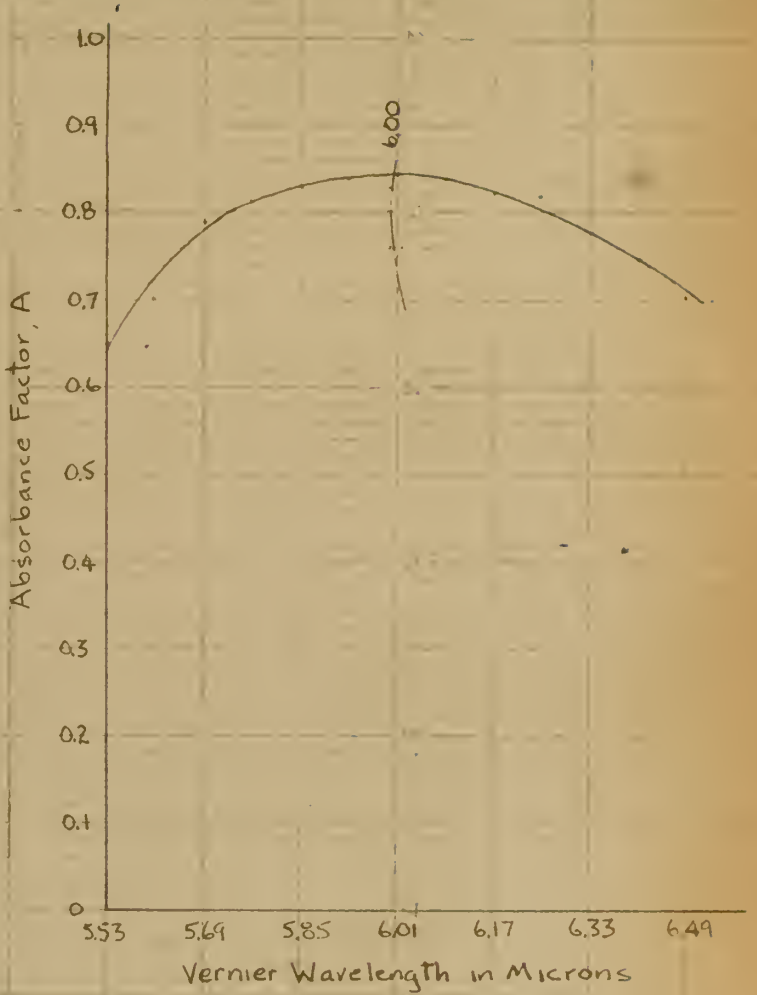

FIGURE 34

6.1 MICRON AMMONIA ABSORPTION BAND

RECORDER TRACE AND ABSORBANCE CURVE

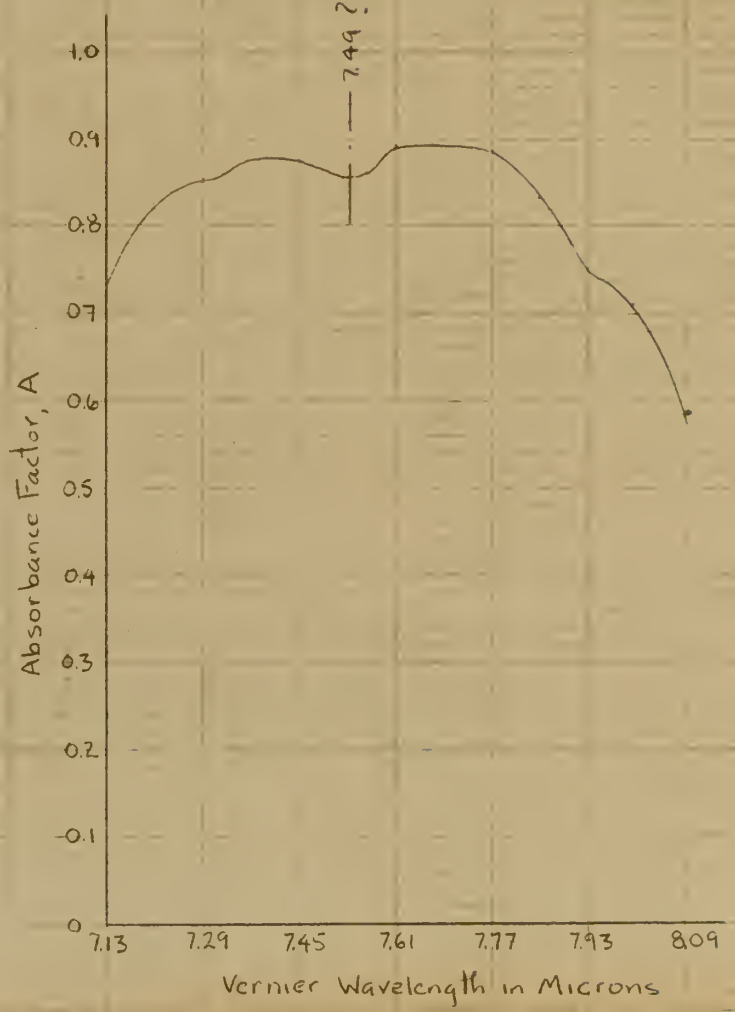

FIGURE 35
7.6 MICRON METHANE ABSORPTION BAND
RECORDER TRACE AND ABSORBANCE CURVE

100 - 4 - 8 - 2.0 - 3.0 - 45 - 5 - 1.2 - 45.1 - 7.8 - 5.20

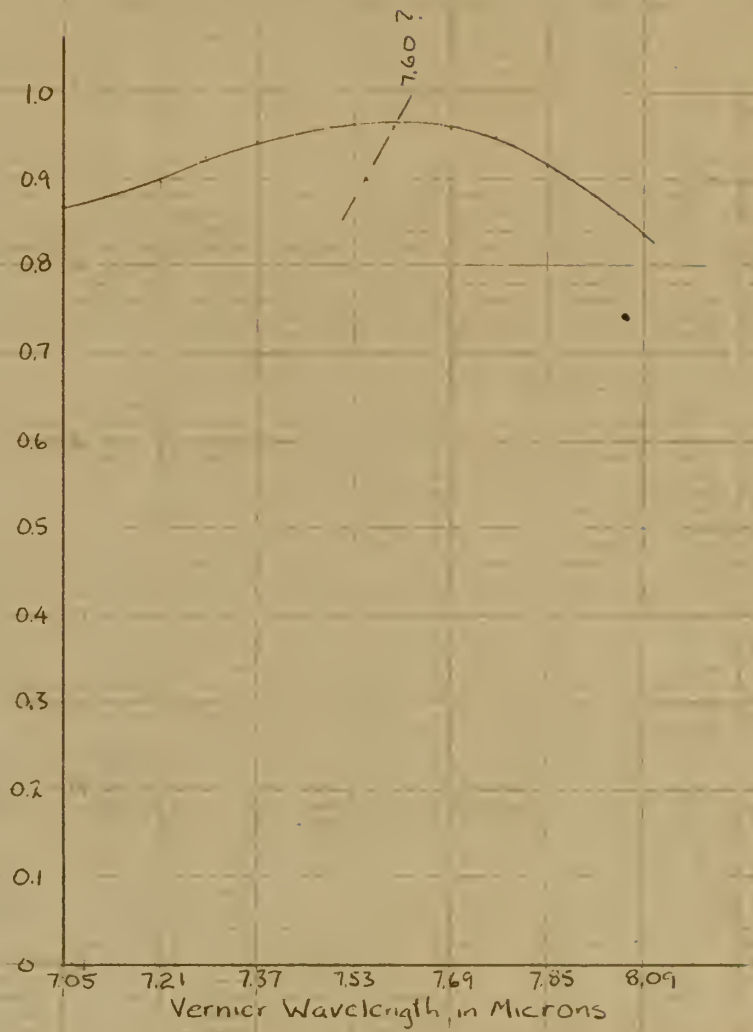

FIGURE 36
7.8 MICRON COLLODION ABSORPTION BAND
RECORDER TRACE AND ABSORBANCE CURVE

CHAPTER V

EVALUATION OF DATA AND CONCLUSIONS

1. Analysis and Summary of Calibration Data

No examples of symmetric absorption bands in a region of symmetric or constant source energy were encountered among the calibration spectra recorded: absorbance factors were therefore calculated for each band used.

In the case of carbon dioxide as a sample absorbant, water vapor effects were negligible in the regions of interest and other contaminating effects were not apparent and were assumed to be absent. Calculation of pseudo-absorbance factor, $A_s = \frac{ky_1 - y_3}{ky_1}$, was therefore carried out, using values from Figure 27 to plot a ky_1 curve on the recorder sheet and then using corresponding values of ky_1 and the recorder trace ordinates, y_3.

In the case of all other sample absorbants, contaminating carbon dioxide and water vapor effects were present in or near the regions of interest, and the calculation of absorbance factor, $A = \frac{y_2 - y_3}{y_2}$, was carried out, using values of y_2 and y_3 from two superimposed recorder traces.

A transparent grid of regularly-spaced wavelength intervals was placed over each response curve and aligned with the wavelength synchronizing signal points: corresponding values of y_3 and y_2 or ky_1 were then read and used to determine the absorbance curves. The point of maximum absorption factor, determined with the aid of absorption curve mid-point axes, was used as the vernier wavelength of calibration points.

Recognized errors in the determination of vernier wavelengths of

calibration points are as follows:

a. Temperature fluctuations during the recording of a spectral response curve. Significant net changes between the times of wavelength synchronizing signals could be recognized and curves showing this effect were discarded. Temperature variations of the order of 1°C occurred in cases where a net change of temperature was not apparent, however, and errors of the order of 0.01 micron were thereby introduced.

b. Errors due to irregular recorder paper feed, the placing of the reading grid, and reading of the ky_1, y_2, and y_3 ordinates. The smoothness of absorption curves obtained indicated that ordinate reading errors were of small significance. Synchronizing signals revealed slight variations in recorder paper feed, however, and this effect and associated translational errors in the location of the grid overlay could yield ultimate errors up to about 0.02 microns.

c. Relative displacement of the y_2 and y_3 traces due to manipulative error in the starting of superimposed traces. Starting the recorder drive first was desirable in order to reduce uneven paper feed, and starting of the monochromator drive motor at a desired point on the recorder trace was generally accomplished within about 0.04 micron. Runs with significant mismatching were discarded and the ultimate calibration error from this effect is considered to have been always less than 0.01 micron, due to the small slopes of the y_2 curve near calibration points.

The mean probable aggregate error in the determination of

the vernier wavelengths of calibration points is judged to be about 0.02 micron.

The data utilized for the true position of the various spectral features is considered to have been in error by less than 0.01 micron in all cases: the error in the true position of the completely symmetric 3.3 micron methane and 4.3 micron carbon dioxide absorption maxima is therefore inconsequential. The previously-mentioned error associated with differences in resolution of unsymmetric absorption bands becomes considerable, however. Estimates of the probable error in the true positions of calibration points are included in the following table of data used:

Absorbant Media	Bibliography Reference Number	Estimated True Wavelength of Low-Resolution Maximum Absorbance Factor and Estimated Probable Error, in Microns
Methane	17	1.79 ± less than 0.01
Ammonia	22	1.97 ± 0.01
Ammonia	1	2.25 ± 0.03
Methane	16	2.33 ± 0.02
Carbon dioxide	2 (abstract)	2.73 ± unevaluated error
Methane	16	3.32 ± 0.00
Carbon dioxide	7	4.26 ± 0.00
Ammonia	1	6.14 ± 0.04
Methane	16	7.59 ± 0.04
Collodion	21 (abstract)	7.79 ± unevaluated error

Figure 37 is the vernier wavelength correction curve determined from the obtained absorption band calibration data at 45°C. Figure 38 is the corresponding calibration curve for the monochromator-spectrometer system.

Preliminary calibration observations revealed the original wavelength corrections to be of the order of + 0.8 micron at 23°C in this region: it is apparent that the process of optical realignment, together with operation at 45°C, has reduced these corrections to a much more suitable level.

2. Recommended Procedure for Operation of the System

The following outline of the recommended operational procedure for this system applies to the most energetic attempts to obtain optimum performance, and steps may be deleted or modified according to the purpose of the run being made:

a. Take a spectral response curve under a set of standardized conditions to verify normal overall system performance.

b. Select and connect the bolometer battery voltage to be used, depending upon the relative needs for maximum response and longer periods of uninterrupted operation.

c. Decide whether or not the constant voltage transformer will be used, depending upon the relative needs for maximum response and the desired degree of trace reproducibility.

d. Make preliminary runs to determine the optimum combination of slits width, amplifier gain, discriminator output shunting resistance, recorder full deflection setting, and recorder stylus position at zero input. Determine the positions at

FIGURE 37

VERNIER WAVELENGTH CORRECTION CURVE FOR 45°C
OPERATION OF THE MONOCHROMATOR - SPECTROMETER SYSTEM.

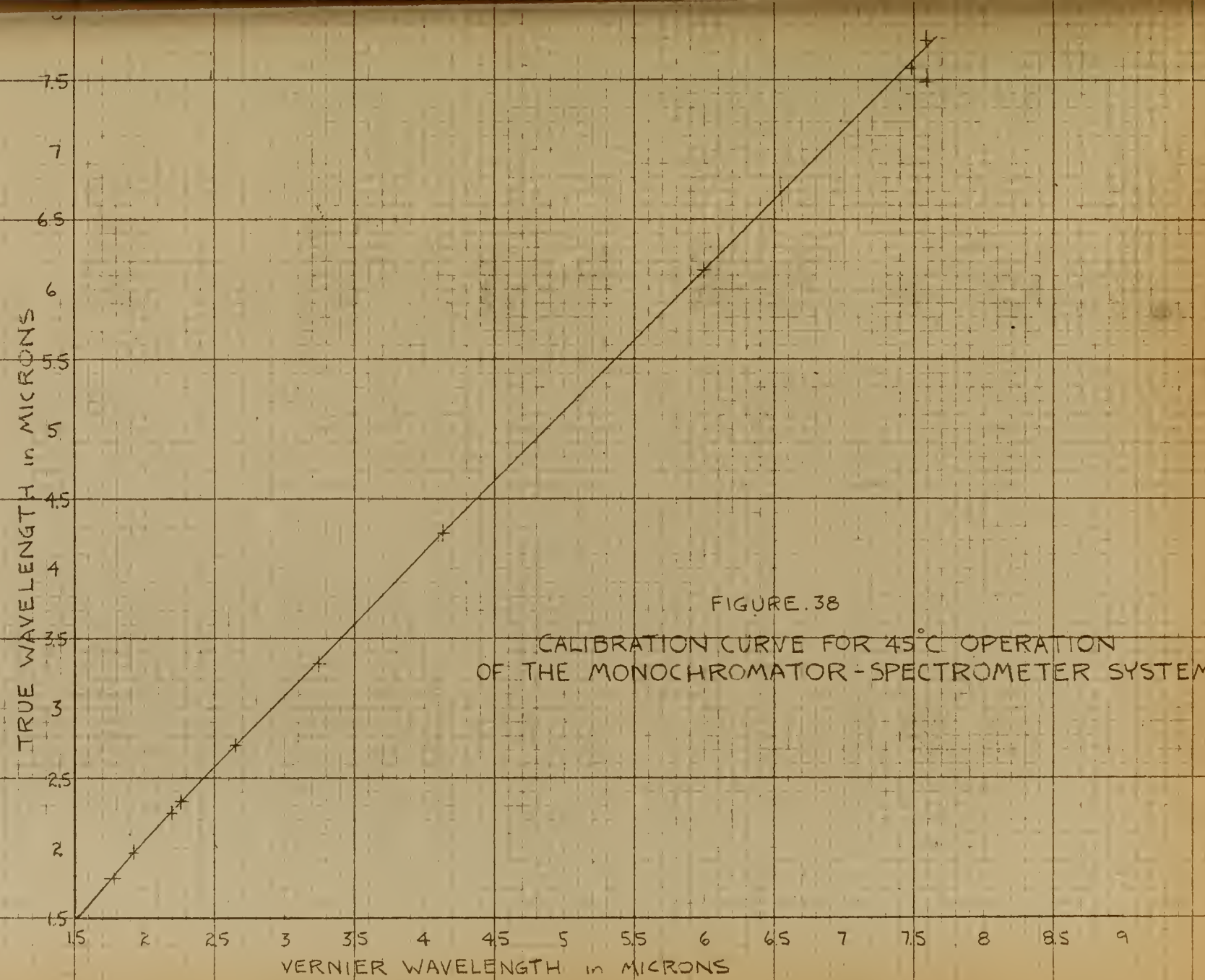

FIGURE. 38

CALIBRATION CURVE FOR 45°C OPERATION
OF THE MONOCHROMATOR-SPECTROMETER SYSTEM

which wavelength synchronizing signals will be introduced.

e. Connect a cathode ray oscilloscope between ground and amplifier terminal 11 and between ground and amplifier terminal 13 while adjusting the reference generator brush rigging for optimum phasing with the detector signal.

f. Put any film or liquid absorber holders to be used in place with wires attached to slide these units in and out of the optical path. Tighten the monochromator casing and check the thermostat setting.

g. Put the constant-temperature enclosure in place. Turn on the circulating air blower and the Globar simulator. (The thermostat system should be on at all times as a moisture safeguard.) Secure all other equipment units.

h. Flush the monochromator casing with dry nitrogen, and then evacuate the casing. Bleed in a gas sample if appropriate.

i. Allow about 6 hours for temperature equalization throughout the outer casing. (If the outer casing is used at all with a high energy source, time must be allowed for temperature equalization, otherwise thermal gradients within the KBr prisms will yield non-reproducible results.)

j. Turn on the recorder and the main power supply about one-half hour before use. Leave the bolometer battery switch off.

k. Turn off the Globar simulator and turn on the source and source cooling air about 10 minutes before use. Bring the source to equilibrium operation.

l. If the run is to be with an evacuated monochromator casing,

restart the vacuum pump and leave it running.

m. Operate the recorder semi-automatic current adjustor. Adjust recorder sensitivity to maximum without hunting.

n. Turn on the bolometer battery voltage and the chopper motor. Operate the snap switch to put the millivoltmeter across the discriminator output. Adjust the discriminator balance control to provide zero signal with median anticipated recorder stylus displacement. Turn off the millivoltmeter snap switch.

o. Disconnect all temporary meters.

p. Operate the monochromator drive motor switch to bring the wavelength vernier to the desired starting position.

q. Record all run data.

r. Start the recorder drive and observe the trace for unusual transient effects.

s. Turn on the monochromator drive and obtain a recorder trace. Manipulate the wavelength synchronizing signal switch according to the previous plan.

t. Turn off the bolometer battery voltage between runs. If gas absorption samples are admitted to the monochromator casing, allow a sufficiently slow flow to assure proper absorption of water vapor from the sample and wait at least one-half hour for the monochromator interior to rereach temperature equilibrium.

In addition to the preceding routine, an occasional calibration check of the vernier wavelength reading for the strong carbon dioxide absorption dip at 4.26 microns is advisable.

3. Suggestions for Further Improvement and Utilization of the System

Following is a list of repairs and modifications which are recommended for eventual accomplishment in the hope of improving the performance and increasing the uses of this system:

a. Resurface the etched back face of the second prism to improve overall energy transmission of the monochromator.

b. Manufacture liquid absorption cells of various thickness, in order to utilize the generally better-defined absorption characteristics of liquids for calibration purposes and to allow the study of liquid absorption spectra.

c. Install a detector at the entrance slit of the monochromator. Use this detector as part of a monitoring device to hold source energy constant over a particular wavelength region or to provide a means of providing an amplifiable signal to be compared with the monochromator output detector signal. Either of these two alternatives would permit the recording of true spectral characteristics with a single run.

d. Obtain more energetic sources, such as larger Globars. Additional source cooling facilities would be required for such sources and filters should be provided to regulate the energy reaching the detector in the high energy wavelength region, but increased long-wavelength responses could thus be obtained.

e. Relocate the chopper mirror as previously described.

f. Replace the thermostat element with one which permits more precise temperature control.

g. Install a clutch arrangement on the monochromator drive gear assembly to provide reversible drive with the outer casing in place.

h. Make further attempts to obtain improved performance from the amplifying system and the Golay units. If these efforts do not yield satisfactory results, design and construct an amplifying system for the bolometer detector to yield a direct current maximum output of about 50 millivolts with minimum self-noise and susceptibility to transient effects.

BIBLIOGRAPHY

1. Barker, E. F. — Perpendicular Vibrations of the Ammonia Molecule. Physical Review. 55:657-662, April, 1939.

2. Barker, E. F. — Absorption of Carbon Dioxide in the Near Infrared. Chemical Abstracts. 16:3261, October, 1922.

3. Barker, E. F. and Adel, A. — Resolution of the Two Difference Bands of Carbon Dioxide Near 10 Microns. Physical Review. 44:185-187, August, 1933.

4. Barnes, R. B. and Bonner, L. G. — The Christiansen Filter in the Infrared. Physical Review. 49:732-740, May, 1936.

5. Barnes, R. B., Gore, R.C. Liddel, U., and Williams, V. Z. — Infrared Spectroscopy, New York, Reinhold Publishing Corp., 1944

6. Brode, W. R. — Chemical Spectroscopy - The Edward Marburg Lecture of 1950. American Society for Testing Materials, 1950.

7. Cameron, D. M. and Nielsen, H. H. — The 4.3 Micron Fundamental Band in the Spectrum of Carbon Dioxide. Physical Review. 53:246-247, February, 1938.

8. Candler, A. — Practical Spectroscopy. Glasgow, Hilger and Watts, Ltd., 1949.

9. Fry, D. L., Nusbaum, R. E., and Randall, H.M. — The Analysis of Multicomponent Mixtures of Hydrocarbons in the Liquid Phase by Means of Infra-Red Absorption Spectroscopy. Journal of Applied Physics. 17:150-161, March, 1946.

10. Golay, M. J. E. — A Pneumatic Infra-Red Detector. Review of Scientific Instruments. 18:357-362, May, 1947.

11. Gundelach, von E. — Die Dispersion von KBr.- Kristallen im Ultraroten. Zeitschrift für Physik. 66:775-783, October, 1930.

12. Harrison, R. H., Lord, R. C., and Loofbourow, J.R. — Practical Spectroscopy. New York, Prentice-Hall, Inc., 1948.

13. Koehler, W. F. — Multiple Beam Fringes of Equal Chromatic Order, Part I, Phase Change Considerations. Journal of the Optical Society of America. 43:738-743, September, 1953.

14. McAlister, E. D., Matheson, G. L., and Sweeney, W. J. — A Large Recording Spectrograph for the Infra-Red to 15 Microns. Review of Scientific Instruments. 12:314-319, June, 1941.

15. Mellon, M. G. — Analytical Absorption Spectroscopy. New York, John Wiley and Sons, Inc., 1950.

16. Nielsen, A. H. and Nielsen, H. H. — Infrared Absorption Bands of Methane. Physical Review. 48:864-867, December, 1935.

17. Norris, W. V. and Unger, H. J. — Infrared Absorption Bands of Methane. Physical Review. 43:467-472, March, 1933.

18. Oetjen, R. A., Kao, Chao-Lan, and Randall, H. M. — The Infra-Red Prism Spectrograph as a Precision Instrument. Review of Scientific Instruments. 13:515-523, December, 1942.

19. Plyler, E. K. and Sleator, W. W. — Further Study of the Absorption of Infra-red Radiation by Water Vapor. Physical Review. 37:1493-1507, June, 1931.

20. Sawyer, R. A. — Experimental Spectroscopy. New York, Prentice-Hall, Inc., 1944.

21. Trowbridge, A. — Optical Properties of Collodion and Celluloid. Chemical Abstracts. 3:19, January, 1909.

22. Unger, H. J. — Infrared Absorption Bands of Ammonia. Physical Review. 43:123-128, January, 1933.

23. Walls, A. J. — The Infra-Red Transmission of Thin Films of Various Organic Materials. Journal of Applied Physics. 11:137-140, February, 1940.

25264

Thesis S56 Skoog
Assembly, adjustment, and partial calibration of an infrared monochromator-spectrometer system.